

**Growth and Electrochemical Properties of LiCoO<sub>2</sub> Single  
Crystals for Application of All Solid State Li-ion Batteries**

全固体リチウムイオン電池応用を目指した  
LiCoO<sub>2</sub>単結晶の育成と電気化学的性質

**PhD Dissertation**

**Interdisciplinary Graduate School of Medicine and Engineering**

**University of Yamanashi, JAPAN**

**March 2021**

**RUMA PARVIN**

*Bismillahir Rahmanir Rahim*

*Dedicated to my beloved Husband*

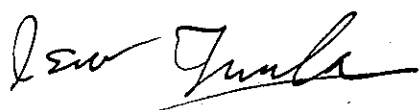
*MD. SHAHAJAN ALI*

## CERTIFICATE

*I hereby certify that the thesis entitled "Growth and Electrochemical Properties of LiCoO<sub>2</sub> Single Crystals for Application of All Solid State Li-ion Batteries" submitted by RUMA PARVIN, has been completed under my direct supervision.*

*This is a bona fide record of the research carried out by the candidate. To the best of my knowledge, this thesis has not been submitted for the award of any degree or award elsewhere.*

***Principal Supervisor***



***Professor Isao Tanaka***

*Center for Crystal Science and Technology*

*University of Yamanashi*

*Miyamae 7-32, Kofu, Yamanashi 400-8511, Japan*

*Phone (+81)55-220-8625 Fax (+81)55-220-8270*

*Mail: [itanaka@yamanashi.ac.jp](mailto:itanaka@yamanashi.ac.jp)*

## *ABSTRACT*

The effects of the mirror tilt angle on the molten zone shape during the growth of LiCoO<sub>2</sub> crystals were investigated for the first time for the traveling solvent floating zone (TSFZ) technique using a tilting-mirror-type image furnace. In our experiments, it was found that the interface shape of the molten zone formed under both tilted and non-tilted conditions was convex. The convexities ( $h/r$ ) of the feed-liquid and crystal-liquid interface were minimum at the tilt angle of  $\theta = 10^\circ$ . It was also found that the lamp power required to maintain the stable molten zone during crystal growth and the amount of Li evaporation from the molten zone were the lowest at  $\theta = 10^\circ$  compared to the other tilt conditions ( $\theta = 5^\circ$  and  $15^\circ$ ). The most effective heating was realized under this tilt condition. We successfully grew large single crystals of LiCoO<sub>2</sub> approximately 7 mm in diameter and 50 mm in length with a shiny visible character at  $\theta = 10^\circ$  due to the lowest convexities and highest stability in this tilt condition.

For the TSFZ growth of larger diameter single crystals of LiCoO<sub>2</sub>, the growth conditions, such as the excess Li content in the feed, amount of Li-excess solvent and the filament shape of the heating lamps, were optimized for various crystal diameters using a tilting-mirror-type image furnace. The stability of the molten zone was affected by the excess Li content in the feed and the amount of solvent. The optimum amount of solvent was linearly related to the square of the crystal diameter during

growth. We successfully grew  $\text{LiCoO}_2$  single crystals with a diameter of 10 mm and 13 (more than  $\frac{1}{2}$  inch) and a length of 50 mm with a shiny visible character under the optimum growth conditions. The charge-discharge characteristics of the grown  $\text{LiCoO}_2$  single crystals were studied using  $\text{LiCoO}_2$  single crystals as cathode and liquid, gel and solid electrolytes. The discharge capacities of Li-ion batteries (LIBs) using  $\text{LiCoO}_2$  single crystals cathode was  $145 \text{ mAhg}^{-1}$  with liquid electrolyte. Almost all solid state LIBs was designed using  $\text{LiCoO}_2$  single crystals cathode with gel electrolyte. The discharge capacities of almost all solid state LIBs was  $90 \text{ mAhg}^{-1}$ . Single crystals growth of 1 at% Nb-doped  $\text{LiCoO}_2$  was tried by TSFZ technique with tilting mirror-type furnace.

---

## CONTENTS

---

<b>ABSTRACT</b>	<b>I</b>	
<b>CONTENTS</b>	<b>III</b>	
<b>CHAPTER I</b>	<b>Introduction</b>	
<b>CHAPTER I</b>	<b>1-43</b>	
1.1	General Introduction	1
	1.1.1 Energy issues and Li-ion batteries (LIBs).	1
	1.1.2 Discussion of cathode materials used in LIBs.	6
1.2	Research background of LiCoO <sub>2</sub> cathode	23
1.3	Purpose of the research	25
1.4	Motivation of the research	27
1.5	Plan of the thesis	28
	References	30

---

## **CHAPTER 2 Effects of mirror tilting on the shape of the molten zone and interfaces during the TSFZ growth of LiCoO<sub>2</sub> single crystals**

---

**44 - 64**

2.1	Introduction	44
	2.1.1 Concept of the solid-liquid interface in the molten zone	44
	2.1.2 Importance of investigation of interface shape	45
	2.1.3 Previous reports about the effects of the interface shape on the crystal growth	45

2.1.4	Control of the solid-liquid interface shape	46
2.1.5	Concept of mirror tilting	47
2.1.6	Advantages of travelling solvent floating zone (TSFZ) method	49
2.2	Experimental procedure	51
2.2.1	Feed preparation	51
2.2.2	Solvent preparation	51
2.2.3	Crystal growth and quenching the molten zone	52
2.2.4	Characterization of the quenched molten zone	54
2.3	Mirror tilting effects on the interface shape of the molten zone	56
2.4	TSFZ growth of LiCoO <sub>2</sub> single crystals as a function of mirror tilting angles	57
2.5	Characterization of grown crystals at mirror tilting angles $\theta = 10^\circ$	61
2.5.1	SEM and Laue XRD measurement	61
2.6	Conclusions	62
	References	63

---

## **CHAPTER 3 Larger diameter single crystals growth of LiCoO<sub>2</sub> by TSFZ**

### **method 65 - 83**

---

3.1	Introduction	65
3.1.1	Background of the study	65

3.1.1.1	Discussion about the previous reports on the growth of $\text{LiCoO}_2$ single crystals	66
3.1.1.2	Importance of the growth of larger diameter single crystals of $\text{LiCoO}_2$	66
3.1.1.3	Problems during the growth of larger diameter single crystals	66
3.1.1.4	Attempts to solve those problems during the growth	67
3.1.1.5	Concept of flat and cylindrical-type heating lamp filament configuration for larger diameter single crystals growth	68
3.2	Optimization of the growth conditions during the single crystals growth	70
3.2.1	Experimental procedure for the TSFZ growth of 10 mm and 13 mm diameter	70
3.2.2	Optimization of the shape of heating lamp filament	72
3.2.3	Optimization of Li excess feed compositions and amount of solvent	74
3.2.4	Relationship among important parameters during the growth	79
3.2.4.1	Optimum excess Li content in feed vs crystal diameter	79
3.2.4.2	Excess Li content in feed vs required lamp power	79
3.2.4.3	Optimum solvent amount vs square of crystal diameter	79
3.3	Conclusions	81
	References	82



---

**CHAPTER 4 Design of next generation all-solid-state Li ion batteries  
(LIBs) using LiCoO<sub>2</sub> single crystals cathode** **84 - 104**

---

4.1	Introduction	84
4.1.1	Background of the study	84
4.1.1.1	Problems of LiCoO <sub>2</sub> polycrystalline cathode in LIBs	85
4.1.1.2	Advantages of single crystals cathode	85
4.1.1.3	Advantages of single crystals solid electrolyte	86
4.2	Experimental section for coin cell preparation	87
4.2.1	Coin cell using liquid electrolyte	87
4.2.2	Coin cell using gel electrolyte	89
4.2.3	Coin cell using LLZO polycrystalline solid electrolyte	90
4.2.4	Coin cell using LLN single crystals solid electrolyte	92
4.3	Charge discharge characteristics of LIBs using LiCoO <sub>2</sub> single crystals cathode	94
4.3.1	Liquid electrolyte	94
4.3.2	Gel electrolyte	97
4.3.3	LLZO Polycrystalline solid electrolyte	98
4.3.4	LLN single crystals solid electrolyte	99
4.4	Conclusions	100
	References	102

---

**CHAPTER 5 Single crystal growth of Nb doped LiCoO<sub>2</sub> by TSFZ method****using tilting mirror furnace 105 - 118**

---

5.1	Introduction	104
	5.1.1 Previous reports on doped LiCoO <sub>2</sub>	106
	5.1.2 Purpose for doping Nb in LiCoO <sub>2</sub> cathode	106
	5.1.3 Motivation	109
5.2	Experimental details	109
5.3	Single crystal growth of LiCo <sub>0.99</sub> Nb <sub>0.01</sub> O <sub>2</sub>	111
5.4	Characterization of grown crystals	115
	5.4.1 Scanning Electron Microscopy (SEM) images	115
5.5	Conclusions	116
	References	116

---

**CHAPTER 6 Social significance and business feasibility of the current****research 119 - 129**

---

---

**CHAPTER 7 Summary and Impact of the present research 130 - 137**

---

7.1	Summary	130
7.2	Impact of the present research	135

---

**APENDIX**

---

List of publications related to this study	138
ACKNOWLEDGEMENT	141

# CHAPTER I

## *Introduction*

### 1.1 General Introduction

#### 1.1.1 Energy issues and Li-ion batteries (LIBs)

In modern society, efficient energy harvest, storage, and management are three essential issues to energy consumption which is shown in the diagram of energy utilization chain in Figure 1-1[1-3].

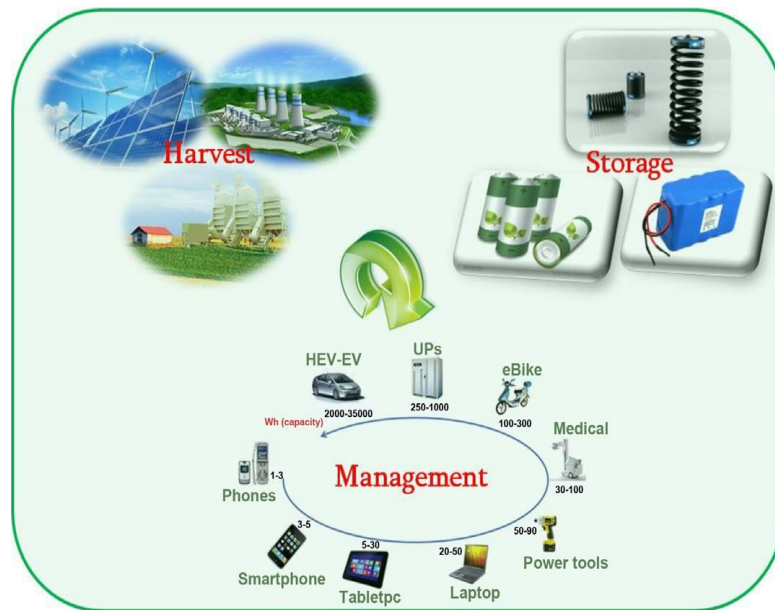


Fig. 1-1 Schematic diagram of the energy utilization chain of modern society [3].

Although, in the past decade, fossil fuels, such as coal, crude oil, and natural gas, were used as primary energy sources to power all high-tech-dependent human activities. However, pollution arising from fossil fuel combustion had a devastating impact on human health and the natural environment. In order to decrease the global warming and environmental pollution, the focus of research has shifted to environmentally benign sustainable energy. Li-ion batteries (LIBs) are one of the most attractive energy storage technologies in which energy is stored in the form of chemical potential [3-12].

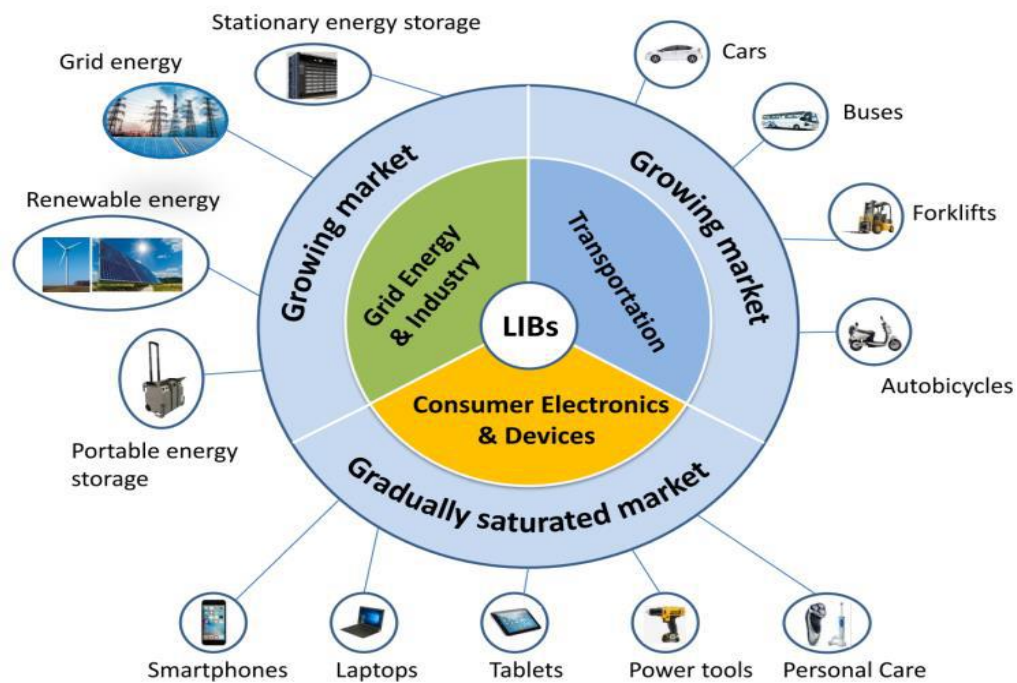


Fig. 1-2 The applications of LIBs in the three main fields including consumer electronics & devices, transportation, and grid energy & industry[13].

This energy storage technologies, particularly for portable electronics and mobile instruments, are based on the conversion of electricity, with the energy being stored in the form of chemical potential [14–17].

Due to their high energy density, batteries have long been used to power portable electronics, as well as stationary and mobile instruments. In the last two decades, Lithium-ion batteries have advanced rapidly with increased energy density and long cyclic stability, which is beneficial for most portable electronics including mobile phones and laptop computers. In addition, research on LIBs has significantly increased due to their high power and high discharge voltages for use as a power source in hybrid electric vehicles and electric vehicles. All solid-state LIBs have also been studied for their safety and stability [18-30]. Currently, lithium-ion batteries have been used in many products, such as consumer electronics, electric/hybrid electric vehicles, stationary energy storage systems etc as shown in Figure 1-2. In 2019, Nobel Prize in chemistry is awarded to Professor John Goodenough (The University of Texas at Austin, USA), M. Stanley Whittingham (Binghamton University, State University of New York, USA), and Akira Yoshino (Asahi Kasei Corporation, Tokyo, Japan, & Meijo University, Nagoya, Japan), for the development of lithium ion battery[31].

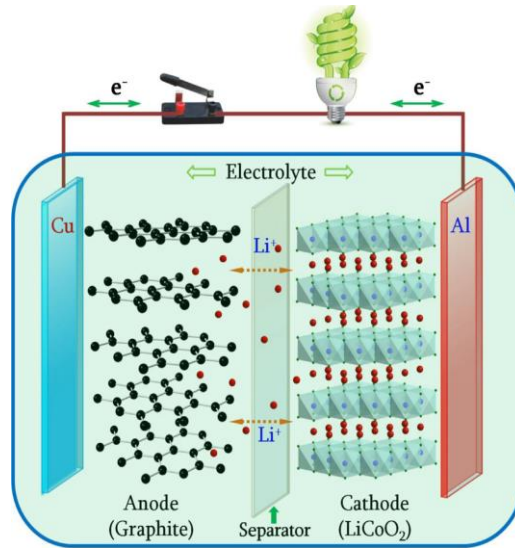


Fig. 1-3 Schematic diagram of the configuration of rechargeable LIBs [3].

A Schematic diagram of the configuration of LIBs is shown in Figure 1-3. Li-ion rechargeable batteries consist of two electrodes, anode and cathode, immersed in an electrolyte and separated by a polymer membrane (Fig.1-3). This basic device configuration has remained unchanged from the earliest developed batteries [32]. The similarities between Li-ion batteries and conventional batteries include the redox reactions at the interfaces between the electrolyte and electrodes, accompanied by the diffusion of ions in the electrolyte. However, the differences between conventional batteries, or galvanic cells, and Li-ion batteries are notable as well. In typical galvanic batteries, the redox reactions proceed simultaneously with the receding or advancing of the electrode surfaces, but not accompanied by either the solid-state mass diffusion in the electrodes or a change in the chemical composition and local atomic

environment [33]. By contrast, the heterogeneous redox reactions in Li-ion batteries are always accompanied by solid-state mass diffusion. Li ions, the working ionic component of electrochemical reactions, are transferred back and forth between the anode and the cathode through the electrolyte. While the concentration of lithium ions remains constant in the electrolyte regardless of the degree of charge or discharge, it varies in the cathode and anode with the charge and discharge states. The basic working mechanism based on which LIBs functions is associated with the transfer of lithium ions from the positive electrode (cathode) to the negative one (anode) and vice versa. During discharging process, lithium ions travel through an electrolyte, often an organic solution of lithium salt such as  $\text{LiPF}_6$ , from the cathode side to the anode side. The exact opposite occurs during charging as an external current is applied [34].

Electrochemical intercalation reactions are widely applied in Li-ion batteries for both anodes, such as graphite [35, 36], and cathodes, such as  $\text{LiCoO}_2$  [37] and  $\text{LiFePO}_4$ [38,39]. Intercalation reactions require the host electrode material to possess space to accommodate Li ions as well as multivalent ions to maintain the electro neutrality. The compounds most commonly studied and widely used for Li-ion intercalation are transition metal-containing compounds with layered, spinel, or olivine structures [40, 41].



### 1.1.2 Discussion of cathode materials used in LIBs

Since the cathode, anode, and electrolyte are the three important active materials of a Li-ion battery. However, a key element that limits the performance of the batteries is the active element of the positive electrode, and it is also the most expensive part.



Fig. 1-4 Schematic illustration of the future EV [42].

Therefore, selection of the cathode material is a key parameter when building reliable batteries for large-format applications such as EVs and energy storage (Fig. 1-4).

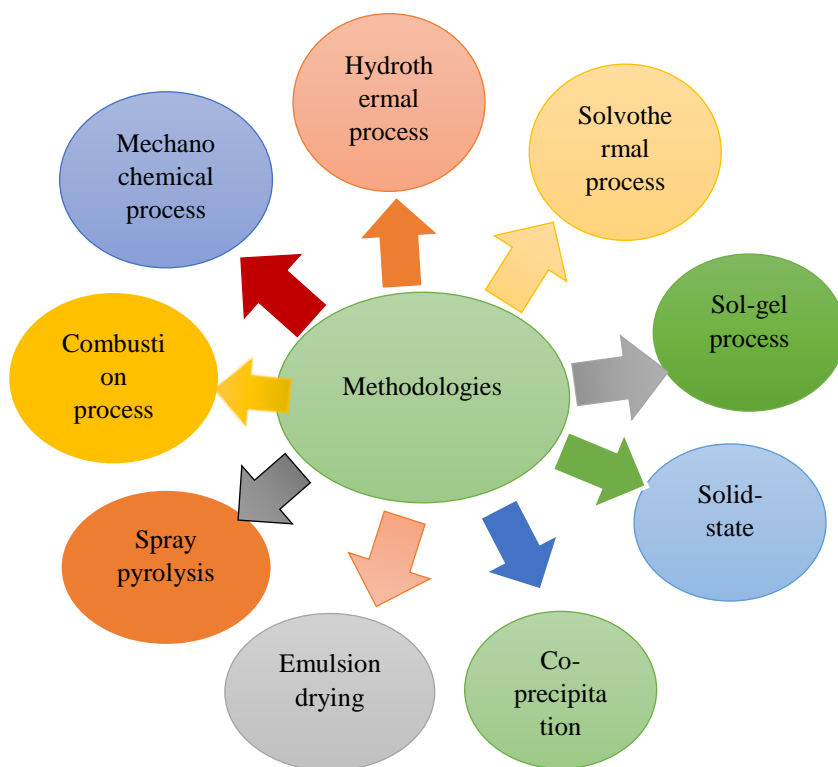


Fig. 1-5 Schematic diagram of different synthesis techniques to produce cathode materials for rechargeable LIBs [36].

**Table 1.** Electrochemical characteristics of the three classes of cathode materials.

<b>Framework</b>	<b>Cathode materials</b>	<b>Theoretical specific capacity(mAh/g)</b>	<b>Practical Specific capacity(mAh/g)</b>	<b>Average potential(V vs. Li<sup>0</sup>/Li<sup>+</sup>)</b>
Layered	LiCoO <sub>2</sub>	272	140	4.2
	LiNi <sub>1/3</sub> Mn <sub>1/3</sub> Co <sub>1/3</sub> O <sub>2</sub>	272	200	4.0
Spinel	LiMn <sub>2</sub> O <sub>4</sub>	148	120	4.1
	LiMn <sub>3/2</sub> Ni <sub>1/2</sub> O <sub>4</sub>	148	120	4.7
Olivine	LiFePO <sub>4</sub>	170	160	3.45
	LiFe <sub>1/2</sub> Mn <sub>1/2</sub> PO <sub>4</sub>	170	160	3.4/4.1

The layered lithium transition metal oxide with the formula LiMO<sub>2</sub>, where M=Co, Mn, Ni or a combination of two or more, have been arguably the most successful category of cathode materials for LIBs due to their superior electrochemical behavior[32].The electrochemical properties of the three classes of cathode materials are summarized in Table 1[43].

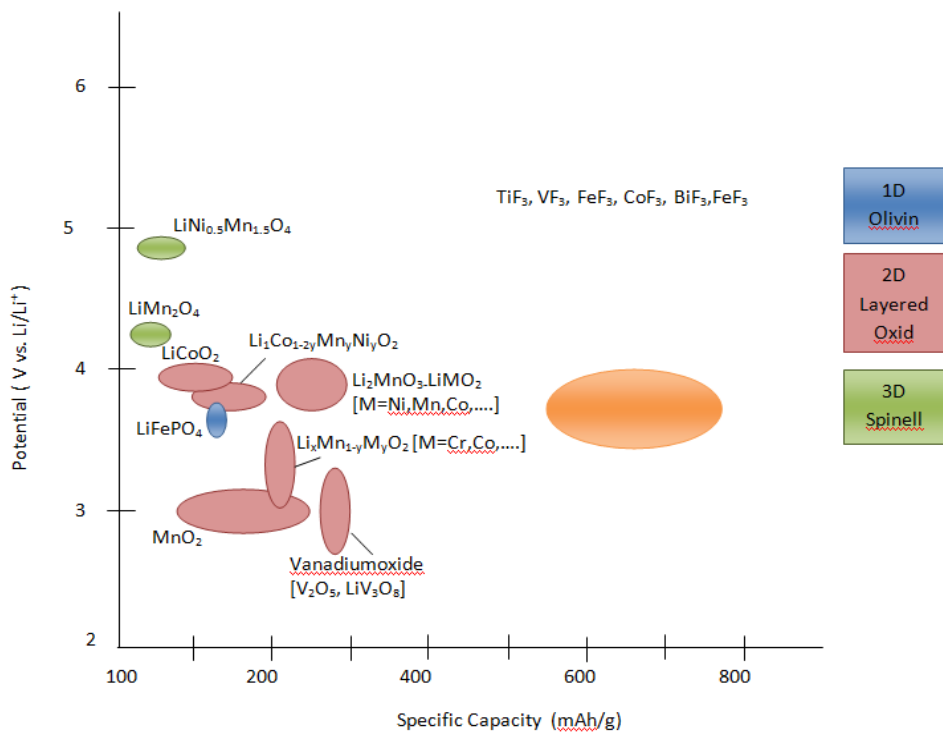


Fig. 1-6 Voltage and specific capacity of different cathode materials [34].

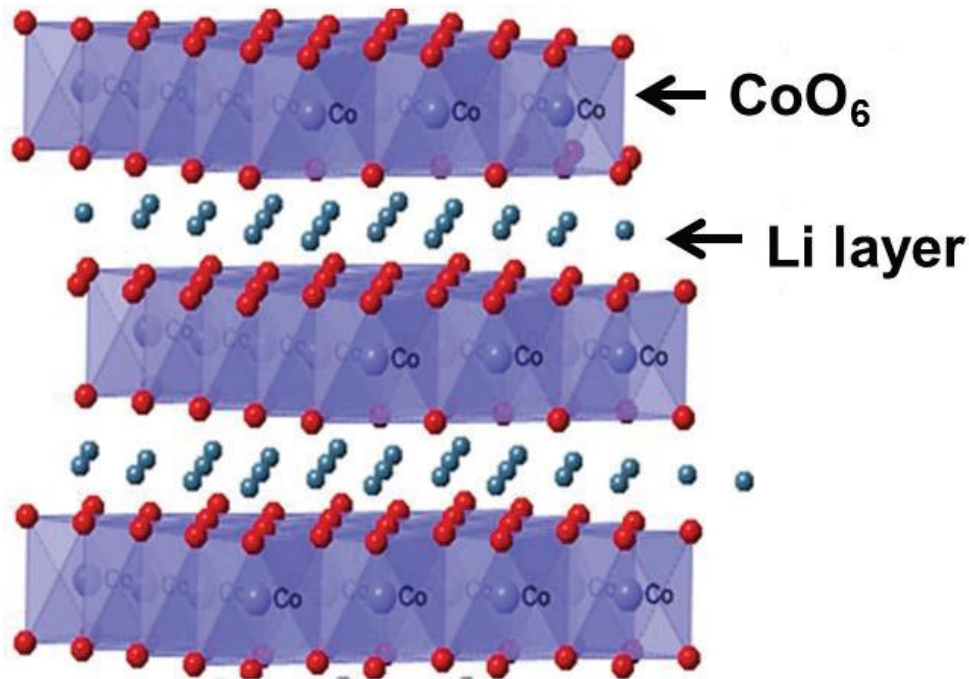


Fig. 1-7 Crystal structure of LiCoO<sub>2</sub>. In the LiMO<sub>2</sub> (M = Co, Mn, Ni) the metal layer is occupied by Mn, Ni, and Co in a random manner [44].

Crystal structure of LiMO<sub>2</sub> (M = Co, Mn, Ni) is shown in Figure 1-7[40]. Schematic diagram of different synthesis techniques to produce cathode materials for rechargeable LIBs [34] are described in Figure 1-5. In addition, comparisons among different cathode materials for LIBs are shown in Figure 1-6. The characteristics of different types of cathode materials for LIBs are discussed in detail as follows:

✓ **Layered lithium manganese oxide,  $\text{LiMnO}_2$  cathode:**

Although  $\text{LiMnO}_2$  has been proposed as a cathode material in LIBs almost as early as  $\text{LiCoO}_2$ , its use has not spread mainly due to performance limitations such as low capacity, difficulty of mass production, and power charge/discharge performance, especially at high temperatures. However, years of extensive research has led to significant improvement of its performance. Compared to  $\text{LiCoO}_2$ ,  $\text{LiMnO}_2$  has major advantages such as high safety and low cost which make it a promising substitute in the future.

✓ **Layered lithium nickel oxide  $\text{LiNiO}_2$  cathode:**

Another cathode material that is lithium nickel oxide ( $\text{LiNiO}_2$ ) which has a comparable layered structure and based cathodes are currently feasible for commercial use, their major drawback is poor solubility in organic electrolyte solutions, particularly at high temperature. Also, synthesis and treatment of  $\text{LiNiO}_2$  often require harsh temperature conditions which further limit its current use in commercial LIBs despite its superior capacity [45]. Nickel has higher energy density than cobalt does; 50% of lithium ions can be transferred between anode and cathode for cobalt at the maximum voltage of a typical battery (4.7 V), while 70% of lithium ions can be mobilized for nickel at only 4.2 V.

In order to enhance the stability and improve the electrochemical behavior of layered cathode materials for the further development of LIBs, many researchers have focused on the derivatives of nickel, cobalt, and/or manganese oxides. The characteristics of some of these derivatives cathode materials for LIBs are discussed as follows:

✓ **Spinel Lithium Transition Metal Oxides ( $\text{LiMn}_2\text{O}_4$ ) cathode:**

Spinel oxides with the chemical formula  $\text{LiMn}_2\text{O}_4$  were first proposed for the LIB oxide cathode by Michael Thackeray in the early 1980s [46].

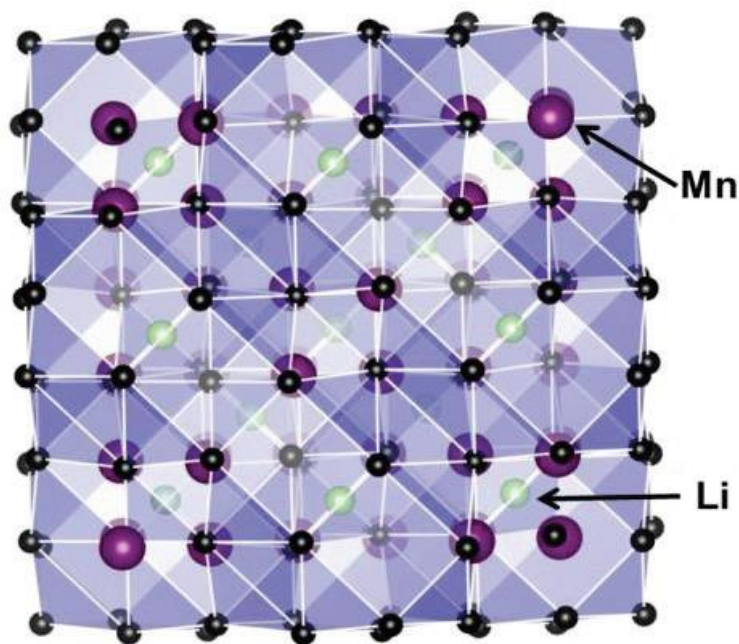


Fig. 1-8 Crystal structure of  $\text{LiMn}_2\text{O}_4$  [44].

Compared to other cathode oxides described above, the spinel lithium manganese oxide  $\text{LiMn}_2\text{O}_4$  is one of the most prospective cathode materials as a non-toxic, environmentally friendly, the high natural abundance of Mn and low-cost candidate [47]. This material has a theoretical capacity of 148 mAh/g for an equivalent weight (M) is 180.8 g/mol [48].

The unique  $\text{MnO}_2$  framework in the structure provides a three-dimensional (3D) diffusion pathway for Li ions. In  $\text{LiM}_2\text{O}_4$  oxide, the M cation always occupies  $\frac{1}{4}$  of the octahedra sites in the lithium layer; hence,  $\frac{1}{4}$  of the octahedra site remains vacant. Lithium ions always occupy the tetrahedra sites and share faces with the empty octahedra site in the TM layer. The structure of the typical  $\text{LiMn}_2\text{O}_4$  is shown in Fig.1-8. The 3D diffusion path in  $\text{LiMn}_2\text{O}_4$  provides excellent rate capability but suffers from severe capacity fading when cycling at elevated temperature. The reasons for this capacity fade were investigated, and two important mechanisms were proposed: 1) the dissolution of  $\text{Mn}^{2+}$  in the electrolyte by the corrosion of  $\text{H}^+$  ions and 2) the irreversible structural transformation from a spinel to a tetragonal structure due to the presence of Jahn-Teller (J-T) active  $\text{Mn}^{3+}$  ions [49,50]. The dissolution of Mn ions proceeds by the disproportionation reaction  $2\text{Mn}^{3+} \rightarrow \text{Mn}^{4+} + \text{Mn}^{2+}$ . Even though these spinel oxides are low cost and safe, the practical capacity and energy density are not comparable to other cathode materials. Various strategies were put forward to suppress the Mn dissolution and minimize the capacity fading.



Some authors have reported the electrical, thermal, and structural properties of  $\text{LiMn}_2\text{O}_4$  as well as the conduction mechanism for this material in a more detailed [51]. Many researchers [52-54] have investigated the electrochemical properties of  $\text{LiMn}_2\text{O}_4$  and reported the discharge capacity in the range of 100-120  $\text{mAhg}^{-1}$  which represent 67-81% of its theoretical capacity (148  $\text{mAhg}^{-1}$ ) [55]. A wide variety of synthetic approaches have been applied to develop spinel  $\text{LiMn}_2\text{O}_4$  including solid-state reaction [56], sol-gel method [57], hydrothermal synthesis [45], combustion synthesis, solution-phase, flame-assisted spray technology [58], and templating method. Within the spinel lithium manganese oxide system, two approaches have been often proposed to improve the structural stability and electrochemical performance of the system: cationic substitution and surface modification.

Many research work has been conducted on the electrochemical properties of derivatives of  $\text{LiMn}_2\text{O}_4$  in order to enhance the specific capacity and power and optimize the operational range of temperature for the original spinel compound. Two derivatives which are  $\text{LiNi}_x\text{Mn}_{2-x}\text{O}_4$  [59], and  $\text{LiCr}_x\text{Mn}_{2-x}\text{O}_4$  [60-62], have attracted strong attention of many researchers due to the improved cyclability of spinel magnesium oxides.

✓ **Olivine Lithium Transition Metal Phosphates (LiMPO<sub>4</sub>) cathode:**

The electrochemical behavior of olivine-structured transition poly anion compounds of the structural formulas of LiMPO<sub>4</sub> and LiMSiO<sub>4</sub> (M=Co, Fe, Mn, Ni or V) have been attracted a great deal of interest as potential cathode materials.

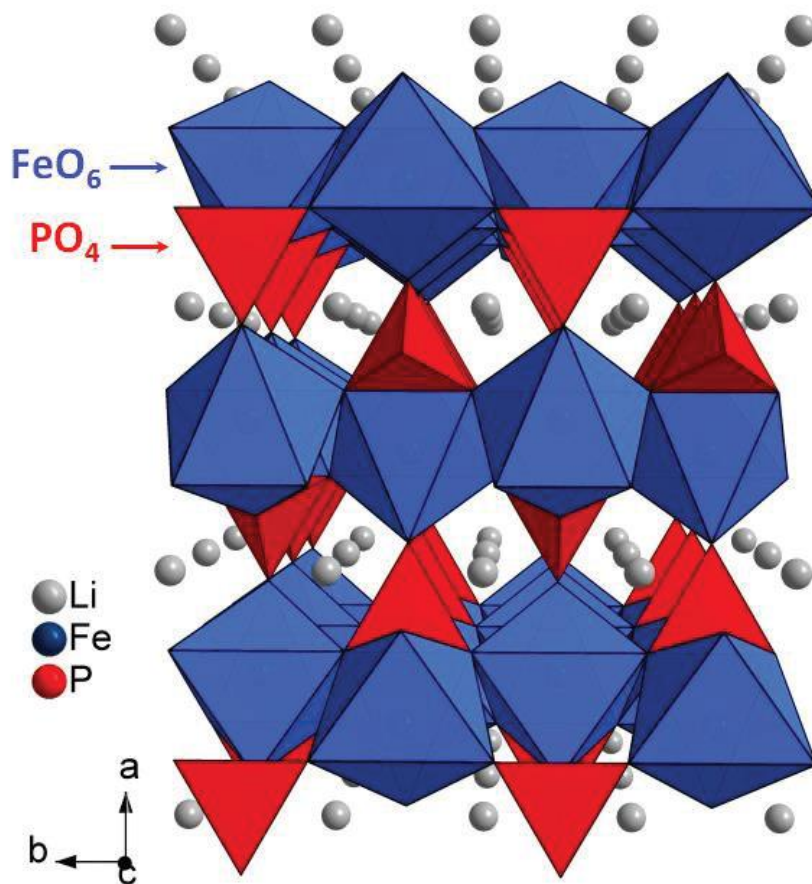


Fig. 1-9 Olivine structure of LiFePO<sub>4</sub> [44].

The crystals structure of Olivine structure of LiFePO<sub>4</sub> is shown in Fig. 1-9, which belongs to space group *Pnma*, with Li, Fe, and P atoms occupying octahedral 4a, octahedral 4c, and tetrahedral 4c sites, respectively. Oxygen atoms are in a slightly

distorted, hexagonal close-packed arrangement. The  $\text{FeO}_6$  octahedra share common corners in the  $bc$  plane, and  $\text{LiO}_6$  octahedra form a linear edge-shared chain parallel to the  $b$  direction. A  $\text{FeO}_6$  octahedron shares edges with two  $\text{LiO}_6$  octahedra and one  $\text{PO}_4$  tetrahedron. The separation of the  $\text{FeO}_6$  octahedra by  $\text{PO}_4$  polyanions significantly reduces the electronic conductivity ( $\sim 10^{-9}$  S/cm at room temperature) [63, 64]. Olivine-structured compounds have several advantages over other cathode materials including its structure of material hardly changes while Li ion intercalation and deintercalation. It holds a long voltage platform. Among phosphate compounds,  $\text{LiFePO}_4$  has received the greatest amount of attention due to a number of desirable features such as low cost, non-toxicity, and good thermal and chemical stability [65]. For example, the main drawback of lithium iron phosphates,  $\text{LiFePO}_4$ , is their low electrochemical performance at room temperature due to low lithium ion diffusion and poor electronic conductivity [65].

✓ **Olivine Lithium Transition Metal Silicates( $\text{LiMSiO}_4$ ) cathode:**

Another group of poly-anionic compounds, silicates, have been examined for their interesting electrochemical potential as cathode materials including  $\text{Li}_2\text{MnSiO}_4$  [66-68],  $\text{Li}_2\text{CoSiO}_4$  [69-71],  $\text{Li}_2\text{FeSiO}_4$  [35,66, 72-81], and  $\text{LiFeSO}_4\text{F}$  [82]. However,

several limitations have to be overcome before a wide use of such materials becomes feasible.

✓ **Nanostructured Metal Oxides Cathode:**

• **Vanadium oxides cathode:**

The vanadium-based oxides have attracted strong interest from researchers due to their good electronic conductivity, excellent chemical stability in polymeric electrolytes, and high energy density [83]. Since vanadium can exist in a number of oxidation states from 2+ in VO to 5+ in V<sub>2</sub>O<sub>5</sub>, vanadium oxides could offer a wide range of capacities as cathode materials [84]. Among these oxides, V<sub>2</sub>O<sub>5</sub>, LiV<sub>3</sub>O<sub>8</sub> and Li<sub>3</sub>V<sub>2</sub>(PO<sub>4</sub>)<sub>3</sub> have shown the most promising electrochemical behavior due to their high discharge capacities and good capacity retention.

• **Vanadium oxides V<sub>2</sub>O<sub>5</sub> cathode:**

As layered compounds with a high theoretical capacity of 442 mAhg<sup>-1</sup>, V<sub>2</sub>O<sub>5</sub> compounds are among the most promising high-capacity cathode materials under development. Several synthetic methods have been employed to prepare V<sub>2</sub>O<sub>5</sub> including sol-gel method, solvothermal route, precipitation process, and electrodeposition. Studies on V<sub>2</sub>O<sub>5</sub> have shown high discharge capacity mostly in

the range of 250-300 mAhg<sup>-1</sup> for V<sub>2</sub>O<sub>5</sub>/polypyrrole composites which represent 57-67% of its theoretical capacity with good capacity retention (15-20% after 50 cycles) [83]. When the structure and composition of lithiated V<sub>2</sub>O<sub>5</sub> nanocomposites are optimized, their electrochemical behavior can be significantly enhanced.

Despite these advantages of V<sub>2</sub>O<sub>5</sub> compounds, two drawbacks still persist: low power density due to their intrinsic low ionic conductivity, and poor cyclability as a result of microstructural failure upon cyclic lithium ion intercalation-deintercalation [83].

- **Vanadium oxides LiV<sub>3</sub>O<sub>8</sub> cathode:**

Another lithium vanadium oxide that has been widely investigated over the last two decades for its good electrochemical properties is LiV<sub>3</sub>O<sub>8</sub>. Such good electrochemical properties include high discharge capacity, high specific energy density, and long cycle life [85]. It was found by several researchers that the synthetic routes affect greatly the capacity of LiV<sub>3</sub>O<sub>8</sub> cathodes [86]. Even though the initial discharge capacity could even reach more than 100% of its theoretical capacity (280 mAhg<sup>-1</sup>) [87] when certain nano structuring techniques or polymeric alloying are applied.

## ✓ **Advanced Cathode Materials**

- **Organic cathodes**

Most of the recent lithium batteries made of inorganic compounds as a cathode are produced from non-renewable resources and because of that they are highly cost [88-91]. Scientists searched for another candidate to improve the power and energy density, safety of Li ion cells and greener Li-ion batteries. Organic electrodes have been proposed as one of the best electrodes for Li-ion batteries due to its inherently flexible, non-toxic, cheap, abundant nature and also their limitation of cycle life, thermal stability, low energy density values and rate capability led to a huge improvement of it [92].

- **Sulfur compounds  $\text{Li}_2\text{S}$**

The sulfur element has the cheapest cathode material for lithium batteries and top theoretical capacity density of 1672 mA/g between all known cathode materials [93].  $\text{Li}_2\text{S}$  cathode material shows a great potential of high-performance rechargeable lithium batteries comparing with other resources of elemental sulfur in nature, like micro-batteries for power sources for electric vehicles and small-size electronic devices emphasizing high charge density [94]. However, because sulfur element has the dissolution of its reaction product polysulfide into the electrolytes and highly insulating nature, it cannot be used directly at low temperature as an electrode material

for lithium batteries, which caused various problems, such as rapid fall of the capacity and short utilization of active material [95].

✓ **Conversion cathodes**

To improve cathode materials, electrochemical conversion reactions have been used as another way to accomplishing the utilization of all the oxidation phases of a transition metal [96-99]. Fluorides metals are one of greatest transition metals that commonly studied in the research because of its stability and its ion considered as a strong and suitable ionic character of the (M-F bond) to transfer charges between two electrodes and produce high operating voltages and reversible capacity [100].

• **Spinel lithium manganese oxyfluorides:**

Spinel lithium manganese oxide  $\text{LiMn}_2\text{O}_4$  has been studied widely as cathode materials due to its features of being non-toxic, inexpensive and environmentally-friendly material. Spinel  $\text{LiMn}_2\text{O}_4$  can deliver 120 mAh/g capacity. However, many different types of research discussed different ways to improve the Spinel lithium manganese oxyfluorides [99-102].

- **Carbon fluorides:**

Carbon fluorides consider as a great theoretically materials for high energy batteries because of its high theoretical potential, low equivalent weight and also most of them produce a very low self-discharge and extraordinary stability which pays high attention for carbon fluorides [103]. Various studies have been studied the lithium batteries contained graphite fluoride as cathode material [104-109]. Therefore, the specific energy densities of covalent graphite fluorides of the (C-F bond) reached 900 W h kg<sup>-1</sup> [110].

- ✓ **Fluorophosphates cathode**

New studies of cathodes materials for LIBs have been conducting about poly-anionic materials containing fluorine as part of their compounds, known as fluorophosphate. LiMPO<sub>4</sub>F and Li<sub>2</sub>MPO<sub>4</sub>F (M=Fe, Ni, Co) were the general formulas of fluorophosphates containing Li and crystallized materials that have been discovered as high-potential cathode materials [111], and thermal stability [112] for rechargeable lithium batteries. Three structured compounds have been widely studies, LiVPO<sub>4</sub>F, NaVPO<sub>4</sub>F, and LiFePO<sub>4</sub>F [113].



- **LiVPO<sub>4</sub>F:**

Lithium vanadium fluorophosphate it is a new class of cathode material that produced high voltage, long cycle life, excellent thermally stability, stable crystalline structure with good quality [105-108]. Carbothermal reduction method used mainly to prepare LiVPO<sub>4</sub>F. The discharge capacity is about 140 mAhg<sup>-1</sup> for the positive electrode with average discharge voltage around 4V [104].

- **NaVPO<sub>4</sub>F:**

Sodium vanadium fluorophosphate characterized as a safer, economical and higher work potential comparing to other materials [114, 115]. Generally, NaVPO<sub>4</sub>F materials synthesis required VPO<sub>4</sub> as the reaction intermediate phase, also it's successfully synthesized by three strategies: first, solid-state which require high temperature, long time-consuming process and complex operation procedure [114,116], second ion exchange or third, hydrothermal approach that considered as a complicated system to collect the results of compounds after the procedures finished [114]. Na<sub>3</sub>V<sub>2</sub>(PO<sub>4</sub>)<sub>2</sub>F<sub>3</sub> classified as the most important among fluorophosphate materials due to the high theoretical capacity 192 mAh/g and its flexibility to be used as a cathode in both Li-ion batteries and Na-ion batteries [117].

- **LiFePO<sub>4</sub>F:**

Another option about olivine-type, tavorite-structured lithium-metal-fluorophosphate as cathode material achieved a good alternative for LIBs [118]. LiFePO<sub>4</sub>F prepared by solid-state routes and produced a reversible capacity approximately 145 mAh.g<sup>-1</sup>, with stable electrochemical cycling (40 cycles at room temperature and 55 °C) [119].

- ✓ **Fluorosulfates cathode LiFeSO<sub>4</sub>F:**

New material of cathode materials reported first by Sebastian et al. was LiMgSO<sub>4</sub>F. LiFeSO<sub>4</sub>F has a theoretical capacity of 148 mA h/g and produced an energy density (543 Wh/kg) as good as LiFePO<sub>4</sub> (581 Wh/kg) [115-123]. LiFeSO<sub>4</sub>F has numerous advantages as cathode material such as it can be prepared from plentiful FeSO<sub>4</sub>·nH<sub>2</sub>O precursor and synthesized at low temperature [124-130].

## **1.2 Research background of LiCoO<sub>2</sub>**

Recently, lithium cobalt oxide LiCoO<sub>2</sub> has attracted strong attention among the research community as a positive cathode material [131,132] and has been commercially used as a cathode material in LIBs for over ten years, with extremely fast market growth [133]. This cathode material has excellent characteristics, such as high discharge potential, low molecular weight, high energy capacity, good

charge/discharge performance, relative ease of synthesis and treatment, and stable and high discharge voltage, which is promising for commercial application of LIBs [7, 26-27,134-140].

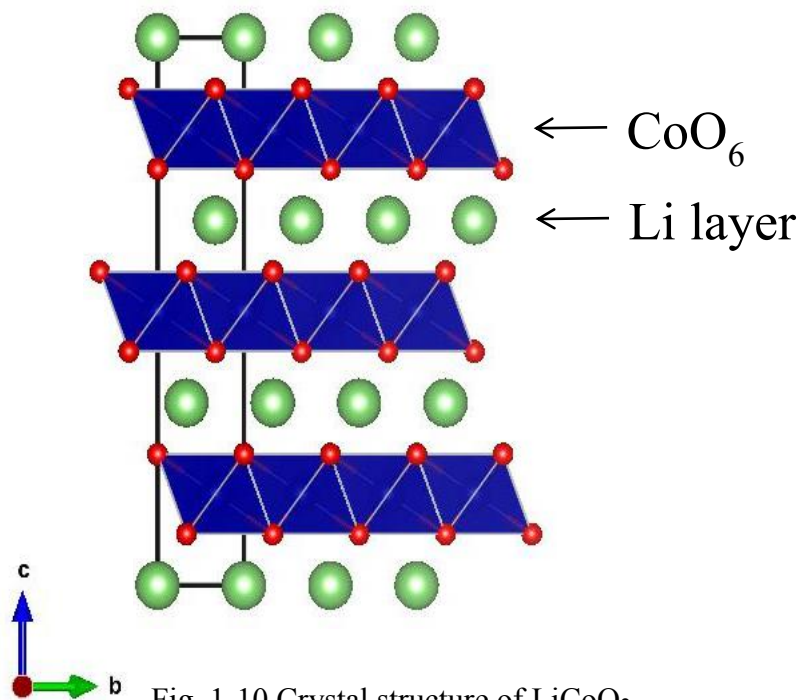


Fig. 1-10 Crystal structure of LiCoO<sub>2</sub>.

LiCoO<sub>2</sub> shows incongruent melting behavior. Melting temperature is within the range of 1100 °C ~ 1300 °C [141]. The crystal structure of LiCoO<sub>2</sub> is a layered structure of CoO<sub>2</sub> layers and Li ion interlayers alternatively stacked along the c-axis in a rhombohedral structure (space group  $R\bar{3}m$  and lattice parameters  $a = 2.816$  and  $c = 14.052$  Å) as shown in Figure 1-10[142,143]. For the layered structure, Li ions can

easily move parallel to the layers in LiCoO<sub>2</sub> [144]. The layered structure is the fundamental reason to expect high ionic conductivity in this type of structure.

Major advantage of LiCoO<sub>2</sub> cathode material is that it has high theoretical capacity of 274 mAhg<sup>-1</sup> compared to other cathode materials that can enhance the performances of next generation all solid state Li-ion batteries (LIBs).

However, in practical discharge capacities of LiCoO<sub>2</sub> are limited to 140 mAhg<sup>-1</sup> [43], only 50% of its theoretical capacity. Many researchers are trying to enhance the practical capacity of LiCoO<sub>2</sub> by applying different synthesis technique. In this study, I have grown high quality, larger diameter single crystals of LiCoO<sub>2</sub> by travelling solvent floating zone (TSFZ) technique to enhance the performance of next generation all solid state Li ion batteries. Due to the highly anisotropic ionic conductivity  $\sigma_a/\sigma_c \approx 500$  in LiCoO<sub>2</sub>, LiCoO<sub>2</sub> single crystals with thicknesses perpendicular to the *c*-axis are strongly required as a cathode to enhance the capacity and charge/discharge rate of LIBs for the development of next generation all solid state LIBs[145]. I have also successfully designed almost all solid state LIBs using LiCoO<sub>2</sub> single crystals for the first time.

## 1.2 Purpose of the research

The purpose of this study is to grow high quality, larger diameter  $\text{LiCoO}_2$  single crystals by travelling solvent floating zone (TSFZ) technique using tilting- mirror-type image furnace for the further development of next generation all solid state LIBs using single crystals cathode. Interface shape is very important to achieve high quality, large single crystals. It is strongly related with the inclusions, cracks, voids that affects the crystal quality. High quality, large diameter  $\text{LiCoO}_2$  single crystals were grown by TSFZ technique by studying the interface shape.

Although some research groups have already reported the growth of  $\text{LiCoO}_2$  single crystals by floating zone (FZ) technique [146,147]. However, the diameter of the grown crystal was limited. The  $\text{LiCoO}_2$  single crystals larger than a half inch diameter are required for the commercial application of cathodes to enhance the performance of LIBs. To the best of our knowledge, there is no report on the TSFZ growth of  $\text{LiCoO}_2$  single crystals of diameter more than half inch diameter that is the main focus of this research. In this study, Larger  $\text{LiCoO}_2$  single crystals with a diameter of 13 mm (more than  $\frac{1}{2}$  inch) was grown successfully with a metallic luster. In addition, charge-discharge characteristics of LIBs using  $\text{LiCoO}_2$  single crystals were investigated.

### 1.3 Motivation of the research

Although  $\text{LiCoO}_2$  polycrystalline material is still commercially used in LIBs as a positive cathode material. However, the capacity of LIBs using  $\text{LiCoO}_2$  polycrystalline material is lower. Actually, grain boundaries (Fig.1-6) in polycrystalline

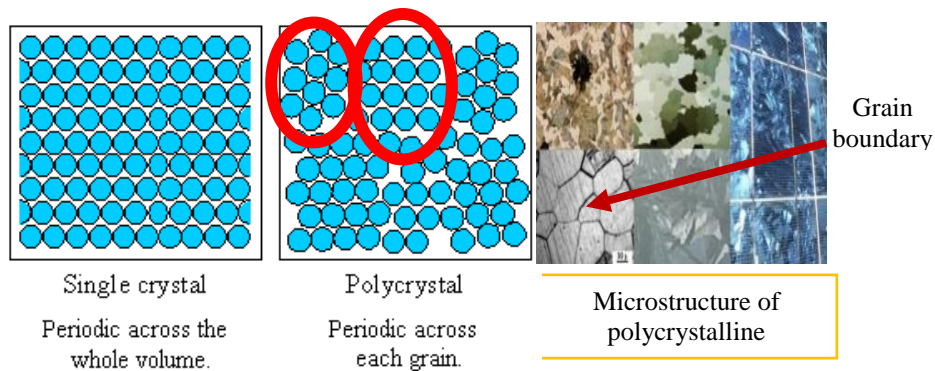


Fig. 1-6 Atomic arrangement in single and polycrystalline materials [148].

materials act as impediments affecting materials intrinsic properties. In addition, grain boundaries are sources of point defects and cause deformation of materials. In Li-ion battery, the movement of Li ion will strongly be affected by defects which is created from the grain boundary of polycrystalline material. As a result, lower capacity is obtained in LIBs using  $\text{LiCoO}_2$  polycrystalline cathode materials.

In order to enhance the capacity for high performance LIBs,  $\text{LiCoO}_2$  single crystals is strongly required due to some excellent characteristics that that making single crystal

precious in industrial and technological application. Single crystals without any defects give true intrinsic materials properties and has no grain boundaries (Fig. 1-6). It has a regular geometric structure and this structure has effect on materials properties. It is unbroken to the edges of the sample.

Actually, high anisotropic ionic conductivity in  $\text{LiCoO}_2$  motivates my research on the growth of high quality  $\text{LiCoO}_2$  single crystals. A single crystalline substrate of  $\text{LiCoO}_2$  perpendicular to the c-axis could be expected to considerably enhance the capacity of Li-ion batteries for the next generation high performance LIBs [149].

#### 1.4 Plan of the thesis

The plan of the present dissertation is as follows:

- In the first chapter (**Chapter 1**), I have tried to give a general introduction of the present work, which delivers the motivation and objective of this study.
- I will discuss the effects of mirror tilting on the shape of the molten zone and interfaces during the TSFZ growth of  $\text{LiCoO}_2$  single crystals in **Chapter 2**. The relation between the mirror tilting angle and convexity of the feed-melt and crystal-melt will also be explained in this chapter. Then,

I will investigate the effects of mirror tilting angles on the growth of large LiCoO<sub>2</sub> single crystals.

- **Chapter 3** is about larger diameter single crystals growth of LiCoO<sub>2</sub> by TSFZ method. In this chapter, I will explain the influences of some important parameters such as of slightly excess Li content (2 mol% to 5 mol%) in the stoichiometric feed, the solvent amount and the filament shape of the heating lamps on the TSFZ growth of larger-diameter LiCoO<sub>2</sub> single crystals of more than half inch(13 mm). In addition, I will establish an interesting relation between the solvent amount and square of the crystals diameter.
- In **Chapter 4**, I will discuss on the design of the next generation all-solid-state Li ion batteries (LIBs) using LiCoO<sub>2</sub> single crystals cathode. I will show the charge-discharge characteristics of LIBs using LiCoO<sub>2</sub> single crystals cathode with liquid, gel and solid electrolytes.
- **Chapter 5** is about Single crystal growth of Nb doped LiCoO<sub>2</sub> by TSFZ method using tilting mirror furnace. In the beginning of this chapter, I will discuss the reason for Nb doping in the LiCoO<sub>2</sub> and then explain the optimized conditions for the growth of Nb doped LiCoO<sub>2</sub> single crystals.
- In **Chapter 6**, I will explain social significance and business feasibility of the current research.



- Finally, in **Chapter 7**, I will summarize all the results of this research. In addition, I will write a short discussion on the impact of the current research.

## References

- [1] F. Zhang, Chem. Soc. Rev. **42** (2013) 3127.
- [2] H. Yoo, E. Markevich, G. Salitra, D. Sharonand, D. Aurbach, Mater. Today, **17** (2014) 110.
- [3] C. Liu, G. N. Zachary, G. Cao Materials Today, **19** (2016)1369.
- [4] IEA, Transport Energy and CO<sub>2</sub>: Moving toward Sustainability, International Energy Agency (IEA), Paris, France, 2009.
- [5] W. Chena, J. Eomb, E. L. Clarke, S. H. Kim, L. Pralit, P. L. Patel ,S. Yub, G. P. Kyle, Energy Policy, **82** (2015) 233.
- [6] D.A Notter, M. Gauch, M, R. Widmer, P. Wager, A. Stamp, R. Zah, , H.J. Althaus, Environ. Sci. Technol.**44** (2010)6550.
- [7] Y. Nishi, Journal of Power Sources, **100** (2001) 101.
- [8] M. Hu,X. Pang, Zhou, Z, Journal of Power Sources, **237** (2013) 229.
- [9] K. Kalyanasundaram, M. Gratzel, J. Mater. Chem. **22** (2012) 24190.
- [10] G.M. Shafiullah, A. Than, M.B. Ali, P. Wolfs, Renew. Sustain. Energy Rev. **20** (2013) 306.
- [11] R. Singh, A.D. Setiawan, Renew. Sustain. Energy Rev. **22** (2013) 332.
- [12] P. Würfel, Physics of Solar Cells: From Basic Principles to Advanced Concepts, Wiley-VCH, 2009.

- [13] J. Lu, Automotive Li-Ion Batteries: Current Status and Future Perspectives, Chemical Sciences and Engineering Division, Argonne National Laboratory, Argonne, IL 60439, USA.
- [14] J.R. Miller, P. Simon, *Science*, **321** (2008) 651.
- [15] P. Simon, Y. Gogotsi, B. Dunn, *Science*, **343** (2014) 1210.
- [16] P. Simon, Y. Gogotsi, *Nat. Mater.* **7** (2008) 845.
- [17] M. Winter, R.J. Brodd, *Chem. Rev.* **104** (2004) 4245.
- [18] M. Armand, J.M. Tarascon, *Nature*, **451** (2008) 652.
- [19] Z. Yang, J. Zhang, C.W. Michael, K. Meyer, X. Lu, D. Choi, J. P. Lemmon, J. Liu, *Chem. Rev.* **111** (2011) 3577.
- [20] P. Ruetschi, *J. Power Sources*, **2** (1977) 3.
- [21] D. Larcher, J.M. Tarascon, *Nat. Chem.* **7** (2015) 19.
- [22] D. Aurbach, G. S. Suresh, E. Levi, A. Mitelman, O. Mizrahi, O. Chusid, M. Brunelli, *Adv. Mater.* **19** (2007) 4260.
- [23] G.L. Soloveichik, *Annu. Rev. Chem. Biomol.* **2** (2011) 503.
- [24] J.M. Tarascon, M. Armand, *Nature*, **414** (2001) 359.
- [25] K. Amine, J. Liu, S. Kang, I. Belharouak, Y. Hyung, D. Vissers, G. Henriksen, *J. Power Sources*, **129** (2004) 14.
- [26] J.B. Goodenough, Y. Kim, *Chem. Mater.* **22** (2010) 587.

- [27] J.B. Bates, N.J. Dudney, B. Neudecker, A. Ueda, C.D. Evans, *Solid State Ionics*, **135** (2000) 33.
- [28] P. Birke, F. Salam, S. Doring, W. Weppner, *Solid State Ionics*, **118** (1999) 149.
- [29] P.H.L. Notten, F. Roozeboom, R. A. H Niessen, L. Baggetto, *Adv. Mater.* **19**(2007)4564.
- [30] J.W. Fergus, *J. Power Sources*, **195** (2010) 4554.
- [31] Ambesh Dixit, Department of Physics & Center for Solar Energy, Indian Institute of Technology Jodhpur, Jodhpur342037, India, Cathode Materials for Lithium Ion Batteries (LIBs): A Review on Materials related aspects towards High Energy Density LIBs.
- [32] A. Yoshino, *Angew. Chem. Int. Ed.* **51** (2012) 5798.
- [33] S.R. Bottone, Nabu Press, 2010.
- [34] Bensalah and Dawood, *J Material SciEng*, **5** (2016) 4
- [35] M. Noel, V. Suryanarayanan, *J. Power Sources*, **111** (2002) 193.
- [36] A.D. Roberts, X. Li, H. Zhang, *Chem. Soc. Rev.* **43** (2014) 4341.
- [37] E. Antolini, *Solid State Ionics*, **170** (2004) 159.
- [38] J. Wang, X. Sun, *Energy Environ. Sci.* **8** (2015) 1110.
- [39] L.-X. Yuan, Z.-H. Wang, W.-X. Zhang, X.-L. Hu, J.-T. Chen, Y.-H. Huang, J. B. Goodenough, *Energy Environ. Sci.* **4** (2011) 269.
- [40] M.S. Whittingham, *Chem. Rev.* **104** (2004) 4271.

- [41] R. Koksang, Solid State Ionics, **84** (1996) 1.
- [42] A. Konarov, S-T. Myung, Y-K. Sun, ACS Energy Lett. **2** (2017) 703.
- [43] C.M. Julien, A. Mauger, K. Zaghbi, H. Groult, Inorganics, **2** (2014)132.
- [44] C. Daniel, D. Mohanty, J. Li, D. L. Wood, Cathode materials review, AIP Conference Proceedings, **26** (2014) 1597.
- [45] D.Y. Zhang, J. Yi, Q. Wei, K. Liu, Z.Z. Fan, Advanced Materials Research, **158** (2010) 256.
- [46] M.M. Thackeray; W.I.F. David; P.G. Bruce; J.B. Goodenough, Materials Research Bulletin, **18** (1983) 461.
- [47] D.K. Kim, P. Muralidharan , H.W. Lee, R. Ruffo, Y. Yang Y, Nano Letters, **8** (2008) 3948.
- [48] Eriksson TOM (2001) LiMn<sub>2</sub>O<sub>4</sub> as a Li-Ion Battery Cathode. Bulk to Electrolyte Interface.
- [49] D. Aurbach; M.D. Levi; K. Gamulski; B. Markovsky; G. Salitra; E. Levi; U. Heider; L. Heider; R. Oesten, Journal of Power Sources, **81**(1999) 472.
- [50] Y.J. Shin, A. Manthiram, J. o. t. E. S. Journal of the Electrochemical Society, **151** (2004) A204.
- [51] J. Marzeca, K. Świerczeka, J. Przewoźnikb , J. Molenda, D.R. Simon , Solid State Ionics, **146** (2002) 225.
- [52] D. Guyomard, J.M. Tarascon, Solid State Ionics, **69** (1994) 222.

- [53] E.I. Santiago, S.T. Amancio-Filho, P.R. Bueno, L.O.S. Bulhões, *Journal of Power Sources*, **98** (2001) 447.
- [54] T.F. Yi, C.L. Hao, C.B. Yue, R.S. Zhu, J. Shu, *Synthetic Metals*, **159** (2009) 1255.
- [55] T.Eriksson, Bifacial carbon nanofoam-fibrous PEDOT composite Supercapacitor in the 3-electrode configuration for electrical energy storage. *Bulk to Electrolyte Interface* (2001).
- [56] T. Li, W. Qiu, H. Zhao, J. Liu, *Rare Metals*, **26** (2007) 280.
- [57] Z. Pegeng Z, F.A.N. Huiqing, F.U. Yunfei, L.I. Zhuo, D. Yongli, *Rare Metals*, **25** (2006) 100.
- [58] X. Zhang, H. Zheng, V. Battaglia, R.L. Axelbaum, *Journal of Power Sources*, **196** (2011) 640.
- [59] J. Lee, J. Hong, D. Jang, Y. Sun, S.M. Oh, *Journal of Power Sources*, **89** (2000) 7.
- [60] D. Zhang, B.N. Popov, R.E. White, *Journal of Power Sources*, **76** (1998) 81.
- [61] G.X. Wang, D.H. Bradhurst, H.K. Liu, S.X. Dou, *Solid State Ionics*, **120** (1999) 95.
- [62] I.J. Davidson, J.J. Murray, *Journal of Power Sources*, **54** (1995) 205.
- [63] S.-Y. Chung, J. T. Bloking, Y.-M. Chiang, *Nat Mater*, **1** (2002) 123.

- [64] G.X. Wang, S. Bewlay, S. A. Needham, H. K. Liu, R. S. Liu, V. A. Drozd, J.-F. Lee, J. M. Chen. *Journal of the Electrochemical Society*, **153** (2006) A25.
- [65] H.J. Guo, K.X. Xiang, X. Cao, X. Li, Z. Wang, *Transactions of Nonferrous Metals Society of China*, **19** (2009) 166.
- [66] R. Dominko, M. Bele, A. Kokalj, M. Gaberscek, J. Jamnik, *Journal of Power Sources*, **174** (2007) 457.
- [67] C. Deng, S. Zhang, B.L. Fu, S.Y. Yang, L. Ma, *Materials Chemistry and Physics*, **120** (2010) 14.
- [68] R.J. Gummow, N.Sharma, V.K. Peterson, Y. He, *Journal of Power Sources*, **197** (2012) 231.
- [69] Z.L. Gong, Y.X. Li, Y. Yang, *Journal of Power Sources*, **174** (2007) 524.
- [70] W.U. Shun-qing, Z.H.U. Zi-zhong, Y. Yong, H.O.U. Zhu-feng, *Transactions of Nonferrous Metals Society of China*, **19** (2009)182.
- [71] S.Q. Wu, J.H. Zhang, Z.Z. Zhu, Y. Yang, *Current Applied Physics*, **7** (2007) 611.
- [72] A. Boucher, M. Ducey, N. McNeff, *Synthesis, Characterization and Electrochemical Performance of  $\text{Li}_2\text{FexMn}_{1-x}\text{SiO}_4/\text{C}$  as Cathode Material for Thin-Film Lithium-Ion Batteries*(2001).
- [73] M. Dahbi, S. Urbonaite, T. Gustafsson, *Journal of Power Sources*, **205** (2001) 456.

- [74] R. Dominko, M. Bele, M. Gaberšček, A. Meden, M. Remškar, *Electrochemistry Communications*, **8** (2006) 217.
- [75] H. Hao, J. Wang, J. Liu, T. Huang, A. Yu, *Journal of Power Sources*, **210** (2012) 397.
- [76] N. Kalaiselvi, A. Manthiram, *Journal of Power Sources*, **195** (2010) 2894.
- [77] K.C. Kam, T. Gustafsson, J.O. Thomas, *Solid State Ionics*, **192** (2011) 356.
- [78] P. Larson, R. Ahuja, A. Nyten, J. Thomas, *Electrochemistry Communications*, **8** (2006) 797.
- [79] A. Liivat, J.O. Thomas, *Computational Materials Science*, **50** (2010) 191.
- [80] A. Nyten, A. Abouimrane, M. Armand, T. Gustafsson, J.O. Thomas, *Electrochemistry Communications*, **7** (2005) 156.
- [81] S. Zhang, C. Deng, B.L. Fu, S.Y. Yang, L. Ma, *Electrochimica Acta*, **55** (2010) 8482.
- [82] L. Liu, B. Zhang, X. Huang, *Materials International*, **21** (2011) 211.
- [83] X. Ren, C. Shi, P. Zhang, Y. Jiang, J. Liu, *Materials Science and Engineering*, **177** (2012) 929.
- [84] A.M. Kannan, A. Manthiram, *Journal of Power Sources*, **159** (2012) 1405.
- [85] X. Xiong, Z. Wang, X. Li, H. Guo, *Materials Letters*, **76** (2012) 8.
- [86] Q. Liu, H. Liu, X. Zhou, C. Cong, K. Zhang, *Solid State Ionics*, **176** (2005) 1549.



- [87] D.G. Jin, K.Y. Yang, H. Lee, W.Y. Yoon, *Electrochemistry Communications*, **12** (2010) 1694.
- [88] Y. Yang, G. Zheng, S. Misra, J. Nelson, M.F. Toney, *J. Am. Chem. Soc.* **134** (2012) 15387.
- [89] T. Li, L. Li, Y. Cao, A. Xing, H. Yang, *The Journal of Physical Chemistry*, **3** (2009) 190.
- [90] F. Gschwind, G. Rodriguez-Garcia, D.J. S. Sandbeck, A. Gross, M. Weil, *Journal of Fluorine Chemistry*, **182** (2016) 76.
- [91] G. Amatucci, N. Pereira, *Journal of Fluorine Chemistry*, **128** (2007) 243.
- [92] S. Goriparti, M.N.K. Harish, S. Sampath, *Chemical Communications*, **49** (2013) 7234.
- [93] J. Wang, J. Yang, C. Wan, K. Du, J. Xie, *Advanced Functional Materials*, **13** (2003) 487.
- [94] K. Bazzi, *Nanostructured Lithium Iron Phosphate As Cathode Material For Lithium Ion-Batteries*. Wayne State University, United States(2014).
- [95] H. Arai, S. Okada, Y. Sakurai, J. Yamaki, *Journal of Power Sources*, **68** (1997) 716.
- [96] P. Poizot, S. Laruelle, S. Grugeon, L. Dupont, J. Tarascon, **407** (2000) 496.
- [97] K. Kubo, M. Fujiwara, S. Yamada, S. Arai, M. Kanda, *Journal of Power Sources*, **68** (1997)553.

- [98] W.C. Choi Understanding the Capacity Fade Mechanisms of Spinel Manganese Oxide Cathodes and Improving their Performance in Lithium Ion Batteries (2007).
- [99] W. Choi, A. Manthiram, *Solid State Ionics*, **178** (2007) 1541.
- [100] F. Gschwind, G.Rodriguez-Garcia, D. J. S. Sandbeck, A.Gross, M.Weil, *Journal of Fluorine Chemistry*, **182** (2016) 76.
- [101] X. Wu, X. Zong, Q. Yang, Z. Jin, H. Wu, *Journal of Fluorine Chemistry*, **107** (2001) 39.
- [102] K. Matsumoto, T. Fukutsuka, T. Okumura, Y. Uchimoto, K. Amezawa, *Journal of Power Sources*, **189** (2009) 599.
- [103] G.G. Amatucci, N. Pereira, *Journal of Fluorine Chemistry*, **128** (2007) 243.
- [104] R.K.B. Gover, P. Burns, A. Bryan, M.Y. Saidi, J.L. Swoyer, *Solid State Ionics*, **177** (2006) 2635.
- [105] X. Liu , H.K. Lee, A simulation study of the spent nuclear fuel cask condition evaluation using high energy X-ray computed tomography. *NDT & E International* **80** (2016): 58.
- [106] R. Sivakami, P. Thiyagarajan, *Optical Materials*, **44** (2015) 1.
- [107] C. Cardenas, M. Ortiz, A. Balbin, J.L. Villaveces, M.E. Patarroyo, *Biochemical and Biophysical Research Communications*, **330** (2005) 1162.

- [108] C.M. Julien, A. Mauger, H.Groult, Chapter 4 - Fluorosulfates and Fluorophosphates As New Cathode Materials for Lithium Ion Battery. Advanced Fluoride-Based Materials for Energy Conversion. Elsevier (2015).
- [109] J.C. Zheng, B. Zhang, Z. H. Yang Journal of Power Sources, **202** (2012) 380.
- [110] R. Yazami, Solid State Ionics, **30** (1988)1756.
- [111] C.M. Julien, A. Mauger, Review of 5-V electrodes for Li-ion batteries: Status and trends. Ionics, **19** (2013) 951.
- [112] H. Liu, C. Cheng, K. Zhang, Materials Chemistry and Physics, **101** (2007) 276.
- [113] R.A. Meyers An influence of carbon matrix origin on electrochemical behaviour of carbon-tin anode nanocomposites. Energy (2012).
- [114] J. Zhao, J. He, X. Ding, J. Zhou, Y. Ma, Journal of Power Sources **195** (2010) 6854.
- [115] R. Gover, A. Bryan, P. Burns, J. Barker, Solid State Ionics, **177** (2006) 1495.
- [116] W. Song, S. Liu Solid State Sciences, **15** (2013) 1.
- [117] M. Bianchini, N. Brisset, F. Fauth, F. Weill, E. Elkaim, Chemistry of Materials, **26** (2014) 4238.
- [118] M. Prabu, M. V. Reddy, S. Selvasekarapandian, G.V.S. Rao, B.V.R. Chowdari Electrochimica Acta, **85** (2012) 572.
- [119] T.N. Ramesh, K.T. Lee, B.L. Ellis, L.F. Nazar, Electrochemical and Solid-State Letters, **13** (2010) A43.

- [120] N. Metals, *Trans Nonferrous Met Soc China*, **17** (2007) 291.
- [121] X. Zhang, W.J. Jiang, A. Mauger, F. Gendron, C.M. Julien, *Journal of Power Sources*, **195** (2010) 1292.
- [122] G. Fey, P. Muralidharan, C. Lu, Y. Cho, *Solid State Ionics*, **176** (2005) 2759.
- [123] Y.K. Sun, D.H. Kim, H.G. Jung, S.T. Myung, K. Amine, *Electrochimica Acta*, **55** (2010) 8621.
- [124] Shin, Manthiram A (2011), *Electrochemistry Communications*, 13: 1213.
- [125] X. Sun, X. Hu, Y. Shi, S. Li, Y. Zhou, *Solid State Ionics*, **180** (2009) 377.
- [126] K. Yang, J. Su, L. Zhang, Y. Long, X. Lv, *Particuology*, **10** (2012) 765.
- [127] T. Yi, A. Zhou, Y. Zhu, R. Zhu, X. Hu, *Rare Metals*, **27** (2008) 496.
- [128] F. Amaral, N. Bocchi, R. Brocenschi, *Journal of Power*, **195** (2010) 3293.
- [129] G.M. Song, Y.J. Wang, Y. Zhou, *Journal of Power Sources*, **128** (2004) 270.
- [130] D. Liu, J. Trottier, P. Charest, J. Fréchette, A. Guerfi, *Journal of Power Sources*, **204** (2012) 127.
- [131] J. Xie, N. Imanishi, T. Zhang, A. Hirano, Y. Takeda, O. Yamamoto, *J. Power Sources*, **189** (2009) 365.
- [132] M. Murayama, R. Kanno, M. Irie, S. Ito, T. Hata, N. Sonoyama, Y. Kawamoto, *J. Solid State Chem.* **168** (2002) 140.
- [133] M. Menetrier, I. Saadoune, S. Levasseur, C. Delmas, *J. Mater. Chem.*, **9** (1999) 1135.

- [134] M. Wakihara, Recent developments in lithium ion batteries. *Materials Science and Engineering: R: Reports*, **33** (2001)109.
- [135] J.M. Tarascon, M. Armand, *Nature*, **414** (2001) 359.
- [136] K. Amine, J. Liu, S. Kang, I. Belharouak, Y. Hyung, D. Vissers, G. Henriksen, J. Power Sources, **129** (2004) 14.
- [137] P. Birke, F. Salam, S. D€oring, W. Weppner, *Solid State Ionics*, **118** (1999) 149.
- [138] P.H.L Notten, F. Roozeboom, R. A. H. Niessen, L. Baggetto, *Adv. Mater.* **19** (2007) 4564.
- [139] J.W. Fergus, *J. Power Sources*, **195** (2010) 4554.
- [140] M. Wakihara, *Materials Science and Engineering: R: Reports*, **33** (2001)109.
- [141] S. Nakamura, A. Maljuk, Y. Maruyama, M. Nagao, S. Watauchi, T. Hayashi, Y. Anzai, Y. Farukawa, C. D. Ling, G. Deng, M. Avdeev, B. Buchner, I. Tanaka, *Cryst. Growth Des.* **19** ( 2019) 415.
- [142] Y. Mizuno, N. Zettsu, K. Yubuta, T. Sakaguchi, T. Saito, H. Wagata, S. Oishi, K. Teshim, *Cryst. Growth Des.* **14** (2014) 1882.
- [143] K. Miyoshi, K. Manami, J. Takeuchi, R. Sasai, S. Nishigori, *Phys. Procedia*, **75** (2015) 278.

- [144] K. Teshima, S. Lee, Y. Mizuno, H. Inagaki, M. Hozumi, K. Kohama, K. Yubuta, T. Shishido, S. Oishi, *Cryst. Growth Des.* **10** (2010) 4471.
- [145] Y. Takahashi, Y. Gotoh, J. Akimoto, S. Mizuta, K. Tokiwa, T. Watanabe, *J. Solid State Chemistry*, **164** (2002)1.
- [146] L. Pinsard-Gaudart, V.-C. Ciomaga, O. Dragos, R. Guillot, N. Dragoe, J. *Cryst. Growth*, **334** (2011)165.
- [147] S.Uthayakumar, M. S. Pandiyan, D. G. Porter, M. J. Gutmann, R. Fan, J. P. Goff *J. Cryst. Growth*, **401** (2014)169.
- [148] DoITPoMS, TLP Library, Atomic Scale Structure of Materials, Introduction, University of Cambridge, 2004.
- [149] R. Parvin, Y. Maruyama, M. Nagao, S. Watauchi, I. Tanaka, *Cryst. Growth Des.* **20** (2020) 3413.

## CHAPTER 2

### *Effects of mirror tilting on the shape of the molten zone and interfaces during the TSFZ growth of $\text{LiCoO}_2$ single crystals*

#### 2.1 Introduction

##### 2.1.1 Concept of solid-liquid interface in the molten zone

In the single crystals growth by floating zone (FZ) technique, molten zone was sustained by the balanced between the surface tension and gravity of the melt during the growth. The molten zone contains two types of solid-liquid interfaces during the growth that are called feed-melt interface and crystal melt interface. During FZ growth, heat coming from the heating lamp is absorbed in the surface of the molten zone. For yttrium orthoferrite ( $\text{YFeO}_3$ ), yttrium iron garnet ( $\text{Y}_3\text{Fe}_5\text{O}_{12}$ ) materials that easily absorb heating radiation show convex interface shape towards the melt [1]. In the case of neodymium gallium garnet ( $\text{Nd}_3\text{Ga}_5\text{O}_{12}$ ), forsterite ( $\text{Mg}_2\text{SiO}_4$ ), Calcium aluminate ( $\text{Ca}_{12}\text{Al}_{14}\text{O}_{33}$ ) materials not easy to absorb heating radiation, the solid-liquid interface shape is concave towards the melt [1]. Solid liquid interface might be cellular depending on the materials to be grown and growth speed [2]. However slightly convex interface shape is significant for the stable single crystals growth by FZ technique.

## **2.1.2 Importance of investigation of interface shape**

### **2.1.3 Previous reports about the effects of the interface shape on the crystal growth**

The interface shape is very important parameter to grow large and high quality single crystals by FZ method. It affects the stability of the molten zone, quality and size of the grown crystal, distribution of solute. An extremely convex interface creates a contact problem between the feed rod and grown crystals during the growth. This contact problem creates instability in the molten zone. An extremely convex interface is unfavorable for the growth of crystals with a low defect density because of the large number of defects caused by thermal stress [3]. Kitamura et al. found that line defects propagate to the edge of a crystal if the solid–liquid interface is more convex toward the melt [1]. In the case of concave crystal-melt interface, dislocations are easily concentrated into the central part of crystals, in which crack often occur [1, 4]. A slightly convex interface is advantageous for the growth of high quality and large single crystals. Kinoshita and Sugii showed that the numbers of low-angle grain boundaries are markedly reduced when the solid–liquid interface during crystal growth is almost flat [5]. Abdur Razzaque Sarker *et al.* reported that low-angle grain boundaries that are associated with dislocations and grain boundaries decreased at slightly convex interface [6]. A slightly convex interface toward the melt is better for improving the quality of the grown crystals [7]. For the FZ growth of rutile, large single crystals up to 19 mm diameter were obtained at slightly convex interface shape of the molten zone during growth [6,8,9]. So control of the interface is very important for the growth of high quality larger diameter single crystals.



#### 2.1.4 Control of the solid-liquid interface shape

Interface shape depends on the various parameters such as the feed diameter, rotation rates and the temperature gradient [1]. Mukter *et al.* studied the effects of lamp power and mirror position on the feed–melt and crystal–melt interfaces during the FZ growth of a silicon crystal. They found that the convexities of the S–L interface shapes at both feed and crystal sides decreased with increasing lamp power. They also reported that interface shapes were independent of the mirror position [10]. In the IR-FZ growth of silicon crystals, the convexity of both the feed and the crystal sides of the molten zone was controlled by the crystal diameter [11]. In addition, during the FZ growth of rutile crystals using tilting-mirror-type infrared heating image furnace, the convexities of the interface was controlled by the mirror tilting angle [9].

In my research, I tried to control the convex interface by the mirror tilting angle during the TSFZ growth of  $\text{LiCoO}_2$  single crystals using the tilting- mirror-type image furnace. In our experiment, other growth parameters such as rotation rates, crystal growth rate, solvent amount were remained constant, only the effects of the mirror tilting on the interface shape was investigated.

### 2.1.5 Concept of mirror tilting

In conventional FZ method, the layout of the mirror and heating lamps is in the same horizontal plane [12]. The schematic diagram of conventional mirror-type image furnace is shown in Figure 2-1. This horizontal mirror symmetrical layout is responsible for the horizontal mirror symmetrical convex interface shape of both the feed-melt and crystal-melt sides. This symmetrical layout is not always necessary to form the molten zone.

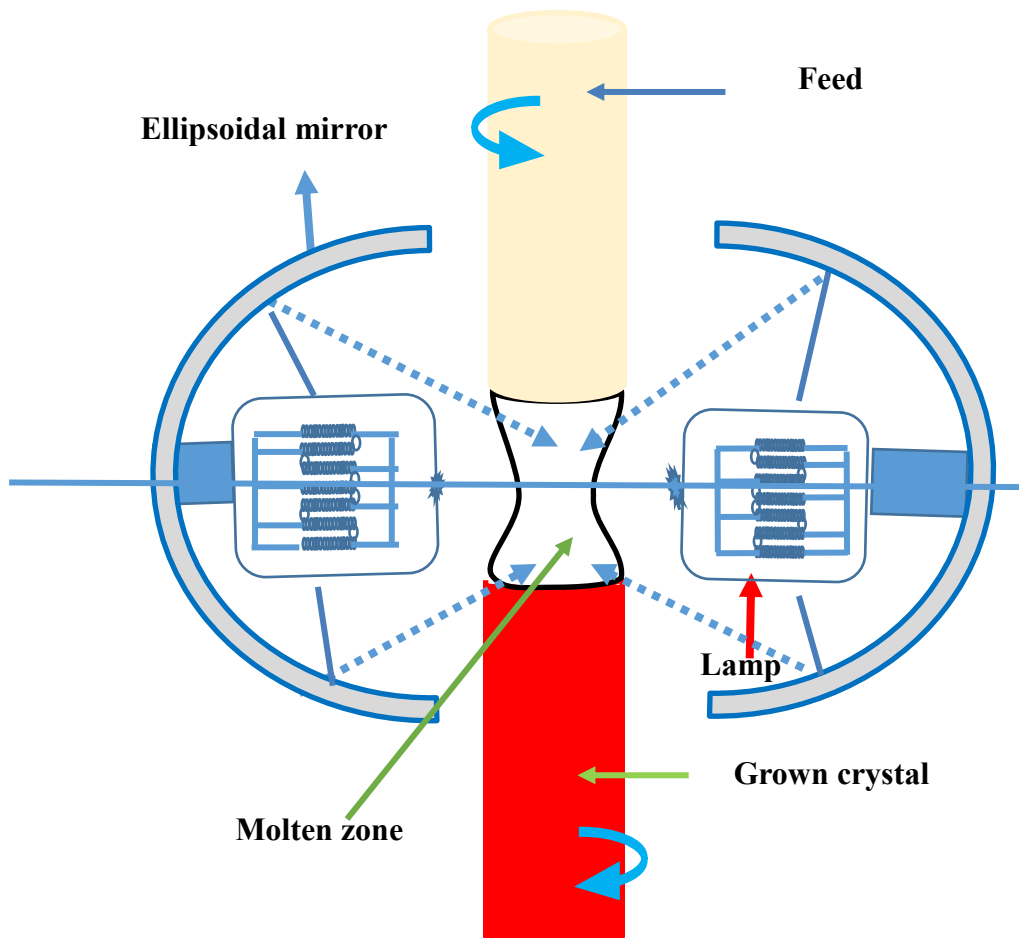


Fig. 2-1 Schematic illustration of a conventional mirror-type furnace.

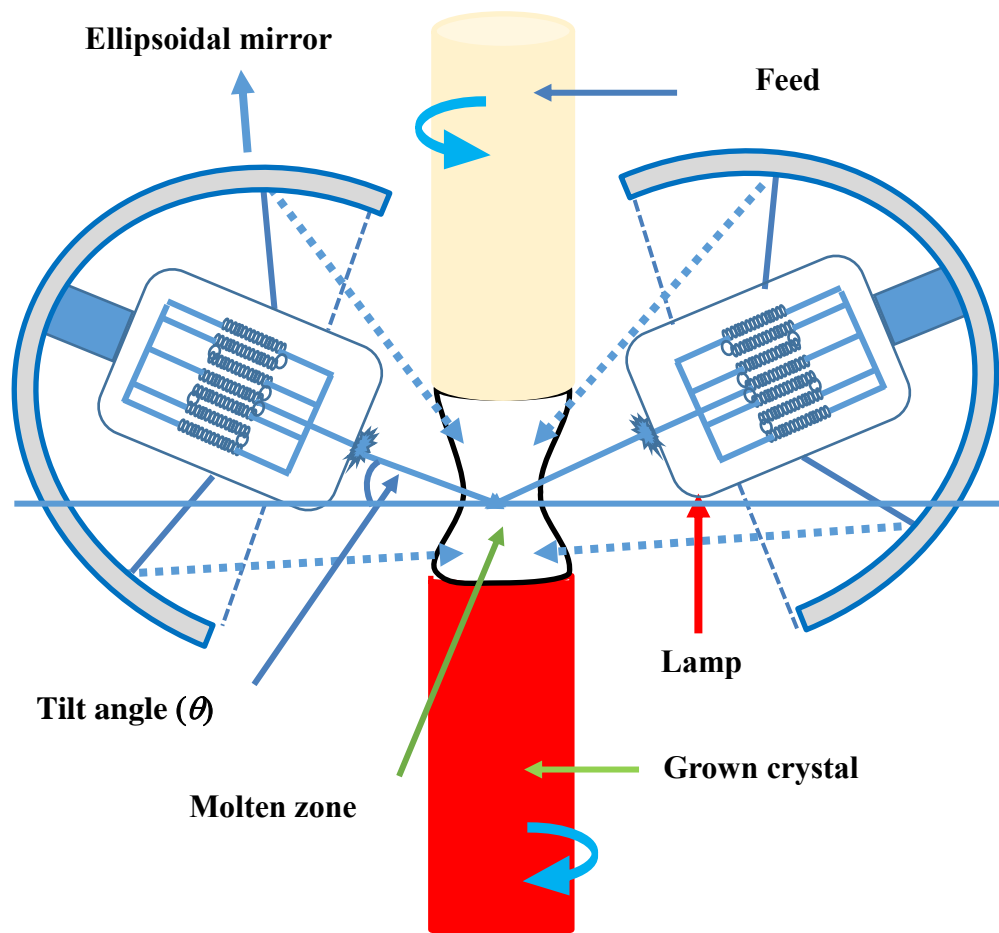


Fig. 2-2 Schematic illustration of a tilting- mirror-type image furnace.

In the tilting-mirror-type image furnace, the layout of the mirror and heating lamps is the asymmetrical [12]. This furnace has four mirrors with halogen lamps of 300 W. The tilting angle ( $\theta$ ) can be changed up to  $15^\circ$  by a motor drive control. As the mirrors are tilted as shown in Fig. 2-2, the fraction of heating light, which incident downward the molten zone, is expected to increase. Interface shape is also expected to change with mirror tilting. It is shown that mirror tilting has a significant effects on the shapes of the solid-liquid interfaces. Convexity of the interfaces ( $h/r$ ) is affected with  $\theta$  which has a significant impact for the growth of high quality single

crystals. Therefore, clarification of the mirror-tilting effects on the TSFZ growth of  $\text{LiCoO}_2$  single crystals could lead to growth of high quality large single crystals.

### **2.1.6 Advantages of travelling solvent floating zone (TSFZ) method**

Single crystals have been grown by a variety of techniques from vapor, gaseous phase, melt and solution; however, growth of crystals via solidification from the melt has been the most widely used technique and is generally preferable when possible, e.g. for the crystal growth of the elemental materials and congruently or near congruently melting compounds [13].

Among the other crystal growth technique, floating zone (FZ) or travelling solvent floating zone (TSFZ) method is a most promising technique because it is a crucible free method that reduces the risk of impurities from the crucible material. TSFZ growth technique can be applied to grow single crystals of many intermetallic materials, oxides, and other systems of interests that can be difficult to grow by other means due to high temperature phase instabilities (e.g. phase transformation, decomposition near the melting temperature or incongruent melting). It has now become the most popular method for the growth of materials with high or very high melting points for which no crucible material is available. The main benefit of the technique is that materials can be grown at temperatures below their melting points, where vapor pressures and decomposition rates are lower. Crystals grown using TSFZ technique are potentially larger and of higher purity than crystals prepared, for example, by flux growth, due to the effects of directional solidification and solvent zone passing, respectively. TSFZ growth at a lower temperature also

decreases the amount of possible contamination from the crucible, potentially reduces the non-stoichiometric defect concentration, and gives crystals in which dislocation densities can be orders of magnitude lower than those prepared by other methods.

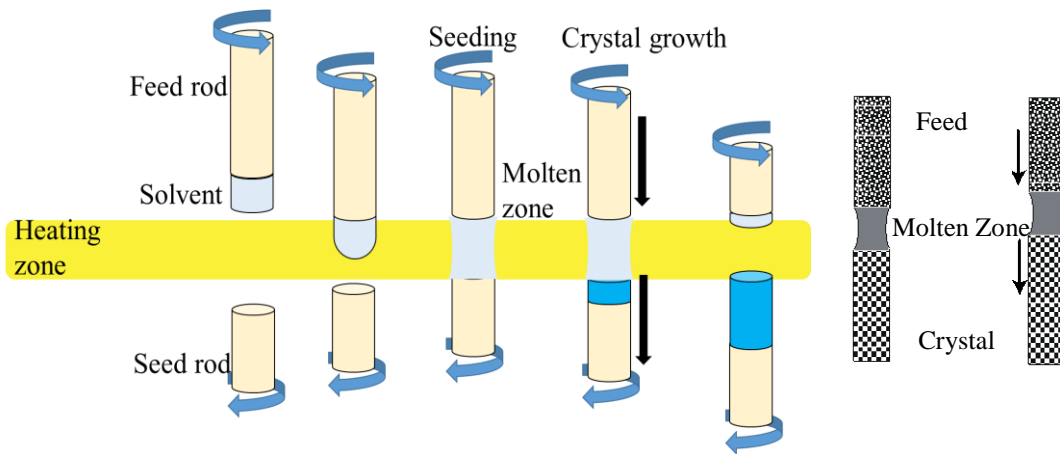


Fig. 2-4 Schematic diagram illustrating the TSFZ growth technique

In the TSFZ technique, the common methodology is to melt a small ‘solvent disk’ of different composition between vertical cylindrical feed and seed rods, which have the same composition as the required crystal. Since the molten solvent is supported against gravity essentially by the surface tension of the liquid, the molten zone stability plays an important role in this technique. The molten zone then retains its composition as zoning progresses since the solidification of crystal from the molten zone is balanced by introduction of feed rod material into the zone. The schematic diagram for the TSFZ growth technique is shown in Figure 2-4. Using the TSFZ technique, a single crystal can be generated by spontaneous nucleation or by using a single-crystalline seed crystal as the initial part of the rod, similar to the floating zone (FZ) technique [14].

## **2.2 Experimental procedure**

### **2.2.1 Feed preparation**

Powders of  $\text{Li}_2\text{CO}_3$  (Rare Metallic Co., Ltd. 99.9% purity) and  $\text{Co}_3\text{O}_4$  (Rare Metallic Co., Ltd. 99.9% purity) were used as starting raw materials. The powders were mixed together in a stoichiometric ratio and calcined at  $750\text{ }^\circ\text{C}$  for 4 hours in air. The calcined powder was formed into a cylindrical shape using a rubber tube, pressed under a cold isostatic pressure of 300 MPa, sintered at  $1050\text{ }^\circ\text{C}$  for 8 hours in oxygen flow, and then used as a feed rod. The feed rod was 7 mm in diameter and approximately 50 mm in length.

### **2.2.2 Solvent preparation and attachment with the feed**

A Li-excess solvent was used for TSFZ growth due to the incongruent melting behavior of  $\text{LiCoO}_2$ . The calcined  $\text{LiCoO}_2$  powder and  $\text{Li}_2\text{CO}_3$  powder were mixed in a Li:Co atomic ratio of 85:15, formed into a cylindrical shape approximately 7 mm in diameter using a hydrostatic press, and then used as a solvent disk for TSFZ growth without sintering. The solvent of 0.8 g was used for the TSFZ growth. Prior to the crystal growth of  $\text{LiCoO}_2$ , a solvent disk was put on the top edge of the feed rod in the image furnace, melted, and then attached with the feed rod in Ar atmosphere. The feed with the solvent and the seed crystal was set at the upper and lower shafts, respectively, and the TSFZ growth was performed in the same as normal FZ growth, as shown Fig. 2-4.

### 2.2.3 Crystal growth and quenching the molten zone

The growth apparatus was a tilting-mirror-type image furnace (Crystal Systems Inc. model TLFZ-4000-H-VPO) with four ellipsoidal mirrors, as shown in Fig. 2-3. This furnace equipped with four flat-filament type 300 W halogen lamps delivering a total lamp power of 1.2 kW was tilted up to  $15^\circ$  by a motor drive controller. Before each growth experiment, molten zone was stirred for approximately 30 mins to maintain steady state due to incongruent melting behavior of  $\text{LiCoO}_2$  material. At this time, lamp power was manually adjusted to realize a stable molten zone at each mirror-tilting angle. The grown crystals of  $\text{LiCoO}_2$  were used as seeds. The direction of seed crystal was [001] and it was same as that of the as-grown crystal throughout the entire growth experiment. For all growth experiments, the growth rate was 5 mm/h under an atmosphere of Ar with a flow rate of 1.5 L/min, and the upper and lower shaft rotation rates were 12 rpm and 25 rpm, respectively, in the opposite directions. In the investigation of the mirror-tilting effects, the tilt angle was varied from 0 to  $15^\circ$ , with the above growth conditions remaining constant during the growth of crystals 7 mm in diameter. The crystal growth was continued until the crystal diameter was uniform (after 20 mm of growth), and then, the heating lamps were quickly turned off to quench the molten zone. The sequence of experimental procedure was shown in Fig. 2-5.

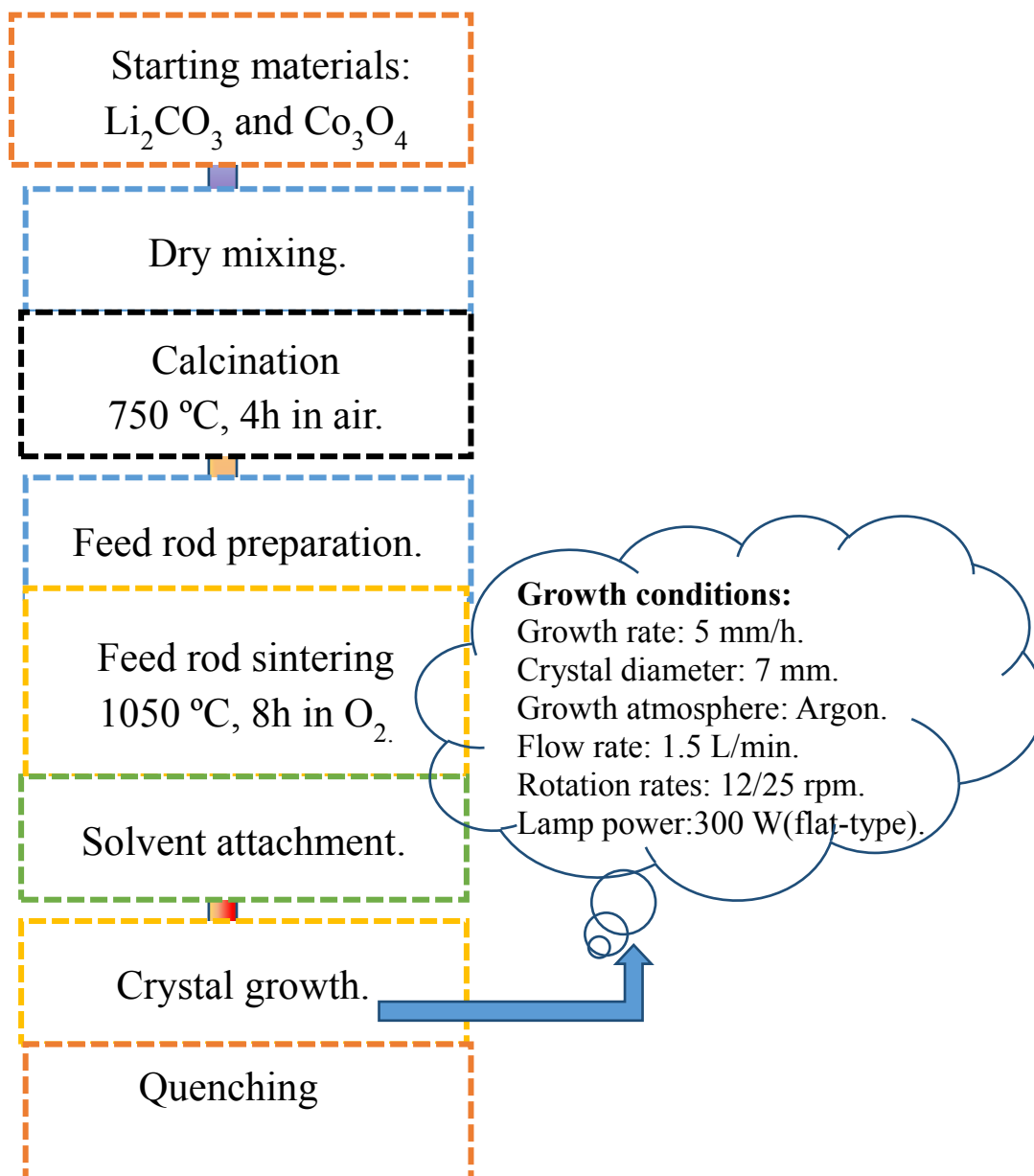


Fig. 2-5 Sequence of experimental procedure for TSFZ growth.



#### 2.2.4 Characterization of the quenched molten zone

The quenched samples were cut through the center along the growth direction and polished to a mirror-like surface. Important parameters characterizing the interface shape, such as the convexities  $h/r$ , molten zone length  $L$  and gap between the feed rod and grown crystal, were directly determined from the photographs of the quenched molten zone obtained during growth as shown in Fig. 2-8. The lamp power required for the crystal growth at each mirror tilt angle was estimated from the applied voltage and the voltage – lamp current proportionality of the halogen lamp.

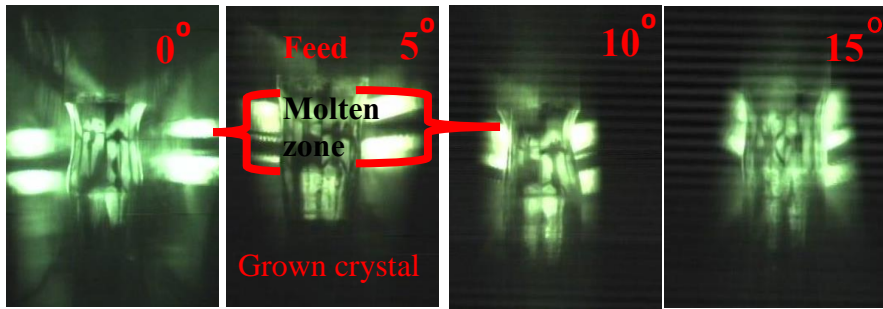


Fig. 2-6 Photographs of the stable molten zones at different mirror tilt angles( $\theta$ ).

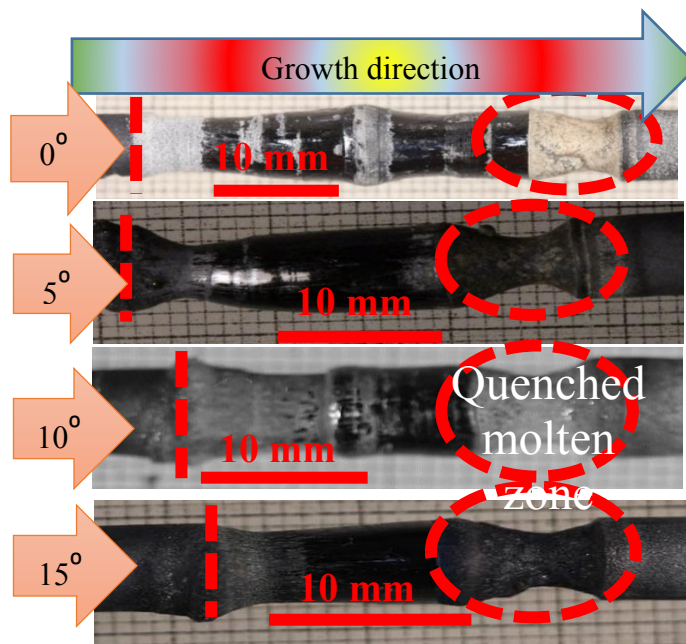


Fig. 2-7 Photographs of the grown crystals at different mirror tilt angles( $\theta$ ).

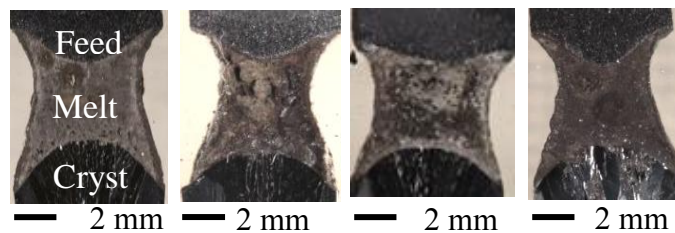


Fig. 2-8 Vertical sections of the molten zones quenched during TSFZ growth of LiCoO<sub>2</sub> at tilt angles of (a) 0°, (b) 5°, (c) 10°, and (d) 15°.

### 2.3 Mirror tilting effects on the interface shape of the molten zone

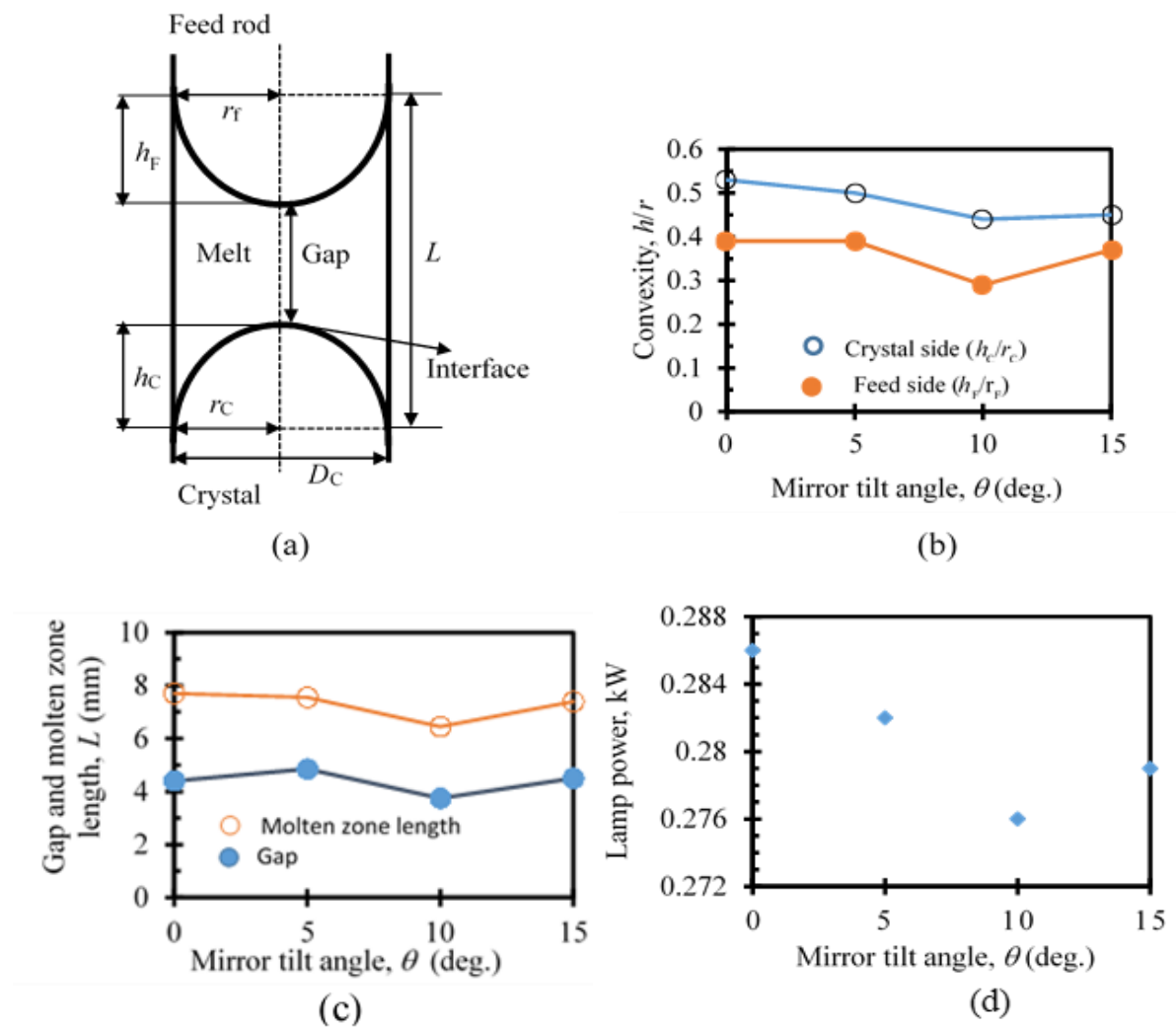


Fig. 2-9 Graphical representation of the characteristic parameters as a function of the mirror tilt angle: (a) schematic diagram exhibiting the definitions of the convexity( $h/r$ ), molten zone length( $L$ ) and gap, (b) convexity( $h/r$ ), (c) molten zone length( $L$ ) and gap, and (d) lamp power required for the growth. Note that the values of  $h/r$ ,  $L$  and the gap were determined using the photographs of the quenched molten zone shown in Fig. 2-8.

The shapes of the feed-liquid and crystal-liquid interfaces were convex and found to be significantly affected by the mirror tilt angle during growth. To examine the interface shape of the molten zone as a function of mirror tilt angle, important parameters characterizing the interface shape, such as the convexity ( $h/r$ ), molten zone length ( $L$ ), and gap between the feed rod and grown crystals, are presented in Fig. 2-9. These parameters were defined as shown in Fig. 2-9(a).

The convexity of the crystal-liquid interface was approximately 0.1 higher than that of the feed-liquid interface at all tilt angles. The convexities of both the feed-liquid interface ( $h_F/r_F$ ) and the crystal-liquid interface ( $h_C/r_C$ ) decreased with increasing mirror tilt angle up to  $10^\circ$  and increased slightly at  $\theta = 15^\circ$ , as shown in Fig. 2-9(b). The change in the convexities for  $\text{LiCoO}_2$  was small compared to that in rutile, from 0.5 to 0.2 at  $\theta = 0^\circ$  to  $20^\circ$  [8]. A low convexity is advantageous in the growth of large crystals to prevent contact between the feed and the grown crystals during crystal growth. The molten zone length ( $L$ ) and the gap between the feed rod and grown crystal were not so affected by the mirror tilt angle and slightly lower at  $\theta = 10^\circ$  due to the minimum lamp power required for the growth under this tilt condition, as shown in Fig. 2-9(c) and (d). The lowest lamp power required to maintain a highly stable molten zone, in which the gap between the feed and crystal is sufficient large, was found at  $\theta = 10^\circ$ . Therefore, this result reveals that the molten zone is stabilized with the most effective heating at the mirror tilt angle of  $\theta = 10^\circ$  for TSFZ growth of  $\text{LiCoO}_2$ .

## 2.4 TSFZ growth of LiCoO<sub>2</sub> single crystals as a function of mirror tilting angles

The amount of solvent is an important factor for maintaining a stable molten zone during the TSFZ growth of LiCoO<sub>2</sub> crystals. The solvent of 0.5 to 0.6 g for a feed diameter of 5 mm was used for the TSFZ growth of LiCoO<sub>2</sub> [12]. The solvent amount was estimated from the feed diameter, assuming that the solvent amount is proportional to the square of the feed diameter since the length of the molten zone is dependent not on the feed diameter but on the width of the lamp filament. The estimation of the solvent amount was consistent with the growth using the feed of 7 mm in diameter.

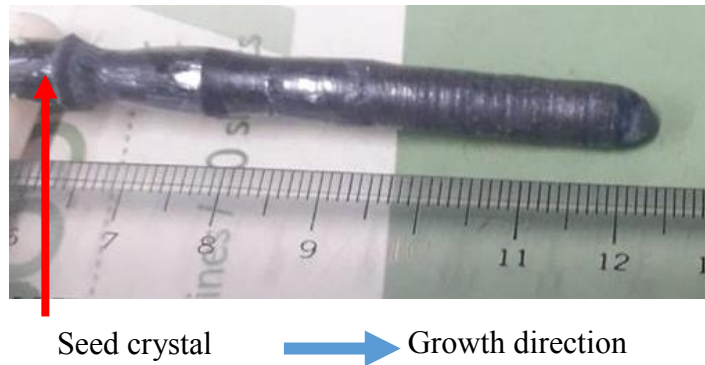


Fig. 2-10 As grown crystals of LiCoO<sub>2</sub> using 0.8 g of solvent at a mirror tilt angle of  $\theta = 10^\circ$ .

In particular, the TSFZ growth using the solvent of 1.1 g for the feed diameter of 7 mm was stable during growth and shiny visible crystals were obtained as described in the next session. In the case of 0.8 g of solvent, however, contact between the feed rod and the grown crystal frequently occurred, disturbing the

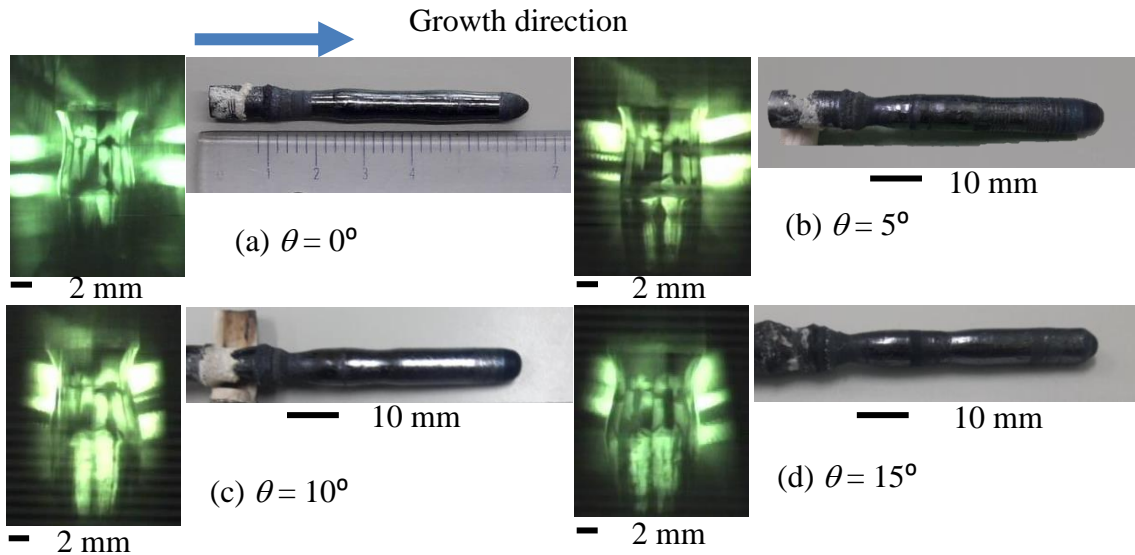


Fig. 2-11 Photographs of molten zones and grown crystals of 7 mm in diameters at different mirror tilt angles  $\theta$ .

molten zone stability during the growth. As a consequence, a rough crystal surface appeared during the growth, as shown in Fig. 2-10.

I tried to grow large  $\text{LiCoO}_2$  single crystals by the TSFZ method using the tilting-mirror-type image furnace. Fig. 2-11 shows photographs of the molten zones and the corresponding crystals of  $\text{LiCoO}_2$ . For the growth using the feed of 7 mm in diameter, the crystal grown at  $\theta = 10^\circ$  was a shiny visible crystal surface as shown in Fig. 2-11(c). In contrast, the crystals grown at the tilt angle other than  $\theta = 10^\circ$  had a periodically rough surface as shown in Fig. 2-11(a), (b) and (d), and contained cracks and inclusions of cobalt oxide. The shapes of the molten zone indicate that the molten zone was almost same during crystal growth at all mirror tilt angles. However, contact between the feed rod and the grown crystals occurred occasionally during growth at the tilt angle other than  $\theta = 10^\circ$ . The phenomenon of the contact is explained the fact that both the convexities of the feed-liquid and

crystal-liquid interfaces are larger than  $\theta = 10^\circ$  as shown in Fig. 2-9(b). In addition, it was found that amount of Li evaporation from the molten zone during growth at  $\theta = 10^\circ$  was minimum as shown in Fig. 2-12. The small of the Li evaporation during at  $\theta = 10^\circ$  is consistent with the lowest lamp power as shown in Fig. 2-9(d).

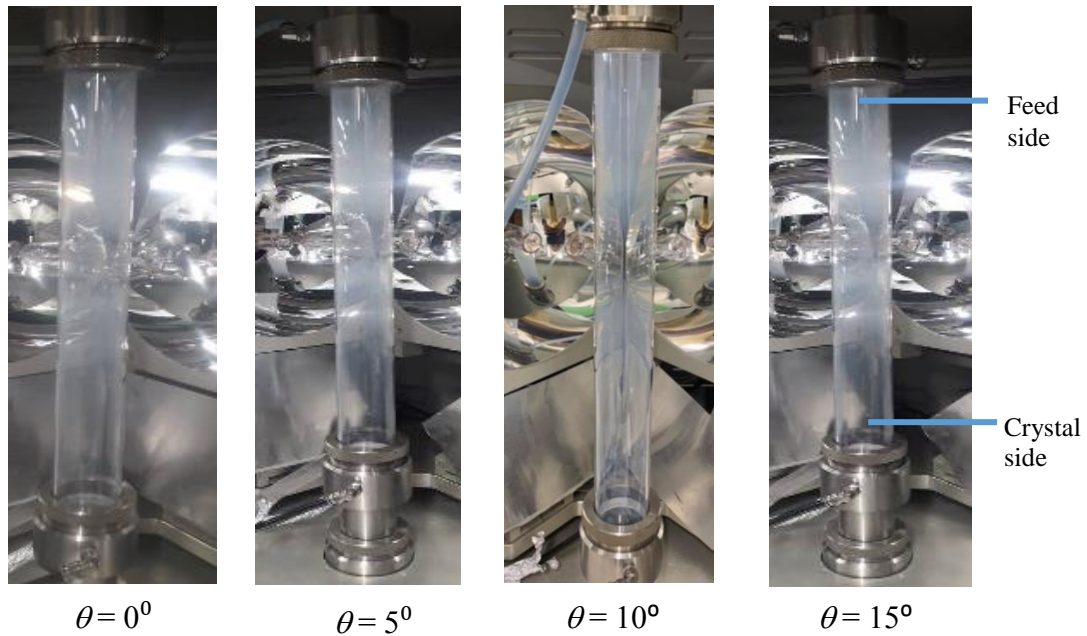


Fig. 2-12 Quartz tubes after the growth of  $\text{LiCoO}_2$  single crystals at different mirror tilt angles. White lithium oxide was deposited on the inner surface of the quartz tube.



## 2.5 Characterization of grown crystal at mirror tilting angles $\theta = 10^\circ$

### 2.5.1 SEM and Laue XRD measurement.

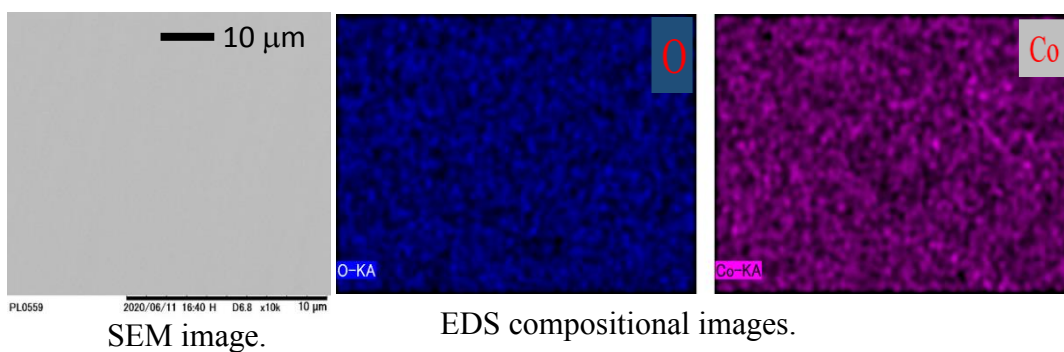
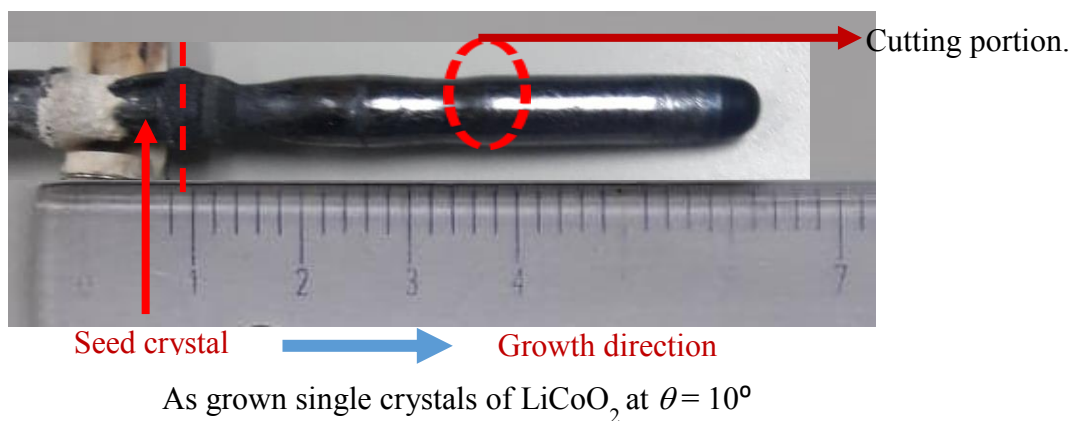


Fig. 2-13 SEM images of the grown crystals of  $\text{LiCoO}_2$  at a mirror tilt angle of  $\theta = 10^\circ$ .

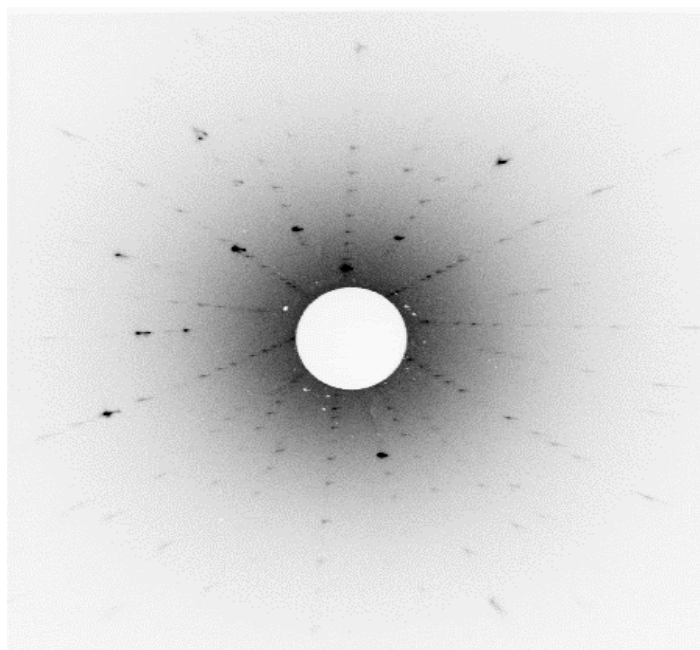


Fig. 2-14 Laue XRD measurement of the grown crystals of  $\text{LiCoO}_2$  at a mirror tilt angle of  $\theta = 10^\circ$ .



Scanning electron microscopy (SEM) and EDS compositional images showed that the LiCoO<sub>2</sub> crystals grown at a mirror tilt angle of  $\theta = 10^\circ$  had a single phase and no inclusion of cobalt-oxide phase as shown in Fig. 2-13. In addition, the Laue XRD measurement confirmed the single crystals of LiCoO<sub>2</sub> grown at a mirror tilt angle of  $\theta = 10^\circ$  by TSFZ technique using tilting-mirror-type image furnace as shown in Fig. 2-14.

## 2.6 Conclusions

The effects of mirror tilt on the shape of the molten zone during the growth of LiCoO<sub>2</sub> single crystals by the traveling solvent floating zone (TSFZ) method using a tilting-mirror-type image furnace were studied. The convexities ( $h/r$ ), molten zone length ( $L$ ) and gap between the feed rod and grown crystal, which are the important parameters characterizing the molten zone shape, were found to be affected by the mirror tilt angle during growth. A highly stable molten zone and a slightly convex interface were observed along with a lower required lamp power at a mirror tilt angle of  $\theta = 10^\circ$ . Therefore, the most effective heating was realized under this tilt condition, and as a result, the best LiCoO<sub>2</sub> single crystals of 7 mm in diameter and 50 mm in length with a shiny visible character were obtained at  $\theta = 10^\circ$ .

## References

- [1] K. Kitamura, S. Kimura, S. Hosoya, J. Cryst. Growth, **48** (1980) 469.
- [2] G.D. Gu, M. Hucker, Y.J. Kim, Tranquada, Q. Li, A.R. Moodenbaugh, J. Cryst. Growth, **287** (2006) 318.
- [3] M. Higuchi, K. Kodaira, Materials Research Bulletin, **29** (1994) 545.
- [4] S.A. Borodin, L.B. Davidova, V. M. Erofeev, A.V. Shanov, S. A. Startsev, V.A. Tatarchenko, J. Crystal Growth, **46** (1979) 757.
- [5] K. Kinoshita, K. Sugii, J. Cryst. Growth, **71** (1985) 283.
- [6] M. Abdur Razzaque Sarker, S. Watauchi, M. Nagao, T. Watanabe, I. Shindo, I. Tanaka, J. Cryst. Growth, **317**(2011) 135.
- [7] C.H. Chiang, J.C. Chen, J. Cryst. Growth, **294** (2006) 323.
- [8] M. Abdur Razzaque Sarker, S. Watauchi, M. Nagao, T.Watanabe, I. Shindo, I. Tanaka, J. Cryst. Growth, **312** (2010) 2008.
- [9] S. Watauchi, M. Abdur Razzaque Sarker, M. Nagao, T.Watanabe, I. Shindo, I. Tanaka,. J. Cryst. Growth, **360** (2012) 105.
- [10] M.M. Hossain, S. Watauchi, M. Nagao, I. Tanaka, CrystEngComm, **16** (2014) 4619.
- [11] M.M. Hossain, S. Watauchi, M. Nagao, I. Tanaka, J. Cryst. Growth, **459** (2017) 105.

- [12] S. Nakamura, A. Maljuk, Y. Maruyama, M. Nagao, S. Watauchi, T. Hayashi, Y. Anzai, Y. Farukawa, C.D. Ling, G. Deng, M. Avdeev, B. Buchner, I. Tanaka, *Cryst. Growth Des.***19** (2019) 415.
- [13] D.T.J. Hurle, *Handbook of Crystal Growth*, Vol. **2**(1994).
- [14] S.M. Koohpayeh, D. Fort, J.S. Abell, *Progress in Crystal Growth and Characterization of Materials*, **54** (2008) 121.

## CHAPTER 3

### *Larger diameter single crystals growth of $\text{LiCoO}_2$ by TSFZ method*

#### 3.1 Introduction

##### 3.1.1 Background of the study

Rechargeable lithium-ion batteries (LIBs) have been used widely in various portable electronics since their first commercialization by Sony Corporation in 1991 and, more recently, in large-scale electrical vehicles (EVs) and energy storage grids (EEGs). Because they are growing rapidly in industrial applications, LIBs are needed that have a higher energy density and greater power output [1–4]. Since LIBs is the most promising battery candidate to power battery-electric vehicles. For these vehicles to be competitive with those powered by conventional internal combustion engines, significant improvements in battery performance are needed, especially in the energy density and power delivery capabilities. However, the cathode material is an extremely important factor when developing high performance rechargeable LIBs. There is an urgent demand for materials with a high energy density because of the miniaturization of electronic equipment and the use of power batteries in EVs/HEVs [5-7]. Recently,  $\text{LiCoO}_2$  has been the most widely used cathode materials in commercial LIBs due to its easy preparation, high specific capacity, low self-

discharge, and excellent cycle life,[8–12] which make it a popular choice for mobile phones, laptops, and digital cameras and other portable electronic equipment.

Improvement in the performance of the LIBs is strongly required in today's informance-rich and mobile society that is significantly related with the properties of the cathode material. Due to the highly anisotropic conductivity  $\sigma_a/\sigma_c \approx 500$  in  $\text{LiCoO}_2$ , a single crystalline substrate of  $\text{LiCoO}_2$  perpendicular to the c-axis is expected to enhance the performance of Li-ion batteries [13].

### 3.1.1.1 Discussion about the previous reports on the growth of $\text{LiCoO}_2$ single crystals

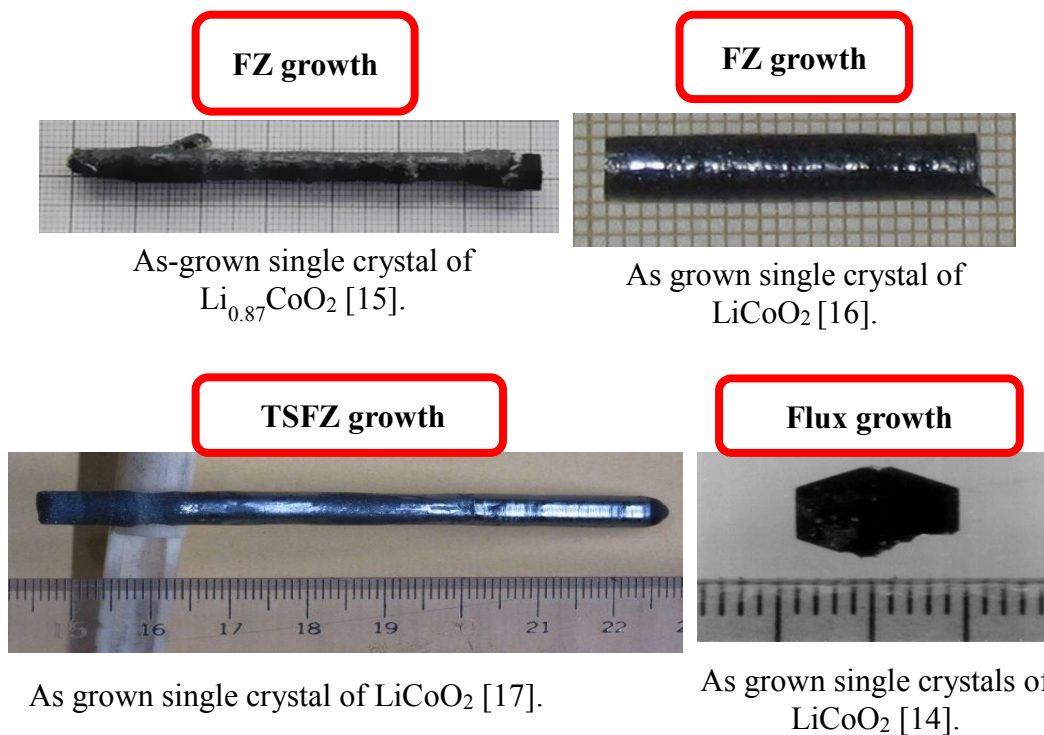


Fig. 3-1 Photographs of previously grown  $\text{LiCoO}_2$  single crystals by different growth techniques.

Akimoto et al; has reported the growth of small  $\text{LiCoO}_2$  single crystals by the flux technique [14]. Some authors have also reported the growth of  $\text{LiCoO}_2$  single crystals by floating zone (FZ) technique(Fig.3-1) using high Li-excess feed of up to (100 mol% excess  $\text{Li}_2\text{CO}_3$ ) to compensate Li evaporation and to decrease the cobalt impurities under high pressure of growth atmosphere without solvent [15,16]. But the diameter of the grown crystals was limited to the 5 mm. We have also grown high-quality single crystals of  $\text{LiCoO}_2$  by the TSFZ technique with the feed of the stoichiometric  $\text{LiCoO}_2$  and a solvent of 85 mol%  $\text{Li}_2\text{O}$  [17, 18]. However, the diameter of the grown crystal was limited to 7 mm.

### **3.1.1.2 Importance of the growth of larger diameter single crystals of $\text{LiCoO}_2$**

The  $\text{LiCoO}_2$  single crystals larger than a half inch diameter are required for the commercial application of cathodes to enhance the performance of LIBs. To the best of my knowledge, there is no report on the TSFZ growth of  $\text{LiCoO}_2$  single crystals of diameter more than half inch diameter that is the main focus of this research.

### **3.1.1.3 Problems during the growth of larger diameter single crystals**

I had tried to grow  $\text{LiCoO}_2$  single crystals with 10 mm in diameter by the TSFZ method using the feed of the stoichiometric  $\text{LiCoO}_2$  and a solvent of 85 mol% $\text{Li}_2\text{O}$  according to references 16 and 17. I found that the main problems on the periodical instability of the molten zone during TSFZ growth of larger-diameter single crystals of  $\text{LiCoO}_2$  were the higher Li evaporation and the contact between feed rod and the

grown crystal. The higher lamp power was required for the crystal growth using the feeds of 10 mm in diameter compared to 7 mm in diameter. The higher lamp power enhanced not only evaporation of Li component from the molten zone but also deposition of cobalt oxide phase in the grown crystals. In addition, contact between the feed rod and the grown crystal occurred due to the deposition of cobalt oxide phase with a high melting temperature, which leads to instability in the molten zone during TSFZ growth. The stability of the molten zone surely affects the crystal quality.

#### **3.1.1.4 Attempts to solve those problems during the growth**

I expected that the filament shape of the heating lamps is effective on the heating efficiency for reduction of Li evaporation and the length of the molten zone for prevention of the contact.

Solvent amount is also an important parameter to control the volume of molten zone during the TSFZ growth with increasing the crystal diameter. The periodic instability of the melting zone suggests that the Li concentration in the melting zone fluctuates periodically due to the alternating Li evaporation and cobalt oxide precipitation from the melting zone for TSFZ growth of the large-diameter crystals using the stoichiometric  $\text{LiCoO}_2$  feeds. Therefore, addition of the excess  $\text{Li}_2\text{CO}_3$  into the stoichiometric feed is necessary to compensate the excess amount of Li evaporation at a higher growth temperature for the growth of  $\text{LiCoO}_2$  single crystals larger than 7 mm in diameter.

In this chapter, I discussed the effects of slightly excess Li content (2 mol% to 5 mol%) in the stoichiometric feed, the amount of solvent and the filament shape of the heating lamps on the TSFZ growth of larger-diameter  $\text{LiCoO}_2$  single crystals.

### **3.1.1.5 Concept of flat and cylindrical-type heating lamp filament configuration for larger diameter single crystals growth**

For the TSFZ growth of larger diameter single crystals of  $\text{LiCoO}_2$ , filament shape of heating lamp is very important because it is strongly related with the molten zone length and stability of the molten zone avoiding the contact problem. Filament shape of heating lamp is also related with the extended heating region and central focusing that has a significant effects to solve the contact problem due to the increased molten zone. This is the main reason for investigation the effects of lamp filament shape for the growth of high quality, larger-diameter single crystals.



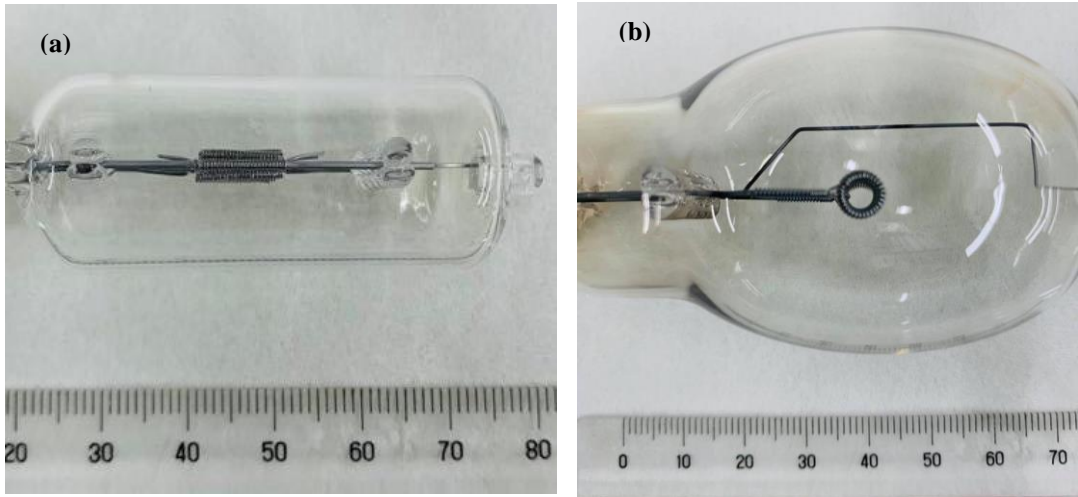


Fig. 3-2 Photographs of 300 W (a) flat filament-type and (b) cylindrical filament-type lamps.

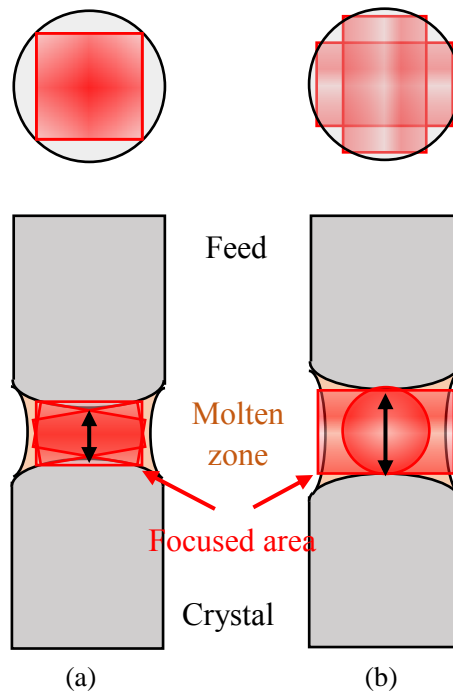


Fig. 3-3 Schematic illustration of focusing images for flat (a) and coil (b) type filament lamps at a mirror tilt angle of  $10^\circ$  for crystal diameter of 10 mm. The upper and lower drawings are the view from above and the side, respectively.

The filament configuration of flat-type and cylindrical-type lamps were shown in Fig. 3-2. In addition, Fig. 3-3 shows a schematic focusing image for flat and cylindrical filament-type lamps. For focusing using flat filament-type lamps as shown in Fig. 3-3(b), with a mirror tilt angle of  $10^\circ$ , the high focusing region is wide and short compared with the cylindrical filament-type lamps. This focusing system is effective for growing small diameter crystals. In the cylindrical filament-type lamp, the focusing rays from the cylindrical-type filament were incident at the center of the molten zone during growth, as shown in Fig. 3-3(b). Therefore, the high focusing region is long for cylindrical-type filament lamps. This effective focusing of the heating lamp to the molten zone is advantageous for the growth of high quality, larger-diameter single crystals of  $\text{LiCoO}_2$ .

## **3.2 Optimization of the growth conditions during the single crystals growth**

### **3.2.1 Experimental procedure for the TSFZ growth of 10 mm and 13 mm diameter**

Experimental procedure for the TSFZ of  $\text{LiCoO}_2$  single crystals of 10 mm and 13 mm in diameter was the same as described in our previous chapter. Only feed composition and diameter was changed in this study to examine the effects of slightly Li excess feed on the growth of larger diameter single crystals. 2-5 mol% excess  $\text{Li}_2\text{CO}_3$  was added to the stoichiometric feed composition and then feed rod of 10 mm and 13 mm in diameter were prepared.

Solvent preparation and attachment process was also same as described in our chapter 2 but only the amount of solvent was varied due to the larger diameter single

crystals growth. The solvent of 2.5 g and 4.9 g was used for the TSFZ growth of  $\text{LiCoO}_2$  single crystals of 10 mm and 13 mm in diameter respectively.

The growth apparatus as described in the previous chapter, a tilting-mirror-type image furnace (Crystal Systems Inc. model TLFZ-4000-H-VPO) with four ellipsoidal mirrors, as shown in Fig. 2-3, was used for the growth. All the growth experiments were performed at mirror tilting angle of  $\theta = 10^\circ$  due to the low convexity and high stability in this tilt condition [17].

To study the effects of the filament shape of the heating lamps on the growth of large-diameter single crystals of  $\text{LiCoO}_2$ , halogen lamps with commercially available flat-type and proto-type cylindrical-type filaments with a rated output of 300 W were used in the growth experiments, as shown in Fig. 3-2. The filament size of the flat filament-type lamp was 7 mm square and 3 mm thick. The filament size of the cylindrical filament-type lamp was 9 mm in length with inner and outer lamp filament diameters of 4.5 mm and 5.5 mm, respectively.

### 3.2.2 Optimization of the shape of heating lamp filament

The molten zone length is an important parameter to maintain a stable molten zone that depends not only on the growth conditions but also on the lamp heating conditions, such as the lamp filament configuration and the focusing conditions from the heating lamp. Fig. 3-4 shows photographs of two molten zones during the TSFZ growth of 10 mm diameter  $\text{LiCoO}_2$  single crystals using tilting-mirror-type image furnaces with different filament types for the heating lamps. In the case of the flat filament-type lamp shown in Fig. 3-3(a), the molten zone length was 6 mm

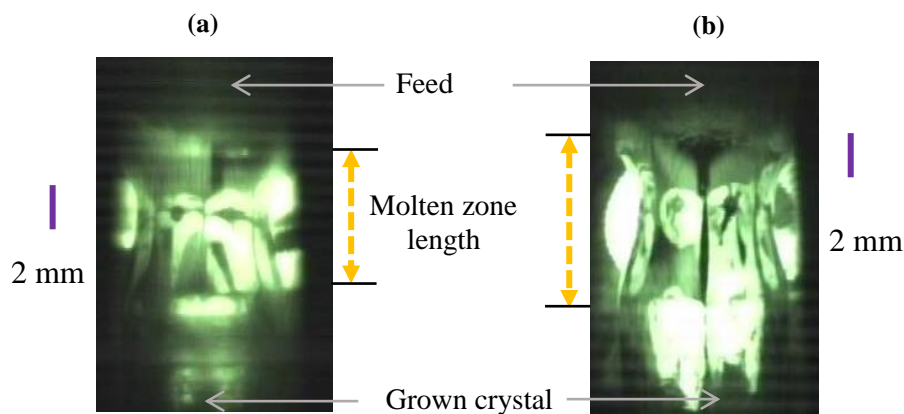


Fig. 3-4 Photographs of molten zones during the growth of  $\text{LiCoO}_2$  single crystals with a diameter of 10 mm using heating lamps of (a) flat-type and (b) cylindrical-type filament.

and shorter as compared with the feed diameter due to the small heating region formed by the flat-type filament, as shown in Fig. 3-4(a). As a result, periodic contact between the feed rod and the grown crystal occurred due to the insufficient gap between the feed rod and the grown crystals. In contrast, the molten zone length was increased to 8 mm, 2 mm longer than that for flat filament-type lamp, due to the large heating region formed by the cylindrical filament-type lamp, as shown in Fig. 3-3(b). As a result, a highly stable molten zone, in which the gap between the

feed rod and grown crystals was sufficient, was obtained during growth using cylindrical filament-type lamp.

The heating region was significantly related to the filament size, which is the filament length and width of the heating lamp. The reason for the increase in the molten zone length was the increase in the filament size of the cylindrical filament-type lamp compared to that of the flat filament-type lamp. This implies that the optimum molten zone length required to sustain stability in the molten zone during the growth of large-diameter single crystals of  $\text{LiCoO}_2$  was strongly affected by the filament shape and size of the heating lamp.

In addition, I realized that the focusing conditions for the heating lamp filament were strongly related to the stability of the molten zone during the growth experiment. Fig. 3-3 shows a schematic focusing image for flat and cylindrical filament-type lamps. For focusing using flat filament-type lamps with a mirror tilt angle of  $10^\circ$ , the high focusing region is wide and short compared with the cylindrical filament-type lamps. In the cylindrical filament-type lamp, the focusing rays from the cylindrical-type filament were incident at the center of the molten zone during growth, as shown in Fig. 3-3(b). Therefore, the high focusing region is long for cylindrical-type filament lamps. A stabilized molten zone avoiding the contact problem was achieved due to the high efficiency of the cylindrical-type filament. This means that effective focusing of the heating lamp to the molten zone had a significant effect on the stable growth of large-diameter single crystals of  $\text{LiCoO}_2$ .

### 3.2.3 Optimization of Li excess feed compositions and amount of solvent

The stability of the molten zone showed a strong relationship with the excess Li content of the feed and the amount of solvent due to high Li evaporation during the TSFZ growth of large-diameter single crystals of  $\text{LiCoO}_2$ . As the feed diameter increased, the amount of Li evaporation also increased due to the highest required lamp power for crystal growth. Therefore, it was difficult to maintain a stable molten zone for an extended period. To compensate for Li evaporation from the molten zone during the TSFZ growth of large-diameter single crystals, excess Li content in the feed was required. Fig. 3-5 and Fig. 3-6 show photographs of  $\text{LiCoO}_2$  crystals with a diameter of 10 mm and 13 mm, respectively, grown with varying excess Li content in the feeds and amount of solvent by the tilting-mirror approach with cylindrical filament-type heating lamps. To study the effects of the excess Li content in the feed on the TSFZ growth, only the percentage of excess Li content in the feed was varied while keeping the other growth parameters constant, as shown in Fig. 3-5(a to c) and Fig. 3-6(a to c).  $\text{LiCoO}_2$  single crystals with a metallic luster were obtained using 2 mol% and 3 mol% excess Li content for feeds with a diameter of 10 mm and 13 mm, respectively, as shown in Fig. 3-5(c) and Fig. 3-6(b). In contrast, for TSFZ growth using feeds with a Li content that was too high, rough and white crystal surfaces appeared during crystal growth. The reason for the appearance of a white crystal surface is the deposition of  $\text{Li}_2\text{O}$  on the crystal surface during growth, as shown in Fig. 3-5(a) and Fig. 3-6(a). In addition, during the growth of  $\text{LiCoO}_2$  crystals using a feed with too low Li content, contact between

the feed rod and grown crystal frequently occurred, creating instability in the molten zone.

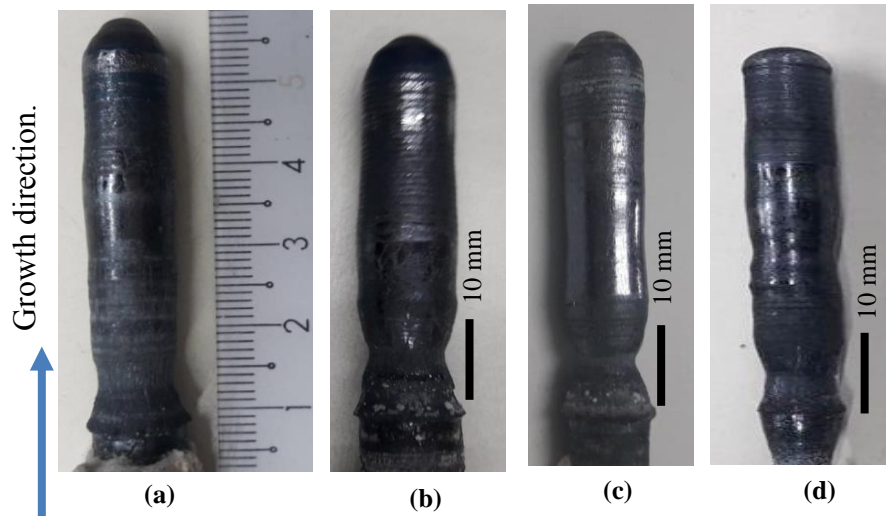


Fig. 3-5 As-grown crystals of  $\text{LiCoO}_2$  of 10 mm in diameter grown at various excess Li content of feed (a) 5 mol%, (b) 3 mol%, (c) 2 mol% using solvent amount of 2.5 g, (d) 2 mol% using 3.0 g solvent.

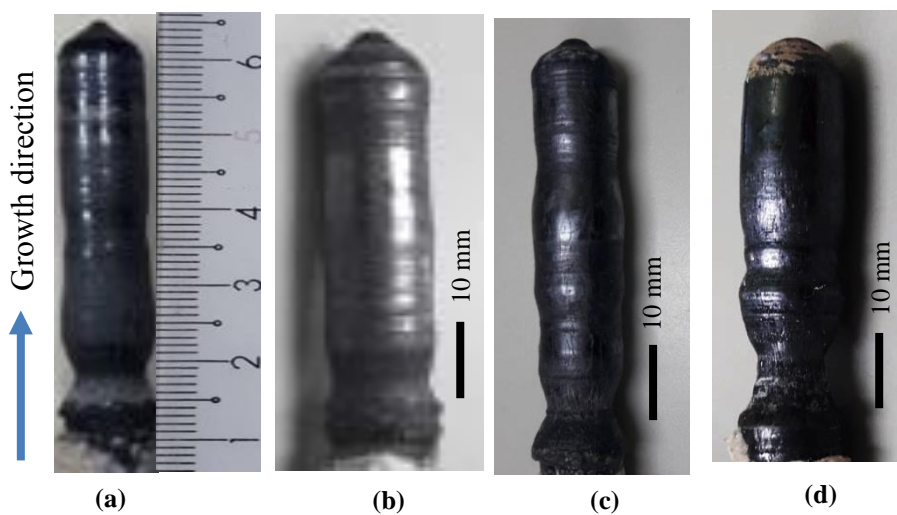


Fig. 3-6 Photographs of  $\text{LiCoO}_2$  crystals with a diameter of 13 mm grown at various excess Li contents in the feed (a) 5 mol%, (b) 3 mol%, (c) 2 mol% using a solvent amount of 4.9 g, (d) 3 mol% using 5.8 g solvent.

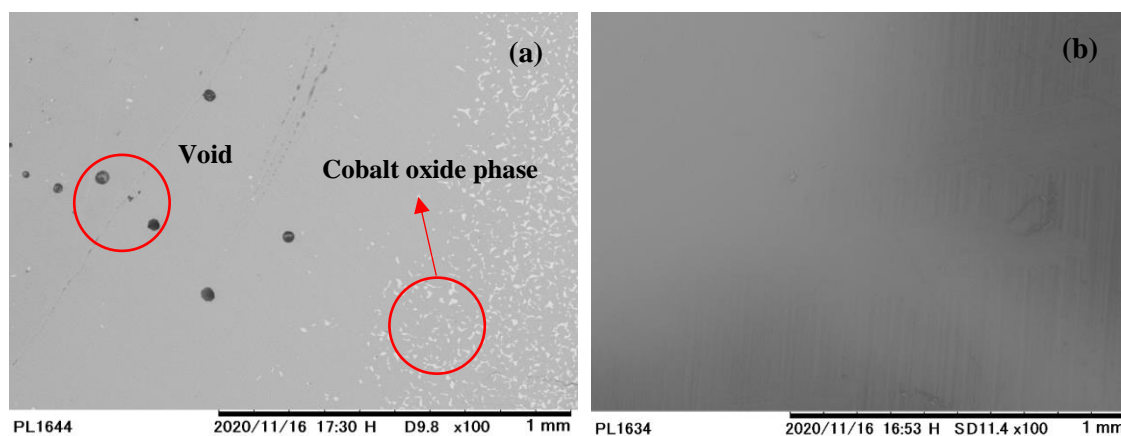


Fig. 3-7 The SEM images at (a) rough surface part and (b) luster surface part in the grown crystal.

As a result, the grown crystals contained cracks and cobalt oxide inclusions, as shown in Fig. 3-5(b) and Fig. 3-6(c). Fig. 3-7 shows SEM images of the insides at a rough and metallic luster surface parts in the grown crystal. Many voids and inclusions of cobalt oxide were observed at the inside of the rough surface part where as the inside of the luster surface part had no inclusion.



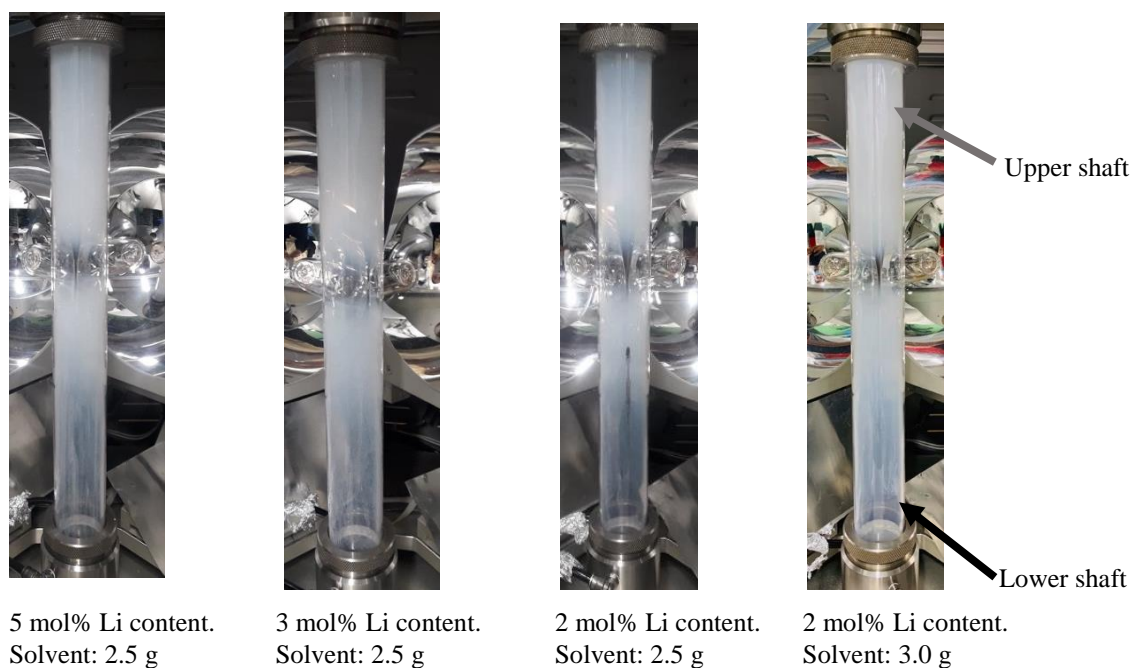


Fig. 3-8 Quartz tubes after the growth of  $\text{LiCoO}_2$  single crystals of 10 mm in diameter at different Li- excess feed and solvent amount. White lithium oxide was deposited on the inner surface of the quartz tube.

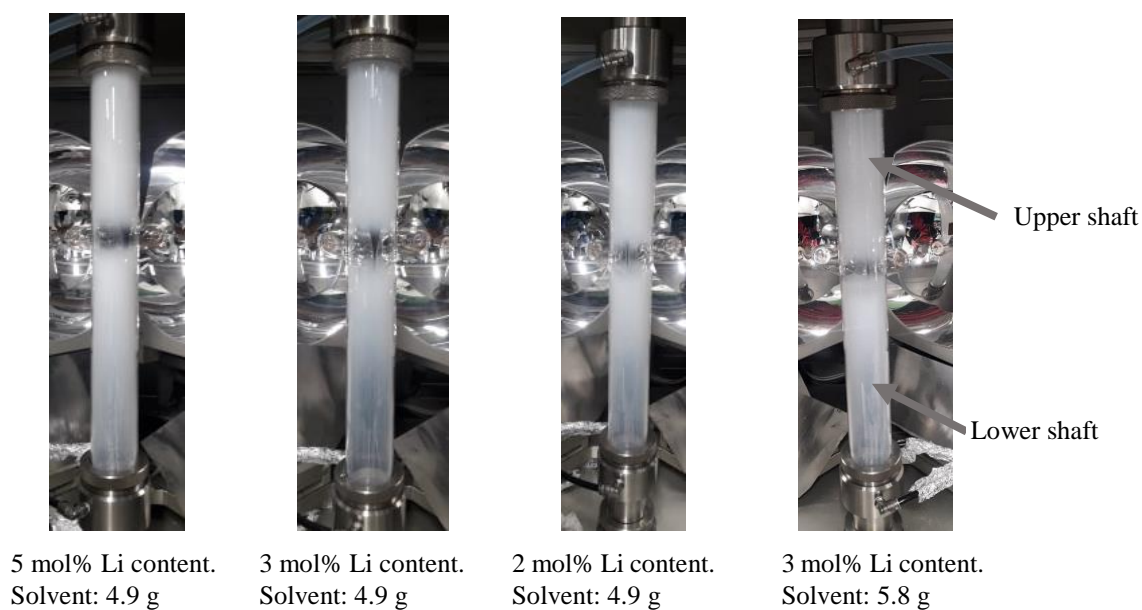


Fig. 3-9 Quartz tubes after the growth of  $\text{LiCoO}_2$  single crystals of 13 mm in diameter at different Li- excess feed and solvent amount. White lithium oxide was deposited on the inner surface of the quartz tube.

The reason for the deposition of excess  $\text{Li}_2\text{O}$  and the instability in the molten zone was strongly related to the high Li evaporation during the TSFZ growth. In our experiment, the Li component evaporated from the molten zone deposited onto the quartz tube surrounding the crystal growth region, as shown in Fig. 3-8 and Fig. 3-9. The quartz tube with the deposited  $\text{Li}_2\text{O}$  behaved as an obstacle for transmitting the effective heat in the molten zone during growth. As a consequence, contact occurred frequently, and the lamp power increased, as shown in Figure 3-8. Therefore, the growth results imply that the optimum excess Li content from the stoichiometric feed is an important parameter for the successful growth of large-diameter single crystals of  $\text{LiCoO}_2$ , avoiding the contact problem between the feed rod and grown crystals during TSFZ growth.

I also investigated the effects of the amount of solvent during the growth of 10 mm and 13 mm diameter crystals of  $\text{LiCoO}_2$  while keeping other growth conditions constant. Fig. 3-5(d) and Fig. 3-6(d) indicate the dependency of the increased amount of solvent on the quality of the grown crystals.

### 3.2.4 Relationship among important parameters during the growth

#### 3.2.4.1 Optimum excess Li content in feed vs crystal diameter

#### 3.2.4.2 Excess Li content in feed vs required lamp power

#### 3.2.4.3 Optimum solvent amount vs square of crystal diameter

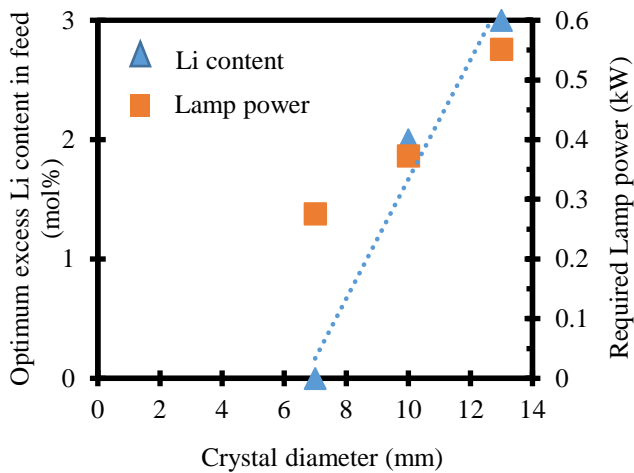


Fig. 3-10 Relationship between the optimum excess Li content in the feed, crystal diameter and required lamp power.

When the amount of solvent was increased, the Li evaporation from the molten zone was also increased due to the longer time required to reach the feed melting temperature. During this time, maintaining the stable molten zone becomes difficult, and contact between the feed rod and grown crystals occurs frequently during growth.

The relation among the optimum excess Li content in the feed, crystal diameter and required lamp power for crystal growth is shown in Fig. 3-10. This relation shows that the excess Li content from the stoichiometric composition is linear with respect to the diameter of the grown crystal. Furthermore, the amount of Li evaporation from the molten zone during the growth was slightly minimized at this optimum condition compared to the other conditions described above for the TSFZ growth

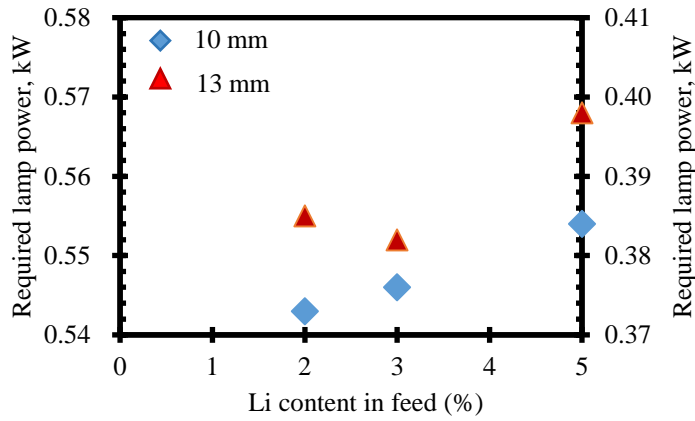


Fig. 3-11 Relationship between excess Li content in the feed and required lamp power.

of 10 mm and 13 mm single crystals, as shown in Fig. 3-8 and Fig. 3-9. The minimum Li evaporation is consistent with the lowest lamp power required for crystal growth, as shown in Fig. 3-11.

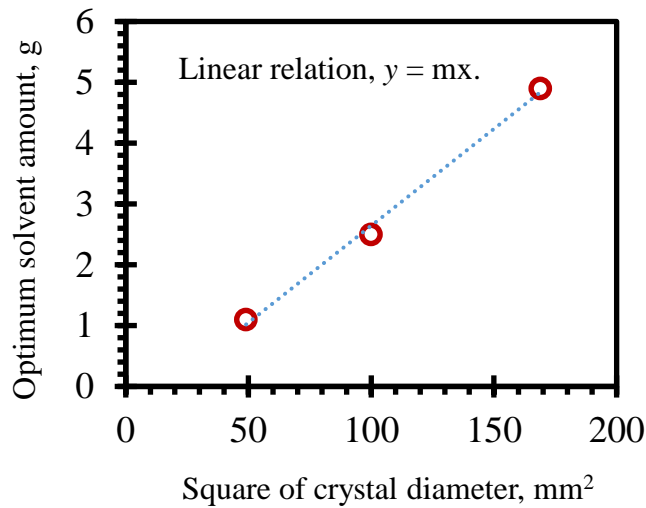


Fig. 3-12 Relationship between optimum solvent amount and crystal diameter.

The relationship between the optimum amount of solvent and the crystal diameter for the TSFZ growth of large-diameter single crystals is shown in Figure 3-12. The optimum amount of solvent was linearly related to the square of the crystal diameter.

This implies that the amount of solvent can be estimated from this linear relationship to grow  $\text{LiCoO}_2$  single crystals with larger diameter.

### **3.3 Conclusions**

The effects of excess Li content in the feed, the amount of solvent and the filament shape of the heating lamps on the growth of large-diameter single crystals of  $\text{LiCoO}_2$  were investigated by the TSFZ technique using a tilting-mirror-type image furnace. The stability of the molten zone during growth is an important factor in increasing the crystal diameter, which was significantly affected by the excess Li content, the feed composition, the amount of solvent and the filament shape of the heating lamp. The cylindrical-type filament was effective in maintaining the optimum molten zone length for the growth of large single crystals of  $\text{LiCoO}_2$  up to 13 mm in diameter. For the 13 mm diameter single crystal growth, a stabilized molten zone avoiding the contact problem was found at the optimum amount of solvent of 4.9 g using a 3 mol% excess Li content feed composition. The required lamp power for crystal growth and amount of Li evaporation from the molten zone during growth was lowest under these optimized growth conditions. A linear relationship between the optimum amount of solvent and the square of the crystal diameter was observed during the growth of large-diameter single crystals of  $\text{LiCoO}_2$ . Research into the growth of 13 mm (1/2 inch) diameter single crystal  $\text{LiCoO}_2$  cathodes is applicable in the industrial applications of LIBs for the further development of next generation all solid state LIBs.

## References

- [1] D. Larcher, J. M. Tarascon, *Nat. Chem.* **7** (2015)19.
- [2] B. Dunn, H. Kamath, J. M. Tarascon, *Science*, **334** (2011)928
- [3] J. B. Goodenough, Y. Kim, *Chem. Mater.* **22** (2010)587.
- [4] J. M. Tarascon, M. Armand, *Nature*, **414** (2001)359
- [5] M. Armand, J.M. Tarascon, *Nature*, **451** (2008) 652.
- [6] K. Kang, Y.S. Meng, J. Br\_egeer, C.P. Grey, G. Ceder, *Science*, **311** (2006) 977.
- [7] Y.K. Sun, S.T. Myung, B.C. Park, J. Prakash, I. Belharouak, K. Amine, *Nat. Mater.* **8** (2009) 320.
- [8] J. Xie, N. Imanishi, T. Zhang, A. Hirano, Y. Takeda, O. Yamamoto, *J. Power Sources*, **189** (2009) 365.
- [9] M. Murayama, R. Kanno, M. Irie, S.Ito, T. Hata, N. Sonoyama, Y. Kawamoto, *J. Solid State Chem.* **168** (2002) 140.
- [10] E. Plichta, S. Slane, M. Uchiyama, M. Saloman, D. Chua, W. Ebner, H.W. Lin, *J. Electrochem. Soc.* **136** (1989) 1865.
- [11] H.F. Gibbard, *J. Power Sources*, **26** (1989) 81.
- [12] J.B. Goodenough, K.S.S Park, *J. Am. Chem. Soc.* **135** (2013) 1167.

- [13] Y. Takahashi, Y. Gotoh, J. Akimoto, S. Mizuta, K. Tokiwa, T. Watanabe, J. Solid State Chem. **164** (2002)1.
- [14] J. Akimoto, Y. Gotoh, O. Akimoto, J. Solid State Chem. **141** (1998) 298.
- [15] L. Pinsard-Gaudart, V.-C Ciomaga, O. Dragos, R. Guillot, N. Dragoie, J. Cryst. Growth, **334** (2011)165.
- [16] S. Uthayakumar, M.S. Pandiyan, D.G. Porter, M.J. Gutmann, R. Fan, J.P. Goff., J. Cryst. Growth, **401** (2014)169.
- [17] S. Nakamura, A. Maljuk, Y. Maruyama, M. Nagao, S. Watauchi, T. Hayashi, Y. Anzai, Y. Farukawa, C.D. Ling, G. Deng, M. Avdeev, B. Buchner, I. Tanaka, Cryst. Growth Des. **19** (2019)415.
- [18] R. Parvin, Y. Maruyama, M. Nagao, S. Watauchi, I. Tanaka, Cryst. Growth Des. **20** (2020) 3413.

## CHAPTER 4

### *Design of next generation all-solid-state Li ion batteries (LIBs)*

#### *using LiCoO<sub>2</sub> single crystals as a cathode*

#### **4.1 Introduction**

##### **4.1.1 Background of the study**

Li-ion batteries (LIBs) are one of the most attractive energy storage technologies that were first introduced into the market by Sony in 1991 and have been widely accepted as power sources for portable electronics and mobile instruments, such as cellular phones, digital cameras and notebooks, because of their high energy and power density [1-6]. Since its first market introduction in 1991, the rechargeable LIBs has proven to be a reliable energy storage device for consumer electronics and has the potential to power electric vehicles (EVs) because of its high energy density, light weight, low maintenance, long service life, and high efficiency [7]. Layered lithium cobaltate LiCoO<sub>2</sub> with a theoretical capacity of 274 mAh/g, has been commercially used as a cathode material in LIBs for over ten years, with extremely fast market growth [8]. The success of this material as a cathode for LIBs is easily evidenced by its utilization in most portable electronic devices. This cathode material has excellent characteristics, such as high discharge potential,



low molecular weight, high energy capacity, good charge/discharge performance, relative ease of synthesis and treatment, and stable and high discharge voltage, which is promising for commercial application of LIBs [9-18].

#### **4.1.1.1 Problems of LiCoO<sub>2</sub> polycrystalline cathode in LIBs**

Although LiCoO<sub>2</sub> polycrystalline material is still commercially used in LIBs as a positive cathode. But the capacity of LIBs using LiCoO<sub>2</sub> polycrystalline material is lower because grain boundaries in polycrystalline materials act as impediments affecting materials intrinsic properties. Grain boundaries are sources of point defects and cause deformation. Grain boundary has a low resistance to creep at high temperature [19]. As a result, In Li-ion battery, the movement of Li ion will strongly be affected by defects which is created from the grain boundary of polycrystalline material.

#### **4.1.1.2 Advantages of single crystals cathode**

Single crystals without any defects give materials intrinsic properties that making single crystal precious in industrial and technological application. It has no grain boundaries and unbroken to the edges of the sample. It has a regular geometric structure and this structure has effect on materials properties [19]. According to high anisotropic conductivity  $\sigma_a/\sigma_c \approx 500$ [20] in LiCoO<sub>2</sub>, single crystalline substrate of LiCoO<sub>2</sub> perpendicular to the *c*-axis could be expected to enhance a performance considerably in LIBs.

#### 4.1.1.3 Advantages of single crystals solid electrolyte

Since LIBs have revolutionized the portable electronics industry. However, safety and stability issues remain a challenge for current commercial batteries based on liquid electrolytes. Significant efforts have been recently focused on the development of all-solid-state batteries, which have the potential to eliminate the use of flammable liquid electrolytes [21-29].

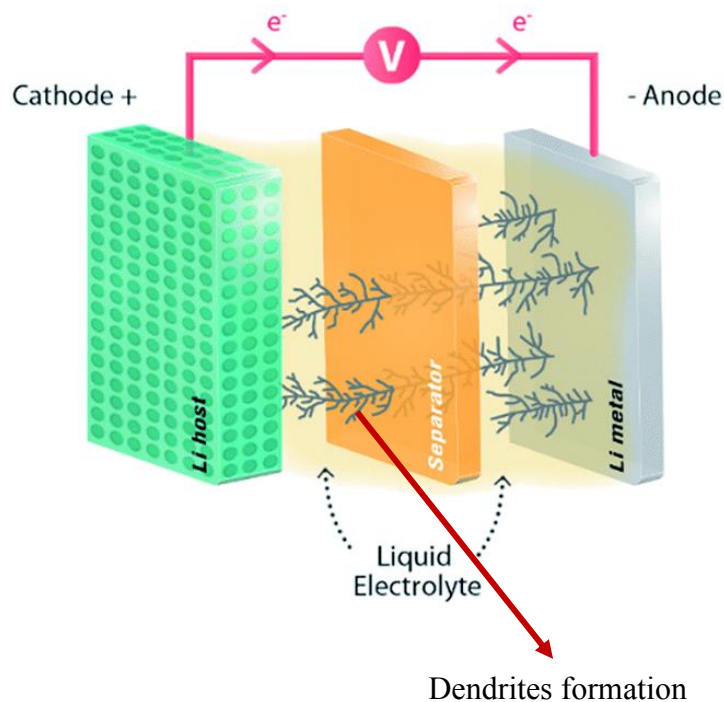


Fig. 4-1 Dendrite formation in LIBs using liquid electrolyte [30].

In LIBs using liquid or polycrystalline solid electrolyte, there is a possibility of dendrite formation during charging-discharging as shown in Figure 4-1 [30-32]. If this dendrite continues to grow, it can eventually punch through the battery separator and cause a short circuit. As a result, firing may occur in

LIBs. In contrast, in the case of single crystals solid electrolyte, there is no risk of dendrite formation or firing problem [33, 34]. Due to the safety and stability, the single crystals solid electrolyte is promising for the next generation all solid state LIBs.

Since in today's information-rich and mobile society, the demands for portable (micro-) electronic devices is rapidly increasing. To meet the increasing demand for those devices, the development of Li-ion rechargeable battery systems with high capacity is strongly required.

In this chapter, we focused on the design of all-solid-state Li-ion batteries using high quality larger diameter LiCoO<sub>2</sub> single crystals cathode for the enhancement of capacities of LIBs. We also tried to design all solid state LIBs using single crystals solid electrolyte for the further development of LIBs.

## **4.2 Experimental section for coin cell preparation**

Coin cells were prepared by changing the type of electrolyte to liquid, gel, Li<sub>7</sub>La<sub>3</sub>Zr<sub>2</sub>O<sub>12</sub> (LLZO) polycrystals, and Li<sub>x</sub>La<sub>(1-x)/3</sub>NbO<sub>3</sub> (LLN) single crystals.

### **4.2.1 Coin cell using liquid electrolyte**

At first the grown single crystals of LiCoO<sub>2</sub> was placed on a wood substrate, cut perpendicular to the growth direction using diamond wire saw, and used as a cathode of thickness 200-400 μm without polishing. The cathode was dried prior to set in a coin-type cell. Additionally, 1 M LiPF<sub>6</sub> in ethylene (EC)/ ethyl methyl carbonate (EMC) solution that is 1 M LiPF<sub>6</sub> / EC : EMC = 3 : 7 was used as liquid electrolyte and Li metal foil was used as anode. Then the coin-type cell was prepared using an argon filled glove box at room temperature as shown in Fig. 4-5. The experimental

procedure for coin-cell preparation using  $\text{LiCoO}_2$  single crystals cathode and liquid electrolyte was shown in Fig. 4-4. Charge-discharge studies of coin-type cells were performed with a battery tester (MACCOR Auto- mated Test System, series 4000) at various current rates and cathode thickness with the voltage limit between 2.5 and 4.2 V at temperature 60 °C.

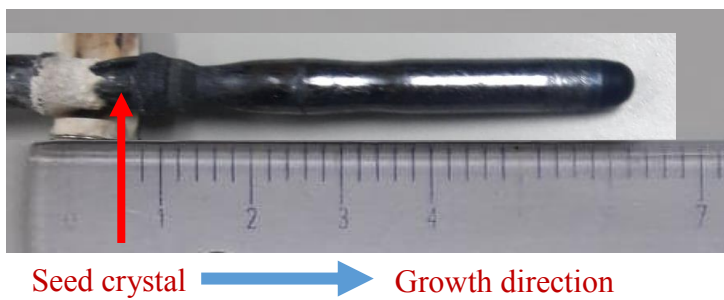


Fig. 4-2. As grown single crystals of  $\text{LiCoO}_2$  used for measuring electrochemical properties.



Fig. 4-3 Coin-cell preparation.

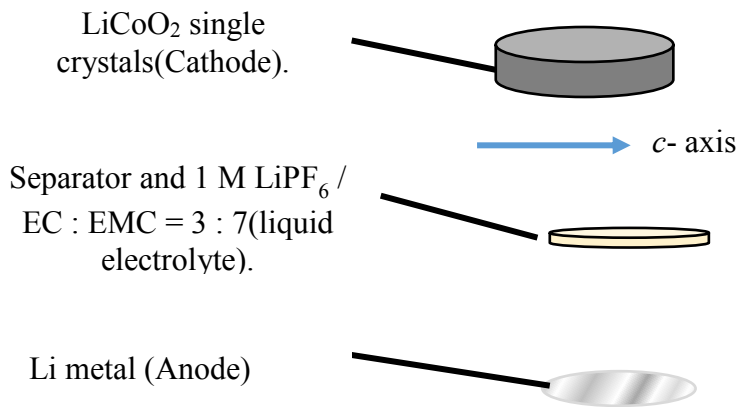


Fig. 4-4 Experimental procedure for coin-cell preparation using liquid electrolyte.



Fig. 4-5 Argon filled globe box used for coin-cell preparation.

Experimental section for coin-cell preparation using  $\text{LiCoO}_2$  single crystals cathode and liquid electrolyte.

#### 4.2.2 Coin cell using gel electrolyte

In next experiment, coin cell was prepared in the same manner but only the electrolyte was changed. The liquid electrolyte was replaced by a 3-dimensionally ordered microporous LiTFSI/ EMITFSI gel electrolyte. LiCoO<sub>2</sub> single crystals of about 180 μm thickness was used as cathode and Li metal foil was used as anode. Aluminum and Copper foils were used as current collector. Experimental procedure for coin-cell preparation using LiCoO<sub>2</sub> single crystals cathode and gel electrolyte was shown in Fig. 4-6. The charge discharge cycles of the prepared cells were studied in the current rate of from 0.1 C and voltage range of 2.5 - 4.5 V.

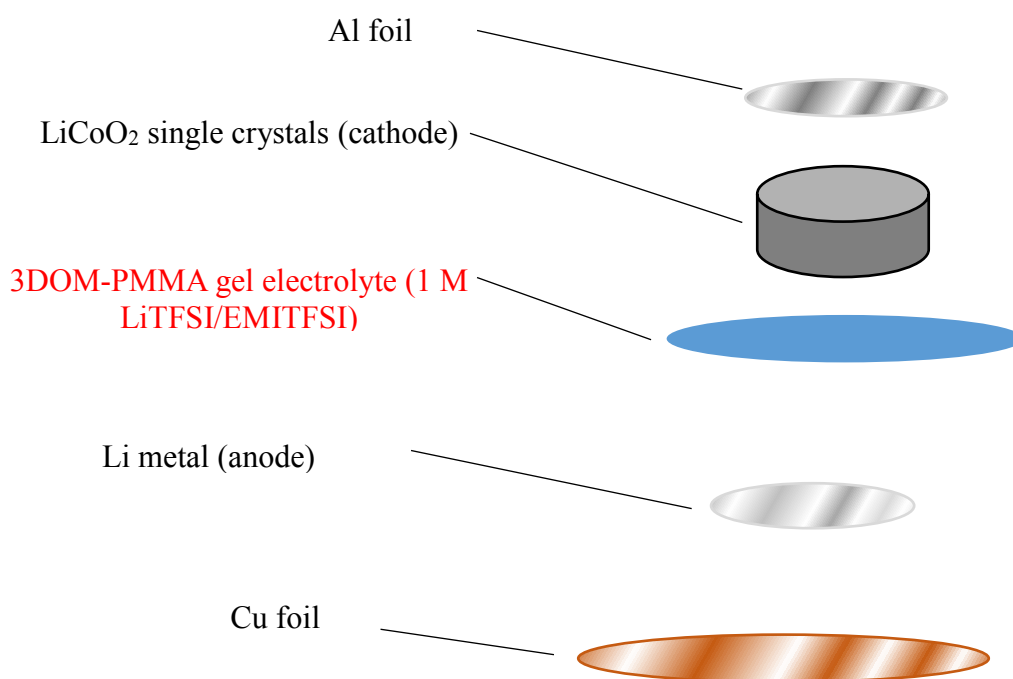
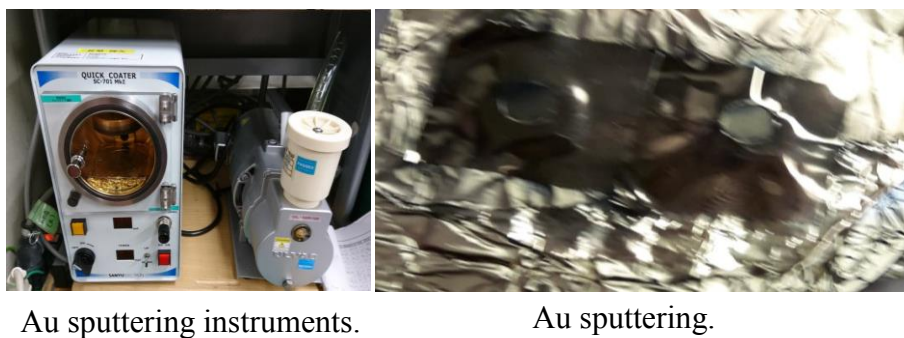


Fig. 4-6 Experimental procedure for coin-cell preparation using LiCoO<sub>2</sub> single crystals cathode and gel electrolyte.

### **4.2.3 Coin cell using LLZO polycrystalline solid electrolyte**

In order to prepare all solid state LIBs, the coin cell was prepared using LLZO polycrystalline solid electrolyte material of thickness 500  $\mu\text{m}$ . Since in this experiment all the parts were solid,  $\text{Li}_3\text{BO}_3$  was used to achieve good interface between the  $\text{LiCoO}_2$  single crystals cathode and LLZO solid electrolyte.  $\text{Li}_3\text{BO}_3$  is a high viscous material and can connect the solid parts efficiently. This is the main reason for using  $\text{Li}_3\text{BO}_3$  between cathode and solid electrolyte. Here, cathode, electrolyte and anode were Li-based materials, so Au sputtering was used to avoid interaction between the Li metal anode and LLZO solid electrolyte. The apparatus used for Au sputtering was shown in Fig. 4-7. The  $\text{LiCoO}_2$  single crystals of 200  $\mu\text{m}$  thickness and 7 mm in diameter was used as cathode, and Li metal foil was used as anode. Experimental procedure for coin-cell preparation using  $\text{LiCoO}_2$  single crystals cathode and LLZO polycrystalline solid electrolyte was shown in Fig. 4-8.



Au sputtering instruments.

Au sputtering.

Fig. 4-7 Apparatus used for Au sputtering.

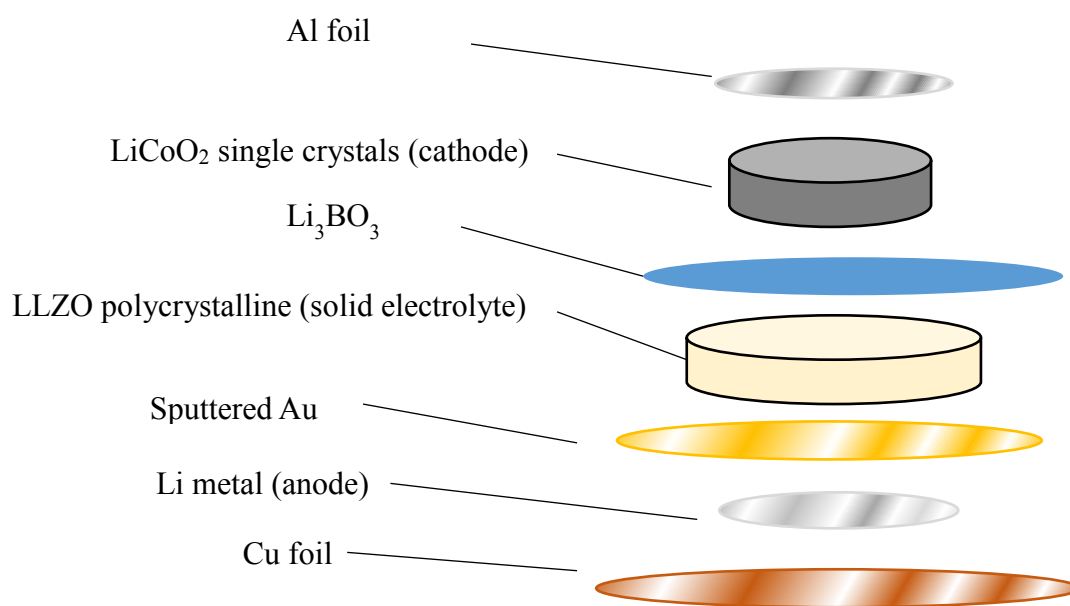


Fig. 4-8 Experimental procedure for coin-cell preparation using LiCoO<sub>2</sub> single crystals cathode and LLZ polycrystalline solid electrolyte.

Experimental section for coin-cell preparation using LiCoO<sub>2</sub> single crystals cathode and LLZ polycrystalline solid electrolyte.

#### **4.2.4 Coin cell using LLN single crystals solid electrolyte**

In addition, to design all solid state LIBs using both single crystals cathode and electrolyte, the coin cell was prepared using  $\text{LiCoO}_2$  single crystals cathode of thickness 200  $\mu\text{m}$  and LLN single crystals electrolyte of thickness 500  $\mu\text{m}$ . One three dimensionally ordered microporous gel that is 3DOM-PMMA gel (LiFSI-G4) was used as separator to avoid the interaction between the  $\text{LiCoO}_2$  single crystals cathode and LLN single crystals electrolyte. Same gel was also as separator to avoid the interaction between the LLN single crystals electrolyte and Li metal anode. Experimental procedure for coin-cell preparation using  $\text{LiCoO}_2$  single crystals cathode and LLN single crystals solid electrolyte was shown in Fig. 4-12. The charge discharge cycles of the prepared cells were studied in the current rate of from 0.01 C and voltage range of 2.5 - 4.5 V.



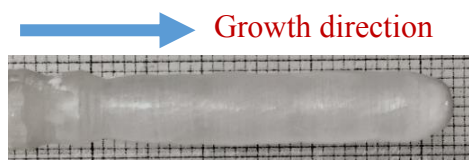


Fig. 4-9 As grown single crystals of LLN used as solid



Fig. 4-10 Samples of thickness 300 ~ 500  $\mu\text{m}$



Fig. 4-11 Coin cell preparation

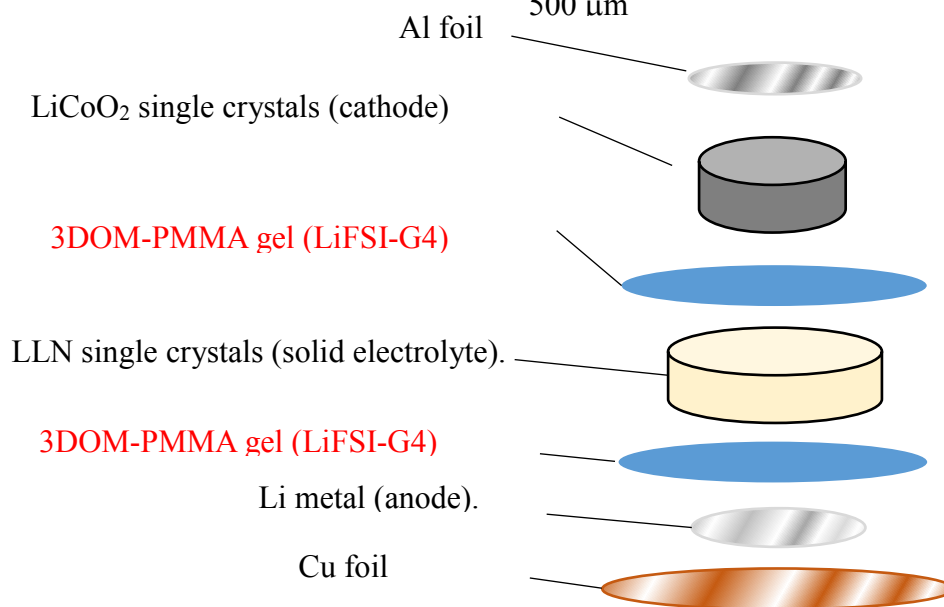
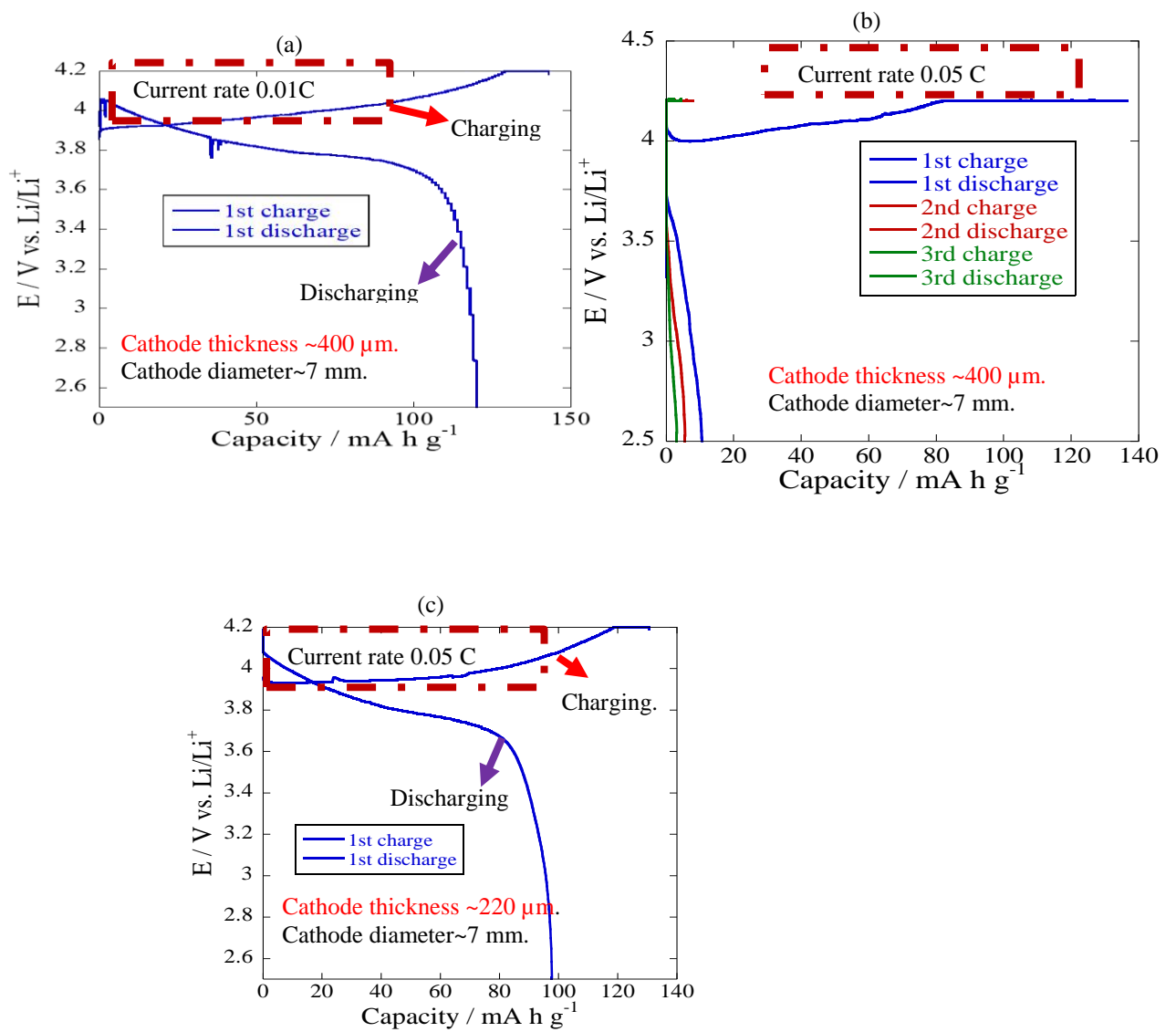


Fig. 4-12 Experimental procedure for coin-cell preparation using LiCoO<sub>2</sub> single crystals cathode and LLN single crystals solid electrolyte.

Experimental section for coin-cell preparation using LiCoO<sub>2</sub> single crystals cathode and LLN single crystals solid electrolyte solid electrolyte.

### 4.3 Charge discharge characteristics of LIBs using $\text{LiCoO}_2$ single crystals cathode

#### 4.3.1 Liquid electrolyte



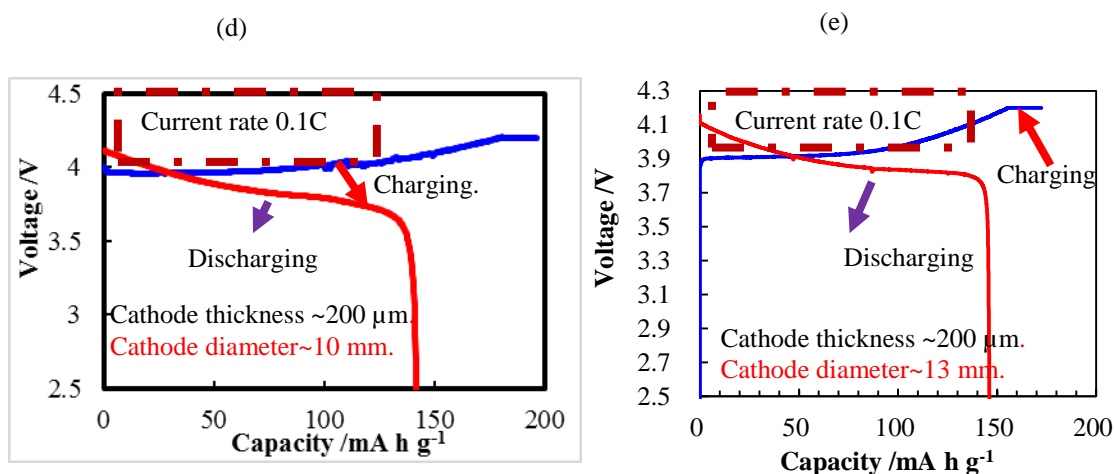


Fig. 4-13 Charge-discharge characteristics of LIBs at different current rate using LiCoO<sub>2</sub> single crystals cathode and liquid electrolyte.

The charge-discharge characteristics of LIBs using LiCoO<sub>2</sub> single crystals cathode with liquid electrolyte at different current rates were shown in Fig. 4-13. First, I tried to prepare coin cell using LiCoO<sub>2</sub> single crystals cathode of thickness 400 μm and studied the charge discharge characteristics at lower current rate of 0.01 C using liquid electrolyte. The coin cell worked successfully and the discharge capacity was 125 mAh/g as shown in Fig. 4-13(a). Next, in order to study the charge-discharge characteristics at higher current rate, the coin cell was prepared in the same condition as that for 0.01 C current rate. The prepared coin cell did not work properly (Fig. 4-13(b)) at higher current rate due to the high impedance of the coin cell. The reason for the high impedance of the coin cell was the high cathode thickness. As the cathode thickness was reduced from the 400 μm to 220 μm, the coin cell worked successfully and the discharge capacity was 90 mAh/g as shown in Fig. 4-13(c). This results implies that the thickness of the cathode had a significant effect on the impedance of the coin cell. I also designed a coin cell using larger diameter that is

10 mm diameter  $\text{LiCoO}_2$  single crystals cathode of thickness 200  $\mu\text{m}$  and studied the charge discharge characteristics at a higher current rate of 0.1 C. In this case, the higher discharge capacity that is 140 mAh/g was achieved as shown in Fig. 4-13(d). As for the practical application of  $\text{LiCoO}_2$  single crystals in LIBs, half inch diameter single crystals cathode is required. In this regards, I prepared the coin cell using the  $\text{LiCoO}_2$  single crystals cathode of more than half inch that is 13 mm diameter and studied the capacity of LIBs. The discharge capacity was increased to 145 mAh/g as shown in Fig. 4-13(e).

Actually, at present,  $\text{LiCoO}_2$  powders are commercially used in mobile electronics. The discharge capacities of commercially used  $\text{LiCoO}_2$  powder cathode was 140 mAh/g [33] with conductive liquid and binder at voltage 4.2 V. The discharge capacities without conductive and binder will be 126 mAh/g. Teshima et al. has reported that the discharge capacity of flux growth  $\text{LiCoO}_2$  crystals using liquid electrolyte with the current rate of 0.1 C and a voltage range from 2.4 to 4.2 V was 130 mAh/g [34]. But this capacity was not the pure  $\text{LiCoO}_2$  capacity because author mixed 80 wt%  $\text{LiCoO}_2$  crystals powder with some ionic conducting liquid and prepared the cathode. Actual capacity of  $\text{LiCoO}_2$  crystals will be 104 mAh/g. Mizuno et al. has also reported the discharge capacity of flux growth  $\text{LiCoO}_2$  crystals of 131 mAh/g[35] using the same cell preparation conditions as mentioned in reference 42. But the actual capacity of pure  $\text{LiCoO}_2$  will be 104.8 mAh/g. Zhiguo et al; has prepared the  $\text{LiCoO}_2$  powder samples by high-temperature solid-state calcination technique and studied the electrochemical performance of  $\text{LiCoO}_2$  power cathode. Author has reported that the discharge capacity of 80 wt%  $\text{LiCoO}_2$  power mixed with ionic conducting solution was 157.7 mAh/g within the voltage range of

3.0 – 4.3 V and a current rate of 0.1 C using liquid electrolyte [36]. The actual capacity of LiCoO<sub>2</sub> power cathode will be 126.16 mAh/g. In all cases, Li-metal was used as anode during coin cell preparation [34-36]. Electrochemical performance of LiCoO<sub>2</sub> powder synthesized by solid-state synthesis route involving the decomposition and intercalation of hydroxide precursors has studied by Huang [37]. The discharge capacity of cathode prepared by mixing 78 wt% LiCoO<sub>2</sub> powders with ionic conducting liquid and binding agents was 142 mAh/g within the voltage range of 2.5-4.25 V and a current rate of 0.2 C. The actual capacity of LiCoO<sub>2</sub> will be 113.6 mAh/g. Liquid electrolyte and graphite anode was used during the coin cell preparation.

Since many research has been conducted on the electrochemical performance of LiCoO<sub>2</sub> polycrystalline materials but the discharge capacity was limited to 126 mAh/g. Actually, grain boundaries in the polycrystalline LiCoO<sub>2</sub> limits the capacity by affecting the movement of Li-ion in LIBs. In addition, polycrystalline LiCoO<sub>2</sub> shows isotropic conductivity.

Actually in our experiment, we have used fair LiCoO<sub>2</sub> single crystals as a cathode without conductive additives and binders. Authors in previous reports prepared the cathode by adding LiCoO<sub>2</sub> powders with conductive additives and binders. Actually, the conductivity of the binder is very low that may effects on reducing capacities of the polycrystalline cathode.

### 4.3.2 Gel electrolyte

The charge-discharge characteristics of LIBs using LiCoO<sub>2</sub> single crystals cathode with gel electrolyte at a current rate of 0.1 C and within the voltage range of 2.5 to 4.2 V was shown in Fig. 4-14. The discharge capacity of LIBs using gel electrolyte was 90 mAh/g which was lower than the capacities using liquid electrolyte due to the high impedance of the prepared coin cell. Actually the capacity of LIBs depends mainly on the impedance of the coin cell and the synthesis process of the coin cell. In addition, the impedance of the coin cell is mainly related with the thickness of the cathode layer. In our experiment, the thickness of LiCoO<sub>2</sub> single crystals was 180 μm, but 100 μm is better. It was very difficult to cut the LiCoO<sub>2</sub> single crystals as thin as 100 μm thickness due to the brittle behavior of the crystals. In addition, in this experiment, gel electrolyte was used that has some impedance that significantly contribute to the total impedance of the coin cell. Although capacity was slightly lower using gel electrolyte compared to the liquid electrolyte, the liquid electrolyte may create leakage and firing problem. In the concern of the safety issue, the design of almost all solid state LIBs is promising for the further development of next generation LIBs.

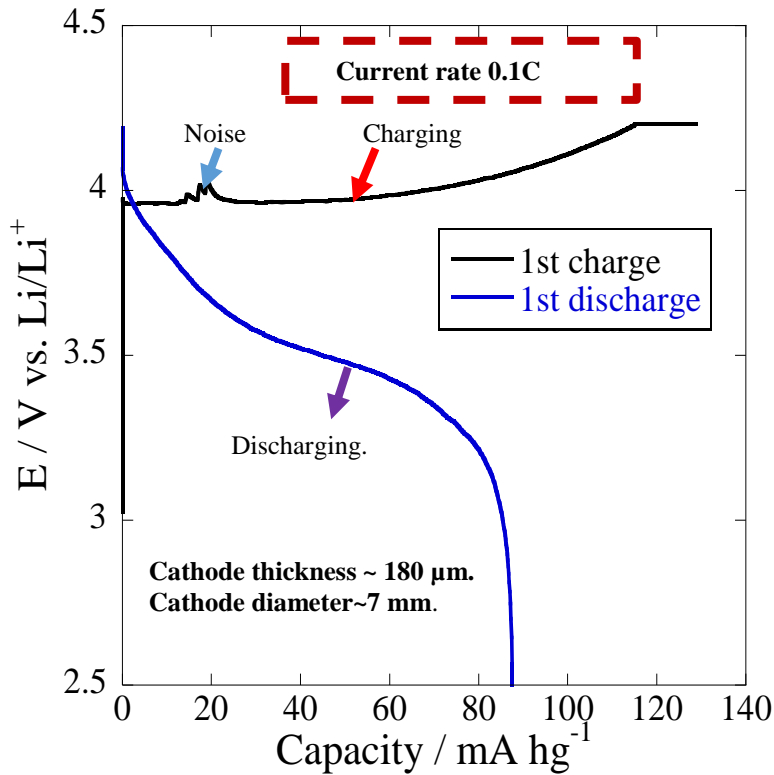


Fig. 4-14 Charge-discharge profiles of the LIBs using the LiCoO<sub>2</sub> single crystals cathode and gel electrolyte.

### 4.3.3 LLZO polycrystalline solid electrolyte

I tried to design all solid state LIBs using LLZO polycrystalline solid electrolyte and studied the charge discharge characteristics of the prepared coin cell. Due to high impedance of coin cell as shown in Fig. 4-15, it was unable to work properly. In the case of all solid state LIBs, cathode, anode and electrolyte all the parts are solid. As a result. The impedance of the coin cell becomes high. In addition, the connection among all solid part is difficult. To connect the cathode with the solid electrolyte, Li<sub>3</sub>BO<sub>3</sub> was used in our experiment. Li<sub>3</sub>BO<sub>3</sub> is a high viscous material, it not only connects the solid parts but also helps to achieve good interface between the cathode

and solid electrolyte. Although  $\text{Li}_3\text{BO}_3$  was used for the interface modification, but the coin cell did not work. So it was difficult to design all solid state LIBs using  $\text{LiCoO}_2$  single crystals cathode and solid electrolyte.

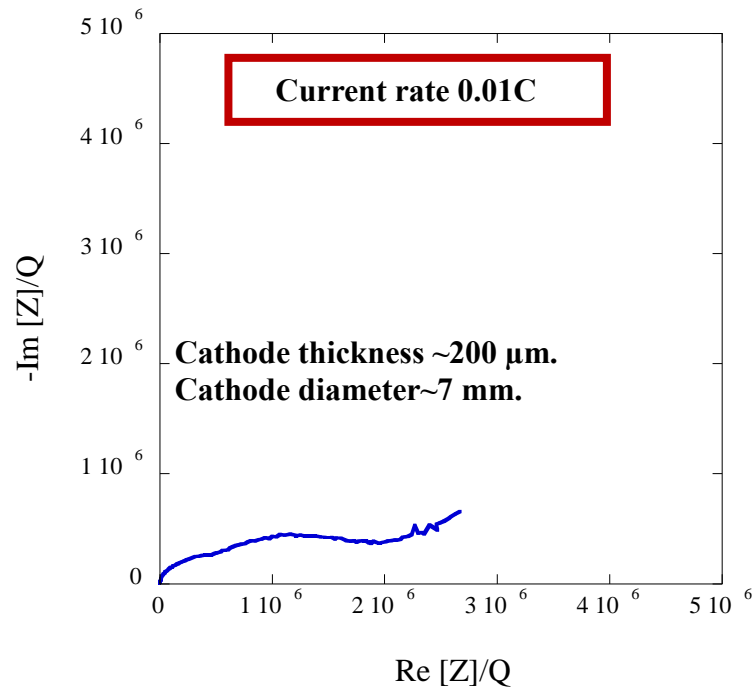


Fig. 4-15 Impedance curve of coin-cell using  $\text{LiCoO}_2$  single crystals cathode and LLZO polycrystalline solid electrolyte.

#### 4.3.4 LLN single crystals solid electrolyte

I also tried to design all solid state LIBs using both  $\text{LiCoO}_2$  single crystals cathode and LLN single crystals solid electrolyte. The charge-discharge characteristics of the prepared coin cell was studied within the voltage range of 2.5 to 4.5 V and lower current rate that is 0.01 C (Fig.4-16). In this experiment, 3 dimensionally ordered micro porous (3DOM) gel was used as a separator to avoid interaction between the  $\text{LiCoO}_2$  single crystals cathode and LLN single crystals solid electrolyte. Also same gel was used between the LLN single crystals solid electrolyte and Li metal anode



as a separator to avoid interaction between them. These gels had some impedance that increases the total impedance of the coin cell. As a result, we failed to design all solid state LIBs using both LiCoO<sub>2</sub> single crystals cathode and LLN single crystals solid electrolyte due to the high impedance of the coin cell.

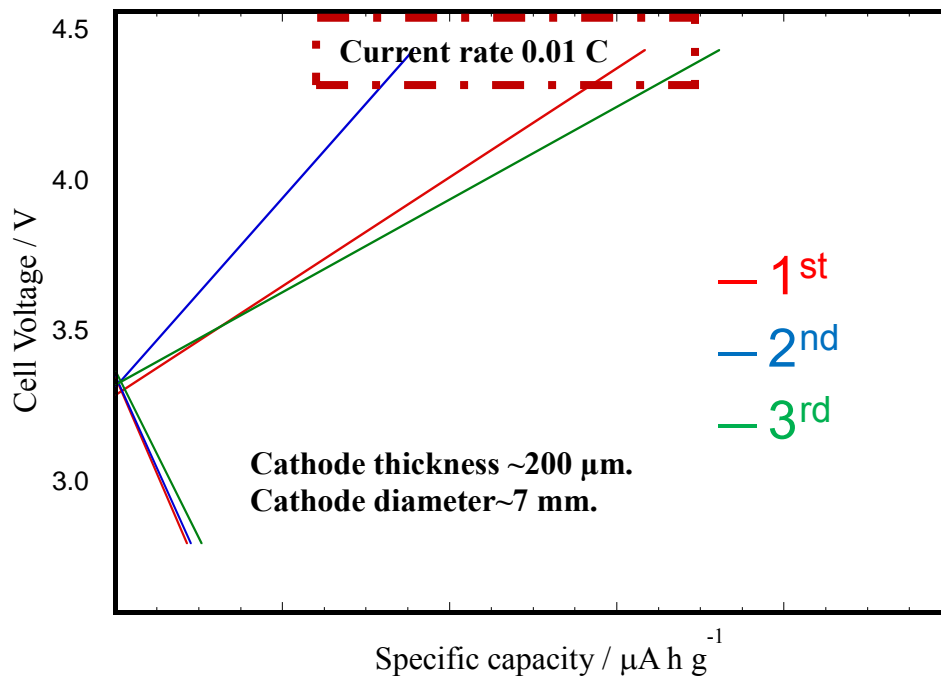


Fig. 4-16 Charge-discharge profiles of the LIBs using the LiCoO<sub>2</sub> single crystals cathode and LLN single crystals solid electrolyte.

#### 4.4 Conclusions

In this chapter, the electrochemical properties of LiCoO<sub>2</sub> single crystals were studied by preparing the coin cell of LIBs. The discharge capacities of LIBs using LiCoO<sub>2</sub> single crystals cathode of 13 mm in diameter and 200 μm thickness with liquid electrolyte was 145mAh/g which was higher than the commercially available LiCoO<sub>2</sub> polycrystalline materials (126 mAh/g). This research is a highly novel

research in the field of further development of LIBs. Nobody has reported the discharge capacity of LIBs using pure  $\text{LiCoO}_2$  single crystals cathode. Although some researchers have reported the discharge capacity of LIBs using  $\text{LiCoO}_2$  crystals grown by flux method, but the capacity was limited due to their cathode preparation process. Authors crushed the crystals and mixed with some ionic conducting solution and prepared the cathode. In this study, I have grown large  $\text{LiCoO}_2$  single crystals by TSFZ technique and cut the grown crystals perpendicular to the growth direction and used the pure single crystals of  $\text{LiCoO}_2$  as a cathode. Due to the use of the fair  $\text{LiCoO}_2$  single crystals without conducting liquid and binders, the capacity was increased compared to the previous studies. I have successfully designed all most all solid state LIBs using  $\text{LiCoO}_2$  single crystals cathode for the first time. The discharge capacity was 90 mAh/g. This is a highly novel research work for the further enhancement of the performance of the next generation all solid state LIBs technologies. Up to now, nobody has reported about the design of almost all solid state LIBs using the fair  $\text{LiCoO}_2$  single crystals cathode. These charge discharge characteristics of LIBs using  $\text{LiCoO}_2$  single crystals cathode could be applicable for the development of next generation all solid state LIBs with regards to the safety issues. In addition, my attempt to design all solid state LIBs using the fair  $\text{LiCoO}_2$  single crystals cathode and single crystals solid electrolyte did not successful due to the high impedance of the coin cells. Although of all solid state LIBs using both single crystals cathode and electrolyte is difficult, improved synthesis technique of coin cell may bring the success in the design of next generation all solid state LIBs.

## References:

- [1] Y. Nishi, *J. Power Sources*, **100** (2001) 101.
- [2] R.F. Nelson, *J. Power Sources*, **107** (2002) 226.
- [3] T. Takamura, *Solid State Ionics*, **152** (2002) 19.
- [4] O. Bitsche, G. Gutmann, *J. Power Sources*, **127** (2004) 8.
- [5] S.S. Zhang, K. Xu, T.R. Jow, *J. Power Sources*, **160** (2006) 1349
- [6] C. Liu, Z.G. Neale, G. Cao, *Materials Today*, **19** (2016) 2.
- [7] M. S. Whittingham, *Materials Research Bulletin*, **33** (2008) 411.
- [8] M. Menetrier, I. Saadoune, S. Levasseur, C. Delmas, *J. Mater. Chem.*, **9** (1999) 1135.
- [9] M. Wakihara, *Materials Science and Engineering: R: Reports*, **33** (2001) 109.
- [10] J.M. Tarascon, M. Armand, *Nature*, **414** (2001) 359.
- [11] K. Amine, J. Liu, S. Kang, I. Belharouak, Y. Hyung, D. Vissers, G. Henriksen, *J. Power Sources*, **129** (2004) 14.
- [12] M. Armand, J.-M. Tarascon, *Nature*, **451** (2008) 652.
- [13] J.B. Goodenough, Y. Kim, *Chem. Mater.* **22** (2010) 587.
- [14] J. B Bates, N. J. Dudney, B. Neudecker, A. Ueda, C.D. Evans, *Solid State Ionics*, **135** (2000) 45.
- [15] P. Birke, F. Salam, S. Döring, W. Weppner, *Solid State Ionics*, **118** (1999) 149.
- [16] P. H. L. Notten, F. Roozeboom, R. A. H. Niessen, L. Baggetto, *Adv. Mater.* **19** (2007) 4564.
- [17] J. W. Fergus, *J. Power Sources*, **195** (2010) 4554.

- [18] M. Wakihara, *Materials Science and Engineering: R: Reports*, **33** (2001) 109.
- [19] DoITPoMS, TLP Library, *Atomic Scale Structure of Materials, Introduction*, University of Cambridge, 2004-2020.
- [20] Y. Takahashi, Y. Gotoh, J. Akimoto, S. Mizuta, K. Tokiwa, T. Watanabe, J. *Solid State Chem.* **164** (2002) 1.
- [21] A. Manthiram, X. Yu, S. Wang, *Nat. Rev. Mater.* **2** (2017) 16103.
- [22] J. Janek, W. G. Zeier, *Nat. Energy*, **1** (2016) 16141.
- [23] M. D. Tikekar, S. Choudhury, Z. Tu, L. A. Archer, *Nat. Energy*, **1** (2016) 16114.
- [24] J. Li, C. Ma, M. Chi, C. Liang, N. Dudney, *J. Adv. Energy Mater.* **5** (2015) 1401408.
- [25] J. C Bachman, S. Muy, A. Grimaud, H.-H. Chang, N. Pour, S. F. Lux, O. Paschos, F. Maglia, S. Lupart, P. Lamp, L. Giordano, Y. Shao-Horn, *Chem. Rev.* **116** (2016)140.
- [26] C. Masquelier, *Nat. Mater.* **10** (2011)649.
- [27] N. Kamaya, K. Homma, Y. Yamakawa, M. Hirayama, R. Kanno, M. Yonemura, T. Kamiyama, Y. Kato, S. Hama, K. Kawamoto, A. Mitsui, *Nat. Mater.* **10** (2011) 682.
- [28] C. Ma, M. F. Chi, *Energy Res.* **4** (2016) 23.
- [29] Y. Wang, W. D. Richards, S. P. Ong, L. J. Miara, J. C. Kim, Y. Mo, G. Ceder, *Nat. Mater.* **14** (2015) 1026.
- [30] A. Varzi, R. Raccichini, S. Passerini, B. Scrosati, *J. Mater. Chem. A*, **4** (2016) 17251.

- [31] M.S. Ali, N. Sato, I. Fukasawa, Y. Maruyama, M. Nagao, S. Watauchi, I. Tanaka, *Cryst. Growth Des.* **19** (2019) 6291.
- [32] NEI Corporation. Battery News. Solid-electrolytes. April 10, 2017.
- [33] C.M. Julien, A. Mauger, K. Zaghbi, H. Groult, *Inorganics*, **2** (2014)132.
- [34] K. Teshima, S. Lee, Y. Mizuno, H. Inagaki, M. Hozumi, K. Kohama, K. Yubuta, T. Shishido, S. Oishi, *Cryst. Growth Des.*, **10** (2010) 4471.
- [35] Y. Mizuno, N. Zettsu, K. Yubuta, T. Sakaguchi, T. Saito, H. Wagata, S. Oishi, K. Teshima, *Cryst. Growth Des.* **14** (2014)1882.
- [36] Zhiguo, W; & Zhixing, W; & Wenjie, P; Huajun, G; Xinhai, L; Jiexi, W; Ai, Q; *Ionics* (2014) 20:1525–1534.
- [37] B. Huang, Y-I. Jang, Y-M. Chiang, D. R. Sadoway, *Journal of Applied Electrochemistry*, 28 (1998) 1365±1369.

## CHAPTER 5

### *Single crystal growth of Nb doped LiCoO<sub>2</sub> by TSFZ method using tilting mirror furnace*

#### 5.1 Introduction

In recent times, Lithium-ion batteries (LIBs) are very promising in our modern society because of their long life cycle, resistance to the memory effect, low contribution to environmental pollution, low self-discharge rate, and high energy density [1–5]. These batteries have been used in mobile phones, computers, digital cameras, etc. [6–11]. The layered LiCoO<sub>2</sub> material is still commercially used in lithium-ion batteries due to its prominent advantages, such as a high working voltage, high specific energy, and high conductivity [12].

Although commercially used LiCoO<sub>2</sub> cathode material has many advantages, some problems limits the improvement of the performance of LIBs. First, its theoretical capacity is 274 mAh g<sup>-1</sup> [13] but the practical achieved discharge capacity is limited. I have designed LiCoO<sub>2</sub> single crystalline cathode to enhance the capacity of LIBs and achieved the maximum practical discharge capacity of 145 mAh g<sup>-1</sup>.

Second, the structure of  $\text{LiCoO}_2$  changes after multiple cycles of deintercalation and intercalation of lithium ions during the charge and discharge process, which increases its internal resistance and decreases its capacity [14].

### **5.1.1 Previous reports on doped $\text{LiCoO}_2$**

#### **5.1.2 Purpose for doping Nb in $\text{LiCoO}_2$ cathode**

Sivajee-Ganesh et al; reported one reason is that cobalt may be dissolved in the electrolyte when the delithiated during charging. Another reason is that the  $\text{CoO}_2$  layer formed after full delithiation shears from the electrode surface and the layered structure collapses [15]. In addition, some authors reported that the lattice parameter changes by the insertion of more Li ions in  $\text{LiCoO}_2$  and can be responsible for the formation of micro cracking in the cathode particles [16–18]. Many researchers are trying to enhance the capacity and cycle performance of  $\text{LiCoO}_2$  beyond 4.2 V, so as to increase the energy density.

Element doping i.e. partial substitutions of bare transition metal (Co) by a different metal elements is an effective way for improving the electrochemical properties of  $\text{LiCoO}_2$ . Previous studies have reported a great deal of information about doping various elements into the  $\text{Co}^{3+}$  site of  $\text{LiCoO}_2$ , such as Mn [19], Mg [20], Cr [21], and

Ca [22]. However, there are few reports about the influence on the electrochemical properties of  $\text{Li}^+$  site doping of  $\text{LiCoO}_2$ . Xie reported that partially substituting the  $\text{Li}^+$  site of  $\text{LiNi}_{0.8}\text{Co}_{0.05}\text{Al}_{0.15}\text{O}_2$  with  $\text{Na}^+$  could broaden the spacing of the Li layer and accelerate the migration rate of lithium ions, thus the rate performance is improved [23]. In addition, Haruki Kaneda suggested that when the  $\text{Li}^+$  site of  $\text{LiNi}_{0.6}\text{Co}_{0.2}\text{Mn}_{0.2}\text{O}_2$  was partially substituted with high-valence  $\text{Nb}^{5+}$ , both the thermal stability and the cycling stability of  $\text{LiNi}_{0.6}\text{Co}_{0.2}\text{Mn}_{0.2}\text{O}_2$  were improved. He also mentioned the reason for improving thermal and the cycling stability by doping of  $\text{Nb}^{5+}$  in  $\text{Li}^+$  site. The doping  $\text{LiNi}_{0.6}\text{Co}_{0.2}\text{Mn}_{0.2}\text{O}_2$  with Nb formed a Nb-O bond that was stronger than the Li-O bond and improved the electrical conductivity, which increased the thermal stability and cycling stability [24].

Kang Wu et al; [14] first synthesized  $\text{LiCoO}_2$ , Na-doped  $\text{LiCoO}_2$ , Zr-doped  $\text{LiCoO}_2$ , and Nb-doped  $\text{LiCoO}_2$  by solid-phase sintering technique and studied the charge/discharge performance of the doped and un-doped  $\text{LiCoO}_2$  cathode. The electrochemical properties showed that the samples doped with the high-valence elements Zr and Nb had a higher capacity, better cycle stability, and better rate performance than those doped with the low-valence element Na. The capacity retention of  $\text{LiCoO}_2$ ,  $\text{Li}_{0.97}\text{Na}_{0.03}\text{CoO}_2$ ,  $\text{Li}_{0.99}\text{Zr}_{0.01}\text{CoO}_2$ , and  $\text{Li}_{0.99}\text{Nb}_{0.01}\text{CoO}_2$  was 68, 42, 85, and 87%, respectively, after 80 cycles at a rate of 10 C at 55 °C. This results



indicates that the capacity retention of  $\text{Li}_{0.99}\text{Nb}_{0.01}\text{CoO}_2$  and  $\text{Li}_{0.99}\text{Zr}_{0.01}\text{CoO}_2$ , was higher than those of the un-doped material and  $\text{Li}_{0.97}\text{Na}_{0.03}\text{CoO}_2$  at a rate of 10 C.

In addition,  $\text{Li}_{0.99}\text{Nb}_{0.01}\text{CoO}_2$  and  $\text{Li}_{0.99}\text{Zr}_{0.01}\text{CoO}_2$  showed higher thermal stability in the charged state than the un-doped material and  $\text{Li}_{0.97}\text{Na}_{0.03}\text{CoO}_2$ .

He also reported that the charge transfer resistance for  $\text{Li}_{0.99}\text{Nb}_{0.01}\text{CoO}_2$  was 134  $\Omega$ , which was smaller than those of  $\text{LiCoO}_2$ ,  $\text{Li}_{0.97}\text{Na}_{0.03}\text{CoO}_2$ , and  $\text{Li}_{0.99}\text{Zr}_{0.01}\text{CoO}_2$ , namely 270, 175, and 178  $\Omega$ , respectively. The results indicate that doping with high-valence elements more effectively reduces the transmission resistance of lithium ions in the electrode and at the electrolyte interface.

This findings highly motivates me on the doping of high-valence Nb ions into the  $\text{Li}^+$  site of  $\text{LiCoO}_2$  for the improvements of the cycling performance, rate capacity, and thermal stability of next generation all solid state LIBs.

Since Kang Wu et al;[14] have measured the electrochemical performance of Nb-doped  $\text{LiCoO}_2$  polycrystalline materials, the grain boundaries in polycrystalline cathode may affect the movement of Li ions, this in turn lowers the capacity of LIBs.

### **5.1.3 Motivation**

I believe that single crystals of Nb-doped  $\text{LiCoO}_2$  can lead to enhance the performance of LIBs compared to Kang Wu work due to no grain boundaries that exhibits the true intrinsic properties of cathode.

In addition, the conductivity of polycrystalline material is isotropic. A single crystalline materials possess anisotropic ionic conductivity and high anisotropic conductivity is expected to enhance the performance of LIBs.

In this study, I have tried to grow 1 at% Nb-doped  $\text{LiCoO}_2$  single crystals by TSFZ technique for further development of cycling performance, rate capacity, and thermal stability of next generation all solid state LIBs.

### **5.2 Experimental details**

High purity of  $\text{Li}_2\text{CO}_3$ ,  $\text{Co}_3\text{O}_4$  and  $\text{Nb}_2\text{O}_5$  powders were used as starting raw materials. The powders were mixed together in a stoichiometric ratio and calcined at  $750^\circ\text{C}$  for 4 hours in air and feed rod was prepared using a rubber tube. The feed rod was pressed under a cold isostatic pressure of 300 MPa, sintered at  $1050^\circ\text{C}$  for 8 hours in oxygen flow, and then used as a feed rod. The feed rod was 7 mm in diameter and approximately 50 mm in length.

A Li-excess solvent was used for TSFZ growth due to the incongruent melting behavior of  $\text{LiCoO}_2$ . The calcined  $\text{LiCo}_{0.99}\text{Nb}_{0.01}\text{O}_2$  powder and  $\text{Li}_2\text{CO}_3$  powder were mixed in a Li:Co atomic ratio of 85:15, formed into a cylindrical shape approximately 7 mm in diameter using a hydrostatic press, and then used as a solvent disk for TSFZ growth without sintering. The solvent of 1.1 g was used for the TSFZ growth. The solvent attachment experiment was same as described in the chapter 2.

The growth apparatus as described in the previous chapter, a tilting-mirror-type image furnace (Crystal Systems Inc. model TLFZ-4000-H-VPO) with four ellipsoidal mirrors, as shown in Fig. 2-3, was used for the growth. Coil-type lamp filament was used in this experiment. All the growth experiments were performed at mirror tilting angle of  $\theta = 10^\circ$  due to the low convexity and high stability in this tilt condition [25]. In this experiment, the growth rate was 5 mm/h under an atmosphere of Ar with a flow rate of 1.5 L/min, and the upper and lower shaft rotation rates were 12 rpm and 25 rpm, respectively, in the opposite directions.

The sequence of experimental procedure was same except the quenching step as shown in Fig. 2-4 in chapter 2.

### 5.3 Single crystals growth of $\text{LiCo}_{0.99}\text{Nb}_{0.01}\text{O}_2$

I tried to grow 1 at% Nb-doped  $\text{LiCoO}_2$  single crystals of 7 mm in diameter by TSFZ technique using tilting mirror type image furnace. First, I have used  $\text{LiCo}_{0.99}\text{Nb}_{0.01}\text{O}_2$  polycrystalline material as a seed and tried to grow.

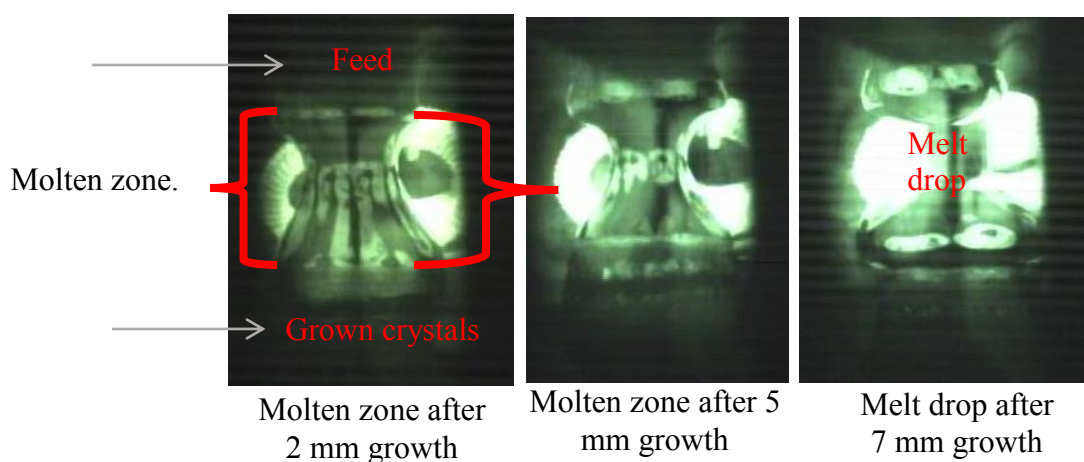


Fig. 5-1 Molten zone at different growth length during the growth of  $\text{LiCo}_{0.99}\text{Nb}_{0.01}\text{O}_2$ .

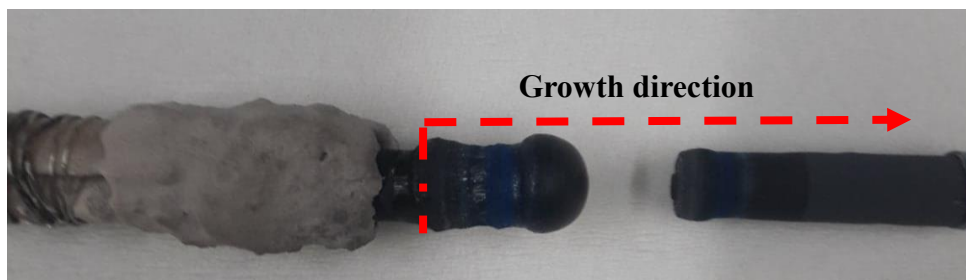


Fig. 5-2 Photograph of unsuccessful crystals of  $\text{LiCo}_{0.99}\text{Nb}_{0.01}\text{O}_2$  due to melt drop.

In this experiment, due to the Nb-doped, the feed melting temperature was increased compared to un-doped  $\text{LiCoO}_2$ . As the seeding was performed at 38% of the total lamp power but the feed melting was noticed at 54% of the total lamp power. As the solvent melts and seeding occurred, it is necessary to increase the lamp power from 38% to 54% to reach the feed melting temperature. Due to the high difference in melting temperature of solvent and feed, it was difficult to maintain the stable molten zone. As a result, melt drop occurred during the growth as shown in Figure 5-1.

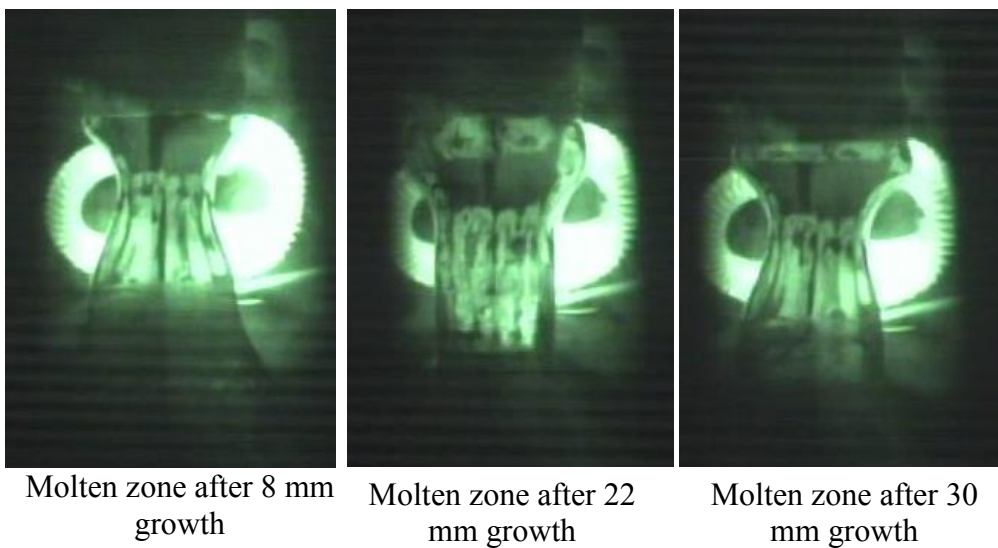


Fig. 5-3 Molten zone at different growth length during the growth of  $\text{LiCo}_{0.99}\text{Nb}_{0.01}\text{O}_2$ .

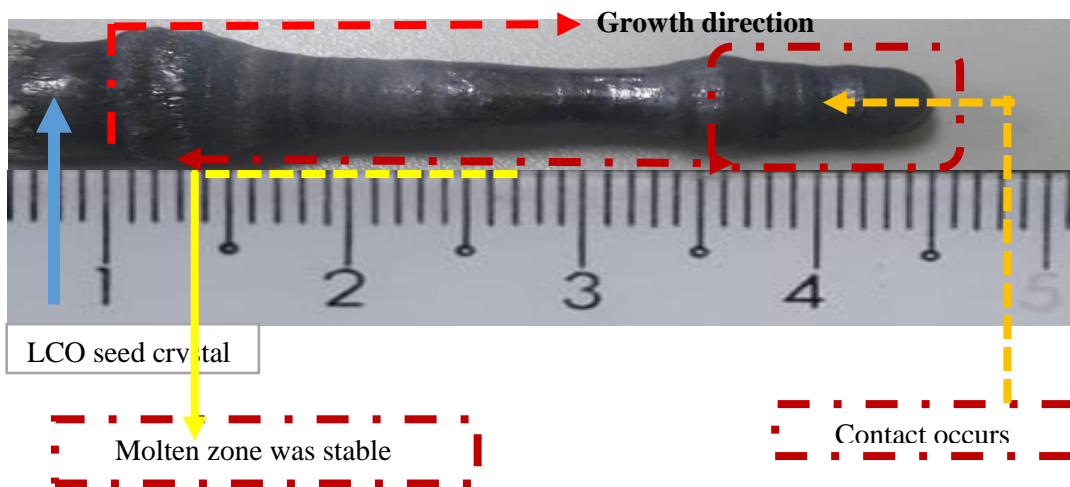


Fig. 5-4 As grown crystals of  $\text{LiCo}_{0.99}\text{Nb}_{0.01}\text{O}_2$  using  $\text{LiCoO}_2$  single crystals seed.

In next experiment, single crystals of  $\text{LiCoO}_2$  was used as a seed. In polycrystalline seed, the melt penetrates into the feed and detached the molten zone. In this time, I have successful to grow the  $\text{LiCo}_{0.99}\text{Nb}_{0.01}\text{O}_2$  crystals as shown in Figure 5-4. The molten zone was stable up to 25 mm growth length but at the end of the growth run the contact between the feed rod and grown crystals occurred. Due to the contact problem, some inclusions were found in SEM images of the grown crystals.

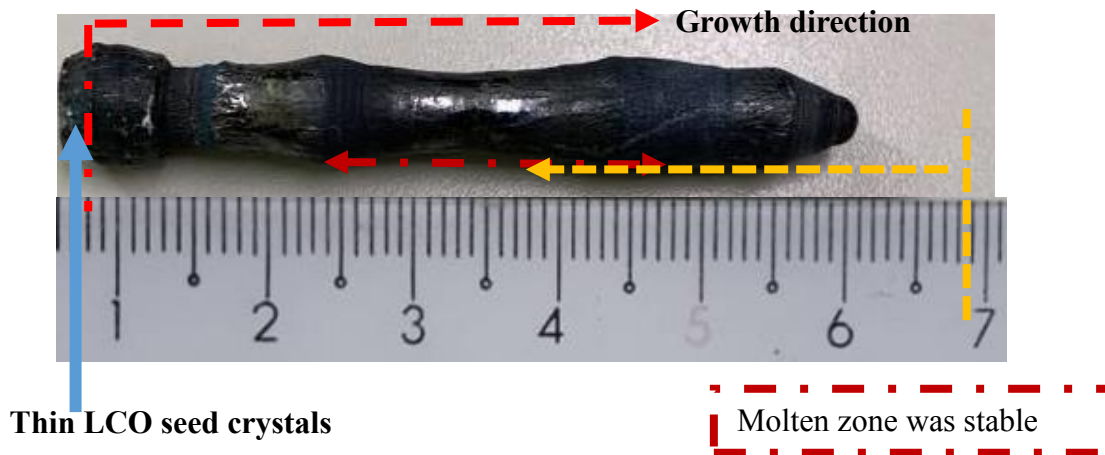


Fig. 5-5 As grown crystals of  $\text{LiCo}_{0.99}\text{Nb}_{0.01}\text{O}_2$  using thin  $\text{LiCoO}_2$  single crystals seed.

I also tried to grow  $\text{LiCo}_{0.99}\text{Nb}_{0.01}\text{O}_2$  crystals using thin  $\text{LiCoO}_2$  single crystals seed but did not successful due to the contact problem at the end of the growth run. So, further experiment is required to the find the optimized growth conditions for the successful TSFZ growth of  $\text{LiCo}_{0.99}\text{Nb}_{0.01}\text{O}_2$  single crystals.

## 5.4 Characterization of grown crystals

### 5.4.1 Scanning Electron Microscopy (SEM) images

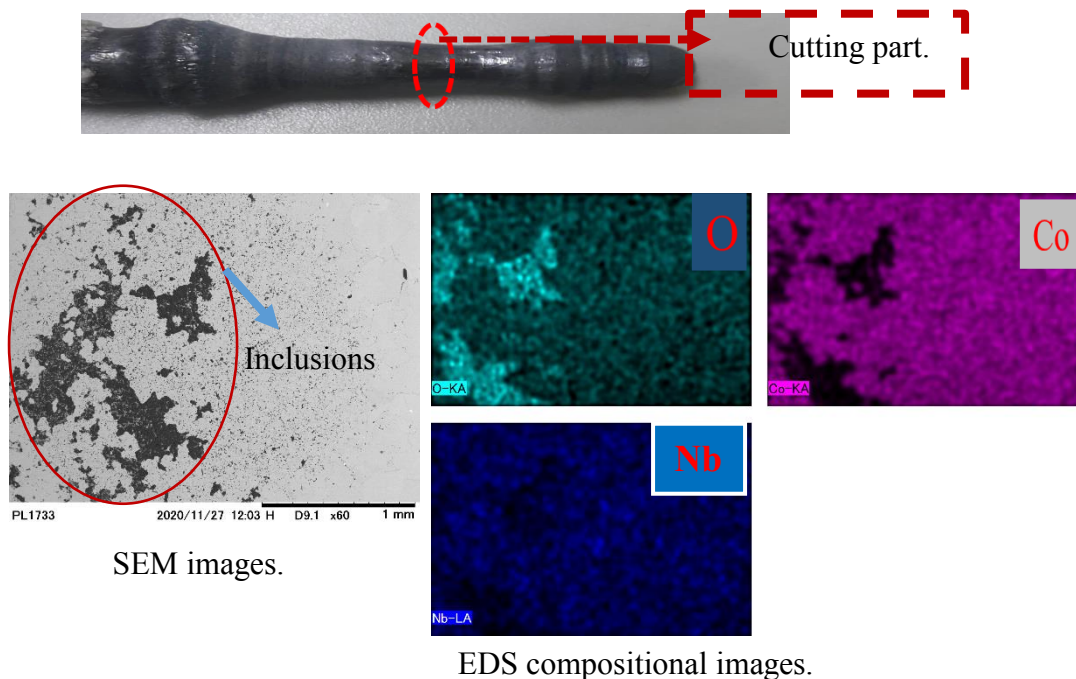


Fig. 5-6 SEM and EDS analysis of grown  $\text{LiCo}_{0.99}\text{Nb}_{0.01}\text{O}_2$  crystals at the center part.

SEM and EDS analysis of the grown crystals showed that some inclusions were observed in the grown crystals. The origin of inclusion may be due to the contact problem between the feed rod and grown crystals during the growth. Also oxygen concentration was high in the grown crystals compared to the undoped  $\text{LiCoO}_2$  single crystals as cleared from the EDS analysis of the grown crystals.



## 5.5 Conclusions

I have tried to grow 1 at% Nb-doped  $\text{LiCoO}_2$  single crystals by TSFZ technique using tilting-mirror-type furnace. Due to the high difference in melting temperature of solvent and feed, it was difficult to maintain the stable molten zone for long time. Instability in the molten zone occurred during the growth. SEM and EDS compositional images showed that some inclusions were observed in the grown crystals. So, further experiment is required for the stable growth of  $\text{LiCo}_{0.99}\text{Nb}_{0.01}\text{O}_2$  single crystals.

## References:

- [1] Z. Wang, C. Wu, L. Liu, F. Wu, L. Chen, X. Huang, *J. Electrochem Soc*, **149** (2002) A466.
- [2] M. Isobe, Y. Ueda, *Cheminform*, **383** (2004) 85.
- [3] Y.H. Wang, L. Chen, Y.G. Wang, Y.Y. Xia, *Electrochim Acta*, **173** (2015) 178.
- [4] Y. Ji, P. Zhang, M. Lin, W. Zhao, Z. Zhang, Y. Zhao, Y. Yang, *J Power Sources*, **359** (2017)391.

- [5] P. Rangaswamy, G.S. Suresh, M.M. Kittappa, *J Solid State Electrochem*, **20** (2016) 2619.
- [6] M. Chen, E. Zhao, D. Chen, M. Wu, S. Han, Q. Huang, L. Yang, X. Xiao, Z. Hu *Inorg Chem*, **56** (2017) 8355.
- [7] M. Chen, E. Zhao, Q. Yan, Z. Hu, X. Xiao, D. Chen, *Sci Rep*, **6** (2016) 29381
- [8] E. Zhao, M. Chen, Z. Hu, X. Xiao, D. Chen, *Electrochim Acta*, **208** (2016) 64.
- [9] B. Shen, P. Zuo, P. Fan, J. Yang, G. Yin, Y. Ma, X. Cheng, C. Du, Y. Gao, J. *Solid State Electrochem*, **21** (2016) 1195.
- [10] A. Swiderska-Mocek, A. Lewandowski, *J. Solid State Electrochem*, **21** (2017) 1365.
- [11] C. Rao, M.M. Liebenow, M. Jayalakshmi, H. Wulff, U. Guth, F. Scholz, *J Solid State Electrochem*, **5** (2001) 348.
- [12] J.M. Tarascon, M. Armand, *Nature*, **414** (2001) 359.
- [13] A. Burukhin, O. Brylev, P. Hany, B.R. Churagulov, *Solid State Ionics*, **151** (2002) 259.
- [14] K. Wu, Q. Li, M. Chen, D. Chen, M. Wu, Z. Hu, F. Li, X. Xiao, *Journal of Solid State Electrochemistry*, **22** (2018) 3725.
- [15] K. Sivajee-Ganesha, B. Purusottam-Reddy, O.M. Hussaina, A. Mauger, C.M. Julienc, *Materials Science and Engineering B*, **209** (2016) 30.

- [16] Q. Liu, H.T. Kuo, R.S. Liu, C.H. Shen, D.S. Shy, X.K. Xing, J.M. Chen, J. Alloys Compd. **496** (2010) 512.
- [17] Y.S. Jung, A.S. Cavanagh, A.C. Dillon, M.D. Groner, S.M. George, S.H. Lee, J. Elec-trochem. Soc. **157** (2010) A75.
- [18] S. Gopukumar, Y. Jeong, K.B. Kim, Solid State Ionics, **159** (2003) 223.
- [19] R. Stoyanova, E. Zhecheva, L. Zarkova, Solid State Ionics, **73** (1994) 233.
- [20] H. Tukamoto, A.R. West, Cheminform, **28** (1997) 3164.
- [21] A. Buyukburc, M.K. Aydinol, Int JMater Res, **105** (2014) 983.
- [22] R. Sathiyamoorthi, R. Chandrasekaran, A. Gopalan, T. Vasudevan, Mater Res Bull. **43** (2008) 1401.
- [23] H. Xie, K. Du, G. Hu, Z. Peng, Y. Cao, J Phys Chem C, **120** (2016) 3235.
- [24] H. Kaneda, Int J. Electrochem Sci, **12** (2017) 4640.
- [25] R. Parvin, Y. Maruyama, M. Nagao, S. Watauchi, I. Tanaka, Cryst. Growth Des. **20** (2020) 3413.

## CHAPTER 6

### *Social significance and business feasibility of the current research*

My research on the preparation of  $\text{LiCoO}_2$  single crystals cathode for the commercial application of Li-ion batteries is directly related with energy issue, social feasibility industrial application and will significantly contribute to the socio-economic development of the world. Lithium-ion batteries (LIBs) are one of the great successes of electrochemical energy storage devices utilized in diverse applications such as portable electronics, hybrid automobiles and even large-scale electrical power storage systems [1–4]. Since the first market emergence of LIBs in the 1990s, the performance of LIBs has been remarkably improved to meet the increasing demand for new energy storage systems with high energy density, high power density, long cycle life and a wide range of operating temperatures [5, 6]. Moreover, rechargeable batteries are rapidly expanding to drivetrains [7, 8], as can be seen from the quadrupled global sales of plug-in light vehicles from 0.55 to 2.21 million cars annually from 2015 to 2019 [9]. The global lithium-ion battery market was valued \$36.7 billion in 2019, and is projected to hit \$129.3 billion by 2027, at a CAGR of 18.0% from 2020 to 2027 [10]. The lithium-ion battery market growth is driven by need for smartphones and other electronics devices and increase in electric vehicles are some of the key factors

that significantly drive the growth of the global lithium-ion battery market. The competitive landscape of the market has also been examined by some of the companies' such which are A123 Systems, Automotive Energy Supply Corp., LG Chem, Panasonic, SAMSUNG SDI, Toshiba, Amperex Technology (ATL), BAK Group, Blue Energy, BYD, CBAK Battery, Tianjin Lishen Battery, Valence Technology, SK innovation, and Hitachi Ltd [11].

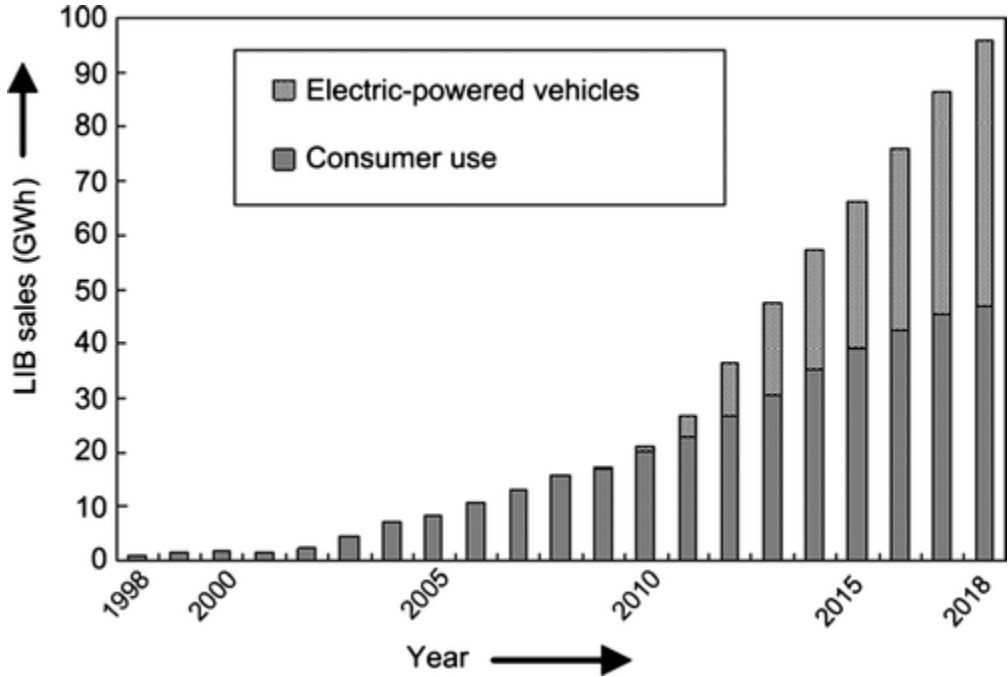


Fig. 6-1 Demands for Li ion batteries in two decades [12].

The demand for Li-ion batteries increases rapidly, especially with the demand from electric-powered vehicles as shown in Fig. 6-1 [12]. Thus, developing revolutionary energy storage systems is an important task in today's energy-dependent society.

Since the birth of the first commercial Li-ion batteries in 1991, portable electronic devices based on Li-ion batteries have been spared up, ranging from mobile phones, laptops, digital cameras, Walkman, MP3 players, and tablets, to wearable electronic devices that have become very popular in recent years [13].



Fig. 6-2 Development of various types of portable electronic devices from 1983 to 2018 [13].

Although LIBs using  $\text{LiCoO}_2$  polycrystalline cathode material is still commercially in many portable electronic devices, the discharge capacity of LIBs is so far from the theoretical capacity due to the limits of intrinsic properties of cathode. The grain boundaries in polycrystalline materials of  $\text{LiCoO}_2$  affects the movement of Li ions in

LIBs that limits the capacity of LIBs. The single crystals has no grain boundaries and exhibit the true intrinsic properties that makes it precious in industrial and technological applications. Due to highly anisotropic ionic conductivity in  $\text{LiCoO}_2$ , single crystals of  $\text{LiCoO}_2$  with thickness perpendicular the c-axis is strongly required to enhance the capacity and charge-discharge rate of LIBs for the further development of next generation all solid state LIBs[14].

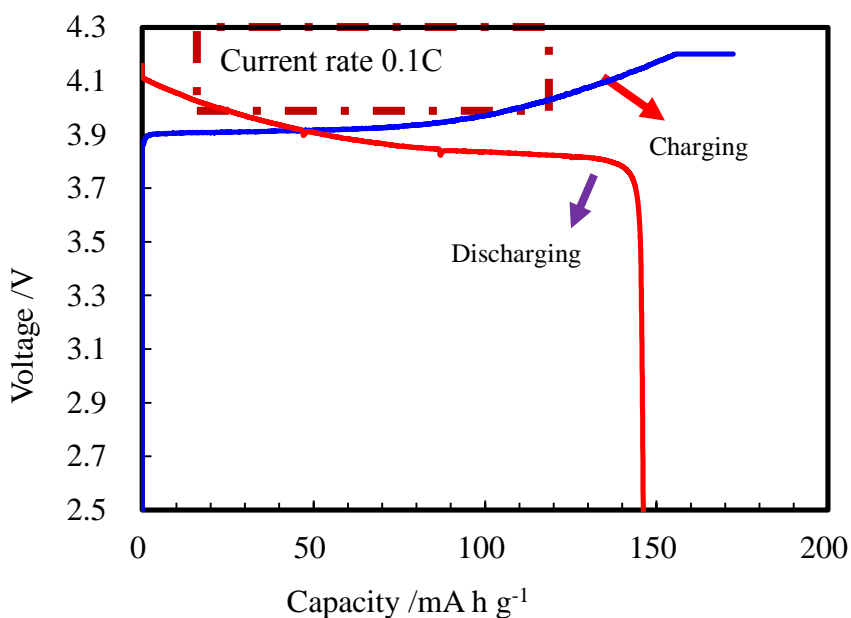


Fig. 6-3 Charge-discharge characteristics of LIBs using  $\text{LiCoO}_2$  single crystals cathode of 13 mm diameter with liquid electrolyte.

In the present research, I prepared single crystals of  $\text{LiCoO}_2$  and designed a LIBs using the fair  $\text{LiCoO}_2$  single crystals cathode with organic liquid electrolyte.  $\text{LiCoO}_2$  single crystals works successfully in LIBs for the first time and higher discharge

capacity that is 145 mAh/g was achieved as shown in Fig.6-3. So this is a highly novel research in the field of the batteries technology. Nobody has reported the higher discharge capacity of LIBs using pure LiCoO<sub>2</sub> single crystals cathode. Although some researchers have focused on the development of the LIBs using the crushed LiCoO<sub>2</sub> single crystals mixing with some ionic conduction solution. However, the capacity was limited to 130-131 mAh/g [15, 16] due to the lack of fair LiCoO<sub>2</sub> single crystals cathode. So, the current research is a highly novel work that could be applicable in the industrial application of LIBs for the enhancement of the performance of next generation LIBs. A new business can be opened worldwide on the development of the next-generation LIBs using LiCoO<sub>2</sub> single crystals cathode that will contribute to the socio economic development of Japan.

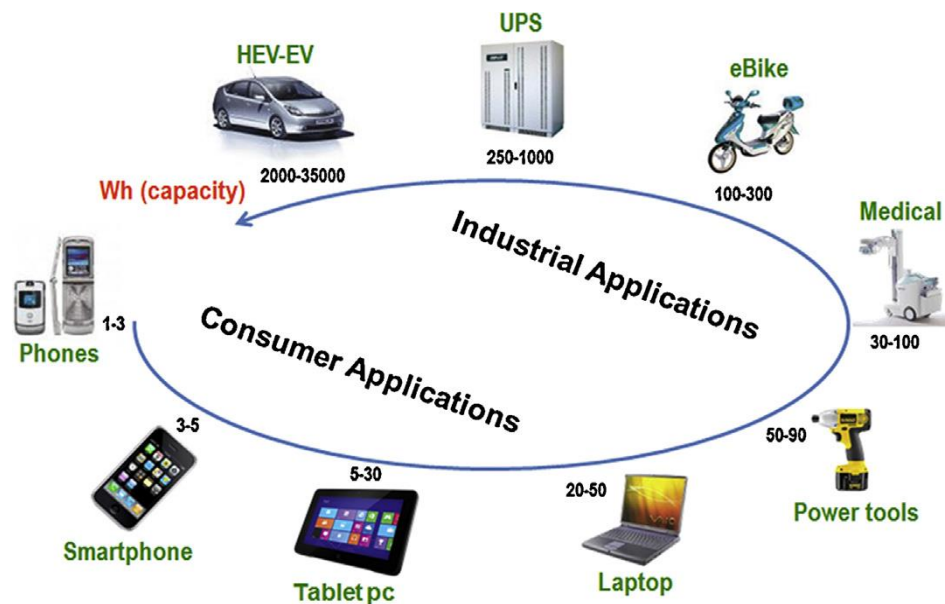


Fig. 6-4 Scope of use of rechargeable batteries [17].



Since Figure 6-4 shows the increasing requirements of modern society for energy storage technology across a broad range of applications. In commercial LIBs usually liquid electrolytes are used due to their large electrochemical voltage windows, high ionic conductivities and great wettability with the internal components of LIBs [18]. Generally, the liquid electrolyte is a mixture of linear and cyclic carbonate-based organic solvents such as diethyl carbonate (DEC) [19], ethyl methyl carbonate(EMC) [19–21], dimethyl carbonate (DMC) [19, 20], ethylene carbonate (EC) [20–22], propylene carbonate(PC) [18], and lithium salt such as lithium hexafluoro phosphate ( $\text{LiPF}_6$ ), lithium hexafluoro arsenate monohydrate ( $\text{LiAsF}_6$ ), lithium perchlorate ( $\text{LiClO}_4$ ) and lithium tetra fluoro borate ( $\text{LiBF}_4$ ) [21,23,24].

However, these liquid electrolytes have severe drawbacks [25], including high flammability, narrow electrochemical stability windows, limited operating temperatures and irreversible decomposition. Due to their high flammability, organic liquid electrolytes are believed to be the main reason for fires and explosions in LIBs [26].

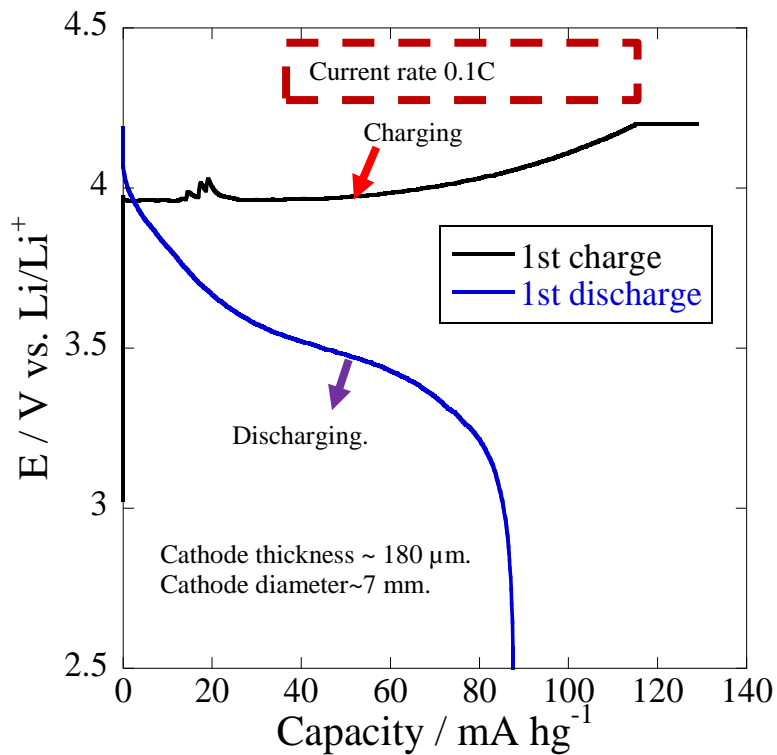


Fig. 6-5 Charge-discharge profiles of the LIBs using the  $\text{LiCoO}_2$  single crystals cathode and gel electrolyte.

In addition, the formation of lithium dendrites with organic liquid electrolytes [27] leads to internal short circuits causing catastrophic failure of lithium-based batteries [28]. Therefore, developing alternative battery systems to prevent such issues of the liquid electrolytes as well as to provide high energy density and power is strongly required.

All-solid-state Li ion batteries may be a promising energy storage technologies that is inherently safer due to the lack of flammable organic components. It has also a large electrochemical stability window, thus enabling a dramatic improvement in the energy density [29–31].

The higher power and energy characteristics of all solid state LIBs motivates me to design all solid state LIBs using  $\text{LiCoO}_2$  single crystals cathode with gel electrolyte. I have successfully designed almost all solid state LIBs using  $\text{LiCoO}_2$  single crystals cathode with high discharge capacity of 90 mAh/g (Fig. 6-5) for the first time. This is a highly novel research that could bring technological breakthroughs in the next-generation all solid state commercial LIBs.

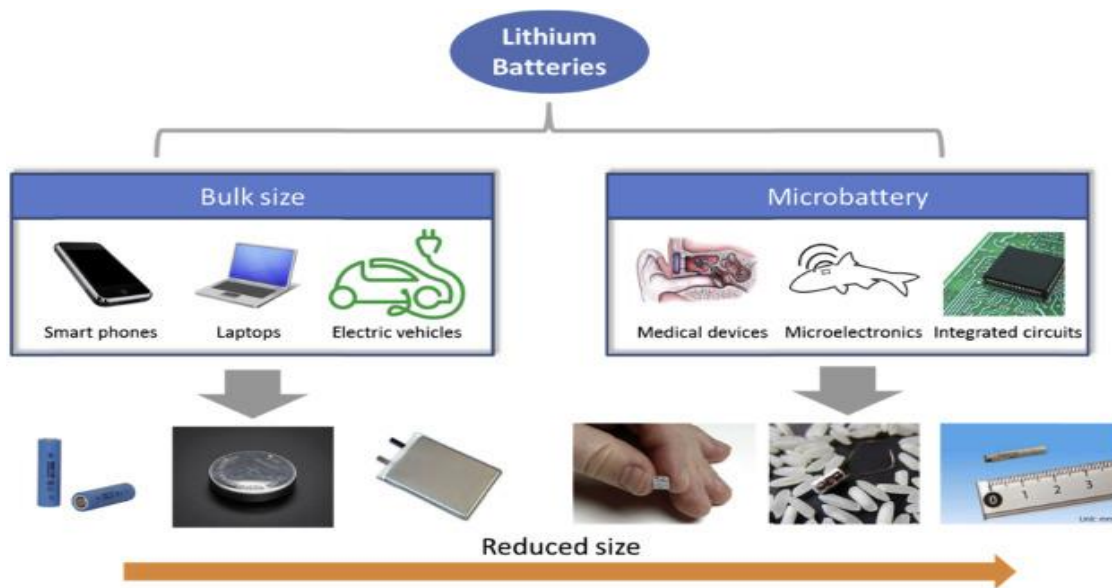
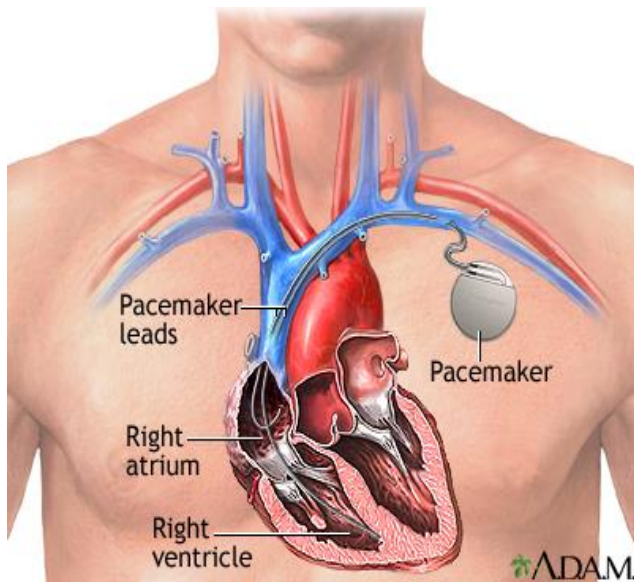


Fig. 6-6 Applications of LIBs and the form of the cells used [32].



Heart pacemaker



Hearing aids

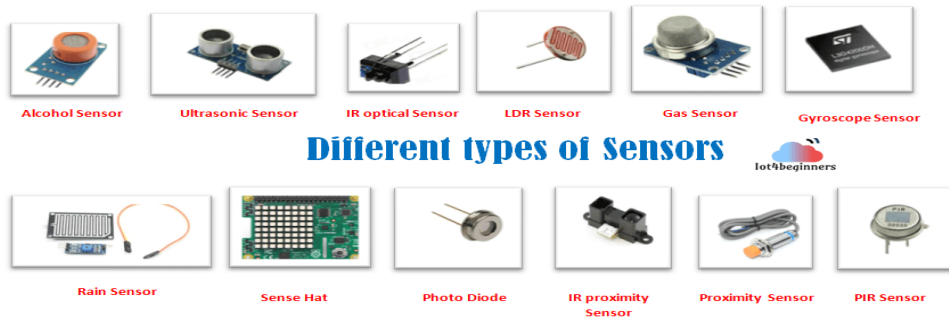


Fig. 6-7 Business feasibility of the current research.

Actually, bulk size LIBs are used in smart phones and laptops, and small sized LIBs are used in medical devices, micro-electronics and integrated circuit as shown in Figure 6-6. My designed LIBs using  $\text{LiCoO}_2$  single crystals cathode is possible to use

in medical devices such as heart pacemaker and hearing aids due to the small, compact size and high capacity. Although the cost will be slightly high but in medical sections safety is most important than the cost. In addition, sensors are very important to the operation of many of today's businesses. They can warn us of potential problems before they become big problems, allowing businesses to perform predictive maintenance and avoid costly downtime. Different types of IoT (Internet of Things) sensors which are expected to grow rapidly in near future may take advantage of high capacity LIBs using  $\text{LiCoO}_2$  single crystals cathode. So, novel design of high performance all solid state LIBs using Single Crystals cathode may be a future directions for the research community for the development of the next generation LIBs in medical and industrial sections that will contribute to the socio-economic development of Japan creating a new business.

## References:

- [1] J. Zhang, L. Zhang, F. Sun, Z. Wang, *IEEE Access*, **6** (2018) 23848.
- [2] M. Dubarry, J. Devie, *Energy Storage*, **18** (2018) 185.
- [3] J. Lopez, M. Gonzalez, J.C. Viera, C. Blanco, Fast-charge in lithium-ion batteries for portable applications. In Proceedings of the INTELEC 2004. 26th Annual International Telecommunications Energy Conference, Chicago, IL, USA, 19–23 September 2004.
- [4] E. Karden, S. Ploumen, B. Fricke, T. Miller, K. Snyder, *J. Power Sources*, **168** (2007) 2.
- [5] Nishi, Y, *J. Power Sources*, **100** (2001) 101.
- [6] S. Ge, Y. Leng, T. Liu, R.S. Long champs, X.G. Yang, Y. Gao, D. Wang, D. Wang, C. Y. Wang, *Sci. Adv.* **6** (2020) 7633.
- [7] M. Schmidt, M. Neuschütz, Lithium-ion batteries key component electrolyte. *ATZ Worldw.* **6** (2011)10.
- [8] A. Kwade, W. Haselrieder, R. Leithoff, A. Modlinger, F. Dietrich, K. Droeder, *Nat. Energy*, **3** (2018) 290.
- [9] Roland Irle, Plug-in Electric Light Vehicle Sales Worldwide, 11 June 2020).
- [10] A. Choudhary, E. Prasad, allied market research.com, lithium-ion-battery-market, April 2020.

- [11] PR Newswire.com, news-releases, Nov 06, 2018, global-lithium-ion-battery-market-report-2018-market-is-expected-to-reach-47-billion-by-2023-from-25billion-in-2017-300744613.
- [12] D. Deng, *Energy Science and Engineering*, **3** (2015)385-418.
- [13] Y. Liang, C. Zhao, H. Yuan, Y. Chen, W. Zhang, J. Huang, D. Yu, Y. Liu, M. Magdalena, Y. Chueh, Q. Zhang, *InfoMat*, **1** (2019) 6-32.
- [14] Y. Takahashi, Y. Gotoh, J. Akimoto, S. Mizuta, K. Tokiwa, T. Watanabe, J. *Solid State Chemistry*, **164** (2002) 1.
- [15] K. Teshima, S. Lee, Y. Mizuno, H. Inagaki, M. Hozumi, K. Kohama, K. Yubuta, T. Shishido, S. Oishi, *Cryst. Growth Des.*, **10** (2010) 4471.
- [16] Y. Mizuno, N. Zettsu, K. Yubuta, T. Sakaguchi, T. Saito, H. Wagata, S. Oishi, K. Teshima, *Cryst. Growth Des.* **14** (2014) 1882.
- [17] H. Yoo, E. Markevich, G. Salitra, D. Sharonand, D. Aurbach, *Mater. Today* **17** (2014) 110.
- [18] P. Peljo, H. H. Girault, *Energy Environ. Sci.* **11**(2018)2306.
- [19] G.G. Eshetu, S. Grugeon, S. Laruelle, S. Boyanov, A. Lecocq, J.P. Bertrand, G. Marlair, *Phys. Chem.Chem. Phys.* **15** (2013) 9145.
- [20] Y. Fu, S. Lu, L. Shi, X. Cheng, H. Zhang, *J. Electrochem. Soc.* **163** (2016), A2022.
- [21] H. Fan, L. Qi, M. Yoshio, H. Wang, *Solid State Ion.* **304** (2017) 107.

- [22] W. Ding, X. Lei, C. Ouyang, *Int. J. Quantum Chem.* **116** (2016) 97.
- [23] R. Younesi, G.M. Veith, P. Johansson, K. Edström, T. Vegge, *Energy Environ. Sci.* **8** (2015) 1905.
- [24] L. Liu, S. Gu, S. Wang, X. Zhang, S. Chen, *RSC Adv.* **10** (2020) 1704.
- [25] T.F. Miller, Z.G. Wang, G.W. Coates, N.P. Balsara, *Acc. Chem. Res.* **50** (2017) 590.
- [26] C. Arbizzani, G. Gabrielli, M. Mastragostino, *J. Power Sources*, **196** (2011) 4801.
- [27] Z.I. Takehara, *J. Power Sources*, **68** (1997) 82.
- [28] Y. Takeda, O. Yamamoto, N. Imanishi, *Electrochemistry*, **84** (2016) 210.
- [29] J. Chen, X. Huang, Y. Zhu, P. Jiang, *Adv. Funct. Mater.* **27** (2017)1604754.
- [30] H. Hou, Q. Xu, Y. Pang, L. Li, J. Wang, C. Zhang, C. Sun, *Adv. Sci.* **4** (2017) 1700072.
- [31] E. Simonetti, M. Carewska, G. Maresca, M. De Francesco, G.B. Appetecchi, *J. Electrochem. Soc.* **164** (2016) A6213.
- [32] Y. Wang, B. Liu, Q. Li, S. Cartmell, S. Ferrara, Z. D. Deng, J. Xiao, *Journal of power sources*, **286** (2015) 330.



## CHAPTER 7

### 7.1 Summary

Recently, sustainable energy as well as efficient and economical energy conversion and storage technologies has become important work in light of the rising environmental issues and dependence on portable and uninterrupted power sources. Li-ion rechargeable batteries play a significant role in the demand for green and sustainable energy. The energy density of a rechargeable battery is determined collectively by the specific capacity of electrodes and the working voltage of the cell, which is the differential potential between the cathode and the anode. Over the past decades, a significant number of studies have focused on enhancing this specific capacity. But the capacity of LIBs using  $\text{LiCoO}_2$  cathode is still lower compared to its theoretical capacity due to the grain boundaries of the  $\text{LiCoO}_2$  polycrystalline cathode. In this study, I have prepared high quality, larger diameter  $\text{LiCoO}_2$  single crystals cathode by TSFZ technique using tilting mirror-type image furnace to enhance the capacities of LIBs. Charge-discharge characteristics of the grown  $\text{LiCoO}_2$  single crystals cathode have been studied.

The summary of my studies is as follows.

In **chapter 1**, I have discussed the characteristics of some cathode materials for LIBs in detail and background of this research on LiCoO<sub>2</sub> cathode. The necessity of the high quality larger diameter LiCoO<sub>2</sub> for the development of the performance of LIBs was described.

In **chapter 2**, I have explained the effects of mirror tilting on the shape of the molten zone and interfaces of LiCoO<sub>2</sub> single crystals during the TSFZ growth using tilting-mirror type image furnace. Interface shape is very important that affects the quality of the grown crystals. In this experiment, mirrors were tilted from 0° to 15° in order to investigate the change of the solid-liquid interface shape in the molten zone during the growth. The interface shape of the molten zone formed under both tilted and non-tilted conditions was convex and convexities were decreased with increasing mirror tilting angle,  $\theta$ . The convexities ( $h/r$ ) of the feed-liquid and crystal-liquid interface were minimum at the tilt angle of  $\theta = 10^\circ$ . I have also grown large single crystals of LiCoO<sub>2</sub> as a function of mirror tilting angle. Best LiCoO<sub>2</sub> single crystals up to 7 mm in diameter and 50 mm in length with a shiny visible character were obtained at a mirror tilt angle of  $\theta = 10^\circ$  due to the lowest convexities at this tilt condition. I have also examined some important parameters that characterizing the molten zone such as molten zone length, gap between the feed and grown crystals and the required lamp power for the crystal growth. The lamp power required to maintain the stable molten zone during crystal growth and the amount of Li evaporation

from the molten zone were the lowest at  $\theta=10^\circ$ . So, slightly convex interface shape is better for the growth of high quality large single crystals of  $\text{LiCoO}_2$ .

In **chapter 3**, I have reported the TSFZ growth of larger diameter single crystals of  $\text{LiCoO}_2$  using tilting-mirror type image furnace. The main problem during the growth of larger diameter single crystals of  $\text{LiCoO}_2$  was the high Li evaporation that increased the required lamp power and the contact problem between the feed rod and grown crystals. The higher lamp power enhanced not only evaporation of Li component from the molten zone but also deposition of cobalt oxide phase in the grown crystals. As a result, contact between the feed rod and the grown crystal occurred due to the deposition of cobalt oxide phase with a high melting temperature, which makes challenging to me for the TSFZ growth of larger diameter single crystals of  $\text{LiCoO}_2$ . In order to overcome these problems, I have studied the effects of slightly excess Li content (2 mol% to 5 mol%) in the stoichiometric feed, the solvent amount and the filament shape of the heating lamps on the growth of larger-diameter  $\text{LiCoO}_2$  single crystals. All these parameters are very important because they are strongly related with the stability of molten zone during the growth. In this study, I have found that the cylindrical type filament shape of the heating lamp had a significant effects to grow the void and inclusion free single crystals of  $\text{LiCoO}_2$  due to the high heating efficiency compared to the flat filament type lamp. For the growth of 10 mm diameter single crystals of  $\text{LiCoO}_2$ , the optimum conditions was found at solvent amount of 2.5 g using a 2 mol% excess Li content feed composition. Optimized conditions for the growth of more than half inch that is 13 mm diameter single crystals of  $\text{LiCoO}_2$  was found at the

optimum amount of solvent of 4.9 g using a 3 mol% excess Li content feed composition. The required lamp power for crystal growth and amount of Li evaporation from the molten zone during growth was lowest under these optimized growth conditions. Finally, I have obtained a linear relationship between the optimum amount of solvent and the square of the crystal diameter during the growth of larger-diameter single crystals of  $\text{LiCoO}_2$ .

In **chapter 4**, I have described the reason for the lower capacity of LIBs using the  $\text{LiCoO}_2$  polycrystalline materials and the advantages of  $\text{LiCoO}_2$  single crystals cathode in LIBs. In this study, charge-discharge characteristics of LIBs using my grown  $\text{LiCoO}_2$  single crystals cathode were investigated using liquid, gel and solid electrolyte. Capacity of LIBs depends on the impedance of the coin cell and the synthesis process of the coin cell. In addition, the impedance of the coin cell is strongly related with the thickness of the cathode. The discharge capacities of LIBs using  $\text{LiCoO}_2$  single crystals cathode with liquid electrolyte was 125 mAh/g at a lower current rate of 0.01 C. At a higher current rate of 0.05 C, the coin cell prepared using  $\text{LiCoO}_2$  single crystals cathode of thickness 400  $\mu\text{m}$  did not properly. The impedance of the coin cell was high due to higher thickness of the cathode. As the cathode thickness was reduced to 200  $\mu\text{m}$ , the higher discharge capacity that is 140 mAh/g was achieved with higher current rate of 0.1 C using liquid electrolyte. In addition, the discharge capacity was also increased to 145 mAh/g as the cathode diameter was 13mm. I have also designed almost all solid state LIBs using  $\text{LiCoO}_2$  single crystals cathode with gel electrolyte and the discharge capacity was 90 mAh/g. In this study, all solid state LIBs

using both polycrystalline and single crystalline solid electrolytes was tried but did not succeed due to the high impedance of the coin cell.

In **chapter 5**, I have discussed the problems during growth of  $\text{LiCo}_{0.99}\text{Nb}_{0.1}\text{O}_2$  single crystals by TSFZ technique using tilting mirror type furnace. Also I have mentioned the necessity for further experiment to find the optimized conditions for the stable growth of Nb-doped  $\text{LiCoO}_2$  single crystals.

In **chapter 6**, I have explained the social significance and business feasibility of the current research.

## 7.2 Impact of the present research

Lithium-ion batteries (LIBs) are small in size, light in weight and high in energy density, so applications of lithium-ion batteries are expanding into new fields such as smart mobile devices, electric vehicles and energy storage systems. LIBs are the powerhouse for the digital electronic revolution in this modern mobile society, exclusively used in mobile phones and laptop computers. The success of commercial LIBs in the 1990s was not an overnight achievement, but a result of intensive research and contribution by many great scientists and engineers. Then much efforts have been put to further improve the performance of Li-ion batteries, achieved certain significant progress. To meet the increasing demand for energy storage, particularly from increasingly popular electric vehicles, intensified research is required to develop next-generation Li-ion batteries with dramatically improved performances, including improved specific energy and volumetric energy density, cyclability, charging rate, stability, and safety. Improvements of the properties of the cathode material is very important in the development of next-generation Li-ion batteries. In this study, I have carried out research on the preparation of high quality and larger diameter  $\text{LiCoO}_2$  single crystals cathode to enhance the performance of next generation all solid state LIBs.  $\text{LiCoO}_2$  is a layered cathode material that exhibits high anisotropic ionic conductivity. Due to the high anisotropic ionic conductivity in  $\text{LiCoO}_2$ , single crystalline substrate perpendicular to c-axis is expected to enhance the capacity and charge/discharge rate of LIBs for the development of next generation all solid state LIBs. For commercial application of  $\text{LiCoO}_2$  single crystals in LIBs,  $\text{LiCoO}_2$  single crystals of

half inch in diameter is extremely required. In the best of my knowledge, any researcher has not reported the TSFZ or FZ growth of  $\text{LiCoO}_2$  single crystals of half inch in diameter. However, the single crystals growth of  $\text{LiCoO}_2$  of half inch in diameter was so challenging due to the contact problem and high Li evaporation during the growth. In this research, I have discussed the present problems, motivation and counterplans on TSFZ growth of larger diameter  $\text{LiCoO}_2$  single crystals in details and finally succeed on the growth of the  $\text{LiCoO}_2$  single crystals of more than half inch (13 mm) in diameter for the first time.

For the practical application of my grown  $\text{LiCoO}_2$  single crystals cathode, I have designed a coin-type cell using the grown  $\text{LiCoO}_2$  single crystals as a cathode, Li metal as an anode and liquid electrolyte. The charge-discharge characteristics of the designed coin-type cell exhibits the high discharge capacity of 145 mAh/g compared to the commercial  $\text{LiCoO}_2$  polycrystalline materials. So this is a highly novel research work for the development of the performances of the next generation LIBs.

Due to the possibility of dendrite formation in LIBs using liquid or polycrystalline solid electrolyte, firing may occur in LIBs. In this regards, the research on the single crystals solid electrolyte is rapidly increasing. Safety issue in LIBs motivated me to design all solid state LIBs using single crystals solid electrolyte. All solid state LIBs using  $\text{LiCoO}_2$  single crystals cathode, single crystals solid electrolyte and Li metal anode was challenging due to the difficulty in the connection of all solid parts that enhances the impedance of the coin cell. Finally, I have successfully designed almost all solid state LIBs using  $\text{LiCoO}_2$  single crystals cathode, gel electrolyte and Li metal anode for the first time. The discharge

capacity of almost all solid state LIBs using  $\text{LiCoO}_2$  single crystals cathode was 90 mAh/g. In concern of the safety issue, this research is a highly novel research that could be helpful in commercial LIBs for the development of the performance of the next generation all solid state LIBs.



## APPENDIX

### List of Publications and Presentations

#### Publications

- [1] **Effects of the Mirror Tilt Angle on the Growth of LiCoO<sub>2</sub> Single Crystals by the Traveling Solvent Floating Zone (TSFZ) Technique Using a Tilting-Mirror-type Image Furnace.**

**Ruma Parvin**, Yuki Maruyama, Masanori Nagao, Satoshi Watauchi, Isao Tanaka, *Crystal Growth and Design*, ACS 2020, 20, 3413-3416.

- [2] **Growth of Large-diameter LiCoO<sub>2</sub> Single Crystals by the Traveling Solvent Floating Zone (TSFZ) Technique using a Tilting-Mirror-type Image Furnace**

**Ruma Parvin**, Md. Shahajan Ali, Yuki Maruyama, Masanori Nagao, Satoshi Watauchi, Isao Tanaka, **Accepted for publication in *Journal of Flux Growth*, Vol. 15 No. 1, June 2021.**

#### **Japanese Patent Application**

*Production method of oxides by traveling solvent floating zone method and single crystals of lithium cobaltate*

Isao Tanaka, Yuki Maruyama, **Ruma Parvin**, Masanori Nagao, Satoshi Watauchi, **Japanese Patent Application, 2020-216337 (2020)**

## **Manuscript Under Preparation**

[1] **Development of all solid state LIBs using LiCoO<sub>2</sub> single crystals cathode (collaboration work with Tokyo Metropolitan University)**

**Ruma Parvin**, Md. Shahajan Ali, Yuki Maryuma, Yuto Yamada, Ryo Oyama, Masanori Nagao, Satoshi Watauchi, Isao Tanaka, Kiyoshi Kanamura(to be submitted to the Journal of **Nature Materials**).

## **On going work**

[1] **Single crystals growth of Nb doped LiCoO<sub>2</sub> by TSFZ method using tilting mirror furnace.**

## **Poster Presentations**

[1] **Ruma Parvin**, Yuki Maruyama, Masanori Nagao, Satoshi Watauchi, Isao Tanaka  
The 7<sup>th</sup> international seminar on Green Energy Conversion Science and Technology, Kofu, University of Yamanashi, Japan. August 22-23, 2018.

- [2] **Ruma Parvin**, Yuki Maryuma, Yuto Yamada, Ryo Oyama, Masanori Nagao, Satoshi Watauchi, Isao Tanaka, Kiyoshi Kanamura, Materials Research Meeting, Yokohama, Japan, December 10-14, 2019.
- [3] **Ruma Parvin**, Yuki Maruyama, Masanori Nagao, Satoshi Watauchi, Isao Tanaka
- The 8<sup>th</sup> international seminar on Green Energy Conversion Science and Technology, Kofu, University of Yamanashi, Japan. October 24-25, 2019.

# *ACKNOWLEDGMENT*

Alhamdulillah, all praises to Allah (SWT) who is the Most Kind and the Powerful, without his kindness, it would be quite impossible to complete this study successfully.

At first, I would like to express my deepest gratefulness to my honorable Supervisor **Professor Isao Tanaka**, Center for Crystal Science and Technology, University of Yamanashi, for his continuous support of my PhD study, for his patience, motivation and immense knowledge. His excellent guidance helped me in all the time of my research and writing this thesis. I could not have imagined having a better advisor and mentor for my PhD study.

I am deeply grateful to **Professor Kyoshi Kanamura** for supervising me during my internship collaboration research work, Department of Applied Chemistry, Tokyo Metropolitan University, Japan. Also, I would like to thank to Yuto Yamada, Ryo Oyama, and Yosuke Khushida for their cordial co-operation.

I also would like to cordial thanks to **Professor Satochi Watauchi, Professor Masanori Nagao and Professor Yuki Maruyama** for their valuable comments and encouragement, especially continuous help to accomplish this research successfully.

Special thanks to Professor Nobuhiro KUMADA, Takahiro TAKEI, Satochi WADA, Kiyokaza NAKAGAYA, Junji YAMANAKA, Yoshinori YONESAKI, and Keisuke ARIMOTO, who provided me an opportunity to access the laboratory and research facilities.

Thanks to the all officials staff of this center for Crystal Science and Technology (CCST), Office of International affairs and University of Yamanashi for their co-operation. I am greatly thankful to all the students of this laboratory for their helpful behavior. In particularly, I am grateful to

Toyoda Nozomi, Hotomomi Hashizume, and Fukasawa for their continuous support inside and outside the laboratory issues. I also want to thanks all of teachers of Nakamura kinder garden School for special cares to my son in the last three years.

I am very much grateful to **Professor A. K. M. A. Islam** my M. Sc. supervisor, my parents, colleagues, relatives, well-wishers and Bangladesh community all members for their mental support and advice to me even though far away from me during my study. I want to express my deepest and infinite love to my husband **Md. Shahajan Ali** and endless affection to my son **Saleh Hasan Rifat**. They were my strength and without their encouragement and continuous help, I could not continue my PhD study.

I want to express my special thanks to the Japanese Government; Ministry of Education, Culture, Sports, Science and Technology (MEXT) for providing me JASSO scholarship for one year. Finally, I would like to express my thanks to Green Energy Conversion Science and Technology and Power Energy Professional (PEP) program for their financial support during time PhD study.

March 2021

Author

A handwritten signature in blue ink that reads "Ruma Parvin". The signature is written in a cursive style and is enclosed within a light blue rectangular border.

(Ruma Parvin)